NTNU
Norwegian University of
Science and Technology

Spin Polarization Effects in Cherenkov Radiation

Jonas Lundeby Willadsen

MSc in Physics
Submission date: May 2018
Supervisor: Bo-Sture Skagerstam, IFY

Norwegian University of Science and Technology
Department of Physics

Abstract

Relativistic quantum mechanics is applied to calculate the transition amplitudes of Cherenkov radiation to first order in perturbation theory, for a spin polarized relativistic particle. Effects related to the spin polarization are derived, and are shown to have a potential for experimental detection greater than that of the effects arising from the established relativistic treatment of Cherenkov radiation.

Sammendrag

Relativistisk kvantemekanikk tas i bruk for å beregne Cherenkovstrålingens transisjonsamplituder til første orden i perturbasjonsteori, for en spinnpolarisert relativistisk partikkel. Effekter relatert til spinnpolarisasjonen utledes, og vises å være lettere eksperimentelt tilgjengelige enn effektene i den etablerte relativistiske teorien for Cherenkovstråling.

Preface

I wish to thank my advisor, Bo-Sture Skagerstam, for his support and contributions to my work, which includes suggesting spin polarized Cherenkov radiation as a thesis topic. This project would not have been possible without the insight and enthusiasm he has offered throughout many a long conversation.

I extend also my gratitude towards my family whose support has kept me working hard, my fellow students whose company and advice have been of great value, and last but not least my lovely Marit, who manages to brighten my days even from many miles away.

Contents

List of Figures

List of Symbols

Symbol	Quantity	SI-unit
l	distance	m
v	speed	$\mathrm{m\,s^{-1}}$
q	charge	C
n	index of refraction	(dimensionless)
P	power	W ($\mathrm{J\,s^{-1}}$)
R	transition rate	Hz ($\mathrm{s^{-1}}$)
k	wavenumber (repetency)	$\mathrm{rad\,m^{-1}}$
ω	angular frequency	$\mathrm{rad\,s^{-1}}$
ϵ	permittivity	$\mathrm{F\,m^{-1}}$
μ	permeability	$\mathrm{H\,m^{-1}}$
ρ	charge density	$\mathrm{C\,m^{-3}}$
$\boldsymbol{j}$	current density	$\mathrm{A\,m^{-2}}$

Physical Constants

Quantity	Symbol	Value[1]	Unit
speed of light	c	2.99792458×10^{8}	$\mathrm{m\,s^{-1}}$ (exact)
vacuum permeability	μ_0	$4\pi \times 10^{-7}$	$\mathrm{H\,m^{-1}}$ (exact)
vacuum permittivity	ϵ_0	$8.85418781 \times 10^{-12}$	$\mathrm{F\,m^{-1}}$ (exact)
reduced Planck constant	$\hbar$	$1.054571726 \times 10^{-34}$	J s
elementary charge	e	$1.602176565 \times 10^{-19}$	C
electron mass	m_e	$9.10938291 \times 10^{-31}$	kg
fine-structure constant	α	$7.2973525698 \times 10^{-3}$	(dimensionless)

[1] All values from [1, p. 107]

1 Introduction

When a charged particle travels through a dielectric medium, at a speed exceeding the velocity of light in said medium, light is emitted in a forward cone coaxial with the path of the particle. This phenomenon is referred to as Cherenkov radiation after the physicist who first detected it experimentally in 1934 [6]. The phenomenon is also known as the Vavilov-Cherenkov effect due to the contributions of S. I. Vavilov, acting as the advisor of P. A. Cherenkov. The effect was first described theoretically by I. M. Frank and I. E. Tamm, who shared the 1958 Nobel prize in physics with P. A. Cherenkov for the discovery and the interpretation of the Cherenkov effect [7].

The effect has found many applications, e.g., in the field of particle physics. For instance, in a so-called Ring-Imaging Cherenkov (RICH) detector, the Cherenkov effect is used to determine the velocity of a particle. If the momentum of the particle is also known one may then determine its mass, thereby identifying the particle [8]. Some notable examples of such detectors are the RICH 1 and RICH 2 detectors at LHCb [5].

The physical interpretation of the Cherenkov effect involves an interesting question which is difficult to answer conclusively, namely that of whether it is the medium or the particle which emits the radiation [9]. In the classical interpretation, the radiation is emitted by the medium under the influence of the field of the charged particle (as opposed to being emitted from the charged particle itself [10, p. 357]). A qualitative explanation, adapted from Reference [11, p. 4–5], is as follows:

A fast moving charge will induce a dipole moment in the atoms of the material in a manner symmetric with regard to rotation about the path of the charge. As a result there is a net effect on the electromagnetic field even at large distances: a brief pulse emitted from each point along the path of the charge. We observe the Fourier components of this pulse as Cherenkov radiation. In general, the wavelets from different points along the track interfere destructively, leaving no observable radiation. In the special case where the charge moves faster than the speed of light in the medium, however, there is an angle θ_C relative to the path of the charge at which the waves interfere constructively, causing light to radiate in this direction.

As will be shown in Chapter 2.1, the classical theory results in the charge radiating an infinite amount of energy per unit length along its path. This problem is circumvented by letting the coefficient of refraction depend on frequency. This enforces a cut-off on the frequencies of light which may be emitted, and thus makes the radiated energy finite. In principle, the classical phenomenon would not respect conservation of energy were it not for the fact that real materials exhibit such a cut-off frequency for their dielectric properties.

The results of the classical theory may, however, be reproduced by quantum mechanical methods, which intrinsically respect conservation of energy and momentum. Thus the principle of the phenomenon may be studied while modelling the medium as dispersionless. In the quantum mechanical theory, as first investigated by V. L. Ginzburg in 1940 [7], a particle coupled to a field moving at higher speeds than the phase-velocity of said field is kinematically permitted to emit a quantum of the field. The Cherenkov angle emerges then, with a relativistic correction, from conservation of energy and momentum rather than the interference of waves. Perhaps it may not be misled to think of the phenomenon as the charged particle itself emitting Cherenkov radiation.

Motivated by the question of whether it is the particle or the medium which radiates, this thesis seeks to employ the framework of relativistic quantum mechanics to describe the radiation emitted by a spin polarized relativistic current. As Chapter 4 will demonstrate, the effects of spin polarization could potentially be non-negligible. The quantum mechanical description of the phenomenon is based on a macroscopic quantization of the electromagnetic field, modelling the medium merely by means of changing the electric permittivity of space. There is to the author's knowledge no analogous way to account for spin polarization effects within macroscopic classical electrodynamics by only altering the electric permittivity of space. Therefore, if spin polarization effects were to be observed experimentally, they may potentially provide a compelling argument for the interpretation wherein it is the particle itself which emits radiation. Additionally, as a practical motivation, the presence of observable spin polarization effects would make it possible for experiments to study the spin degrees of freedom of a beam of charged particles.

2 Theoretical Background

We here provide an overview of the established theory of Cherenkov radiation. We first apply classical electrodynamics to calculate the power spectrum of the radiation. Thereupon, we reproduce the result within quantum mechanics. Finally, we calculate the transition amplitude of the phenomenon within relativistic quantum mechanics, whereupon in the next chapter we consider the resulting corrections to the results from the previous theories.

2.1 Classical Electrodynamics

The following is adapted from Ref. [11, Ch. 2].

Overview

The classical theory of Cherenkov radiation is based on a few simplifying assumptions:

1. The medium is treated as an unbounded continuum, i.e., its microscopic structure and boundary are neglected.
2. The medium is treated as a linear isotropic dielectric, with characteristic frequency independent permittivity ϵ, and $\mu = 1$.
3. We neglect absorption of radiation in the medium, i.e., $\mathrm{Im}\{\epsilon\} = 0$.
4. The calculations are performed on a sufficiently large, finite, time scale but such that the velocity of the charge may nevertheless be considered constant.

In a linear isotropic dielectric, the macroscopic Maxwell equations take on the same form as the microscopic equations, except with the permittivity of the medium, $\epsilon\epsilon_0$, substituted for that of the vacuum

$$\begin{aligned} \boldsymbol{\nabla} \cdot \boldsymbol{E}(\boldsymbol{r},t) &= \frac{\rho(\boldsymbol{r},t)}{\epsilon\epsilon_0} \,, & \boldsymbol{\nabla} \times \boldsymbol{E}(\boldsymbol{r},t) &= -\frac{\partial}{\partial t}\boldsymbol{B}(\boldsymbol{r},t) \,, \\ \boldsymbol{\nabla} \cdot \boldsymbol{B}(\boldsymbol{r},t) &= 0 \,, & \boldsymbol{\nabla} \times \boldsymbol{B}(\boldsymbol{r},t) &= \mu_0 \boldsymbol{j}(\boldsymbol{r},t) + \epsilon\epsilon_0\mu_0 \frac{\partial}{\partial t}\boldsymbol{E}(\boldsymbol{r},t) \,. \end{aligned} \tag{2.1}$$

Here, $\rho(\boldsymbol{r},t)$ and $\boldsymbol{j}(\boldsymbol{r},t)$ denote a classical free charge density and a classical free current density respectively. We define a vector potential $\boldsymbol{A}(\boldsymbol{r},t)$ by

$$\boldsymbol{B}(\boldsymbol{r},t) = \boldsymbol{\nabla} \times \boldsymbol{A}(\boldsymbol{r},t) \,, \tag{2.2}$$

and a scalar potential $V(\boldsymbol{r}, t)$ by

$$\boldsymbol{E}(\boldsymbol{r}, t) = -\boldsymbol{\nabla} V(\boldsymbol{r}, t) - \frac{\partial}{\partial t}\boldsymbol{A}(\boldsymbol{r}, t) \, . \tag{2.3}$$

Furthermore, we impose the Lorenz gauge

$$\boldsymbol{\nabla} \cdot \boldsymbol{A}(\boldsymbol{r}, t) = -\frac{n^2}{c^2}\frac{\partial}{\partial t} V(\boldsymbol{r}, t) \, , \tag{2.4}$$

where we have defined the index of refraction by $n = \sqrt{\epsilon}$. With this choice of gauge, Maxwell's equations as expressed in Eqs.(2.1) lead to the wave equations

$$\nabla^2 \boldsymbol{A}(\boldsymbol{r}, t) - \frac{n^2}{c^2}\frac{\partial^2}{\partial t^2}\boldsymbol{A}(\boldsymbol{r}, t) = -\mu_0 \boldsymbol{j}(\boldsymbol{r}, t) \, , \tag{2.5}$$

and

$$\nabla^2 V(\boldsymbol{r}, t) - \frac{n^2}{c^2}\frac{\partial^2}{\partial t^2} V(\boldsymbol{r}, t) = -\frac{1}{\epsilon\epsilon_0}\rho(\boldsymbol{r}, t) \, . \tag{2.6}$$

For these fields, a freely propagating sinusoidal wave behaves as $\sin(\omega t - \boldsymbol{k} \cdot \boldsymbol{r})$, where ω denotes the angular frequency of the wave and $\boldsymbol{k}$ denotes the wave vector. The wave vector points in the direction of propagation of the wave, and obeys the dispersion relation

$$k = \frac{\omega n}{c} \, , \tag{2.7}$$

where $k = |\boldsymbol{k}|$.

Under these assumptions we are able to evaluate the field originating from a point charge, q, travelling through a dielectric at a speed v greater than the phase velocity of light, c/n. We shall do so by inserting the corresponding parameters in Eq.(2.5) to find an expression for the vector potential in the presence of such a charge. We will then use this expression to evaluate the physical fields $\boldsymbol{E}(\boldsymbol{r}, t)$ and $\boldsymbol{B}(\boldsymbol{r}, t)$, by Eq.(2.2) and Eq.(2.3). Finally, we will calculate the radiated power. The calculations will be performed using cylindrical coordinates ρ, ϕ, z, in order to utilize the azimuthal symmetry of the problem. We place the charge at the origin of the $\rho\phi$-plane, and align $\hat{\mathbf{z}}$ with its direction of motion, $\boldsymbol{v} = v\hat{\mathbf{z}}$ where $v = |\boldsymbol{v}|$ (see Figure 2.1). Before solving the wave equation we will, however, make an intuitive argument to predict the wave vector of the solution.

Each point along the path of the charge may be considered the source of a disturbance in the electromagnetic field. As each such disturbance propagates in all directions at the speed c/n, they will interfere constructively at an angle θ_C relative to the z-axis (see Figure 2.2). This angle is called the Cherenkov angle and is determined by the relation

$$\cos\theta_C = \frac{c}{nv} \, . \tag{2.8}$$

Note that θ_C is not defined for v smaller than the speed of light in the medium. Knowing the angle at which we expect emitted light to propagate allows us to

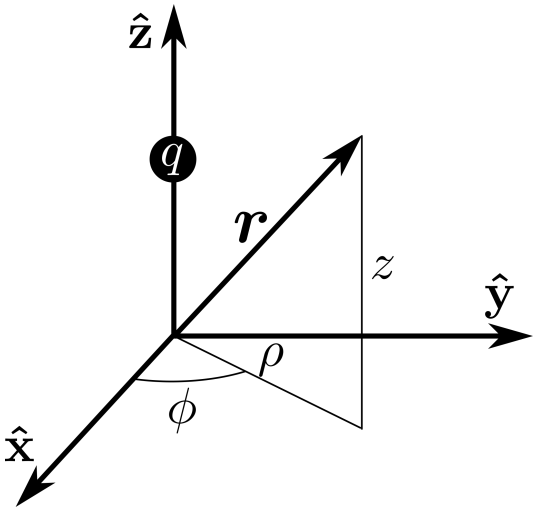

FIGURE 2.1: The point $\boldsymbol{r}$ in a cylindrical coordinate system, with the charge q on the z-axis.

determine the corresponding wave vector

$$\boldsymbol{k} = \frac{\omega n}{c}[\hat{\boldsymbol{\rho}} \sin\theta_C + \hat{\mathbf{z}} \cos\theta_C] \ . \tag{2.9}$$

Here we have also used the dispersion relation, Eq.(2.7), to set the magnitude of the wave vector. Note that $\boldsymbol{k}$ is orthogonal to $\hat{\boldsymbol{\phi}}$ due to the azimuthal symmetry of the problem. We expect $\boldsymbol{k}$ to emerge as the wave vector of the solution to the wave equation.

The Vector Potential

Provided a specified current density, Eq.(2.5) may be solved for the resulting vector potential. The current density corresponding to the moving charge in our scenario is

$$\boldsymbol{j}(\boldsymbol{r}, t) = \hat{\mathbf{z}} q v \delta_\rho(\rho)\delta(z - vt) \ . \tag{2.10}$$

Here $\delta_\rho(\rho)$ is a radial delta function, defined in accordance with Appendix C. Performing the Fourier transforms of $\boldsymbol{A}(\boldsymbol{r}, t)$ and $\boldsymbol{j}(\boldsymbol{r}, t)$ with respect to time, according to Eq.(A.4), we may express Eq.(2.5) as

$$\left(\nabla^2 + \frac{\omega^2 n^2}{c^2}\right) \boldsymbol{A}(\boldsymbol{r}, \omega) = -\mu_0 \boldsymbol{j}(\boldsymbol{r}, \omega) \ . \tag{2.11}$$

Here, the Fourier transform of the current density is

$$\boldsymbol{j}(\boldsymbol{r}, \omega) = \hat{\boldsymbol{z}} q e^{-i\omega z/v} \delta_\rho(\rho) \ , \tag{2.12}$$

by Eq.(C.4). In view of this expression, we make an Ansatz for the vector field

$$\boldsymbol{A}(\boldsymbol{r}, \omega) = \hat{\mathbf{z}} A_z(\boldsymbol{r}, \omega) \ , \quad A_z(\boldsymbol{r}, \omega) = u(\rho, \omega) e^{-i\omega z/v} \ . \tag{2.13}$$

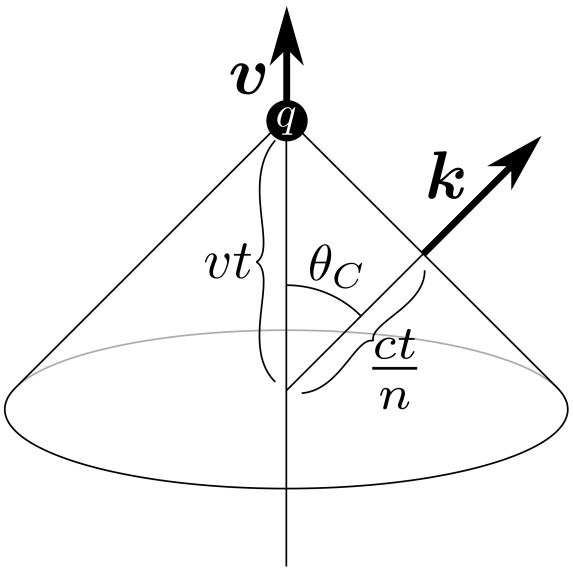

FIGURE 2.2: A light pulse originating at the charge q, propagating with azimuthal symmetry at an angle θ_C relative to the direction of propagation of the charge.

The problem is then reduced to obtaining an expression for $u(\rho, \omega)$. Inserting in Eq.(2.11) the Fourier transform of the current, Eq.(2.12), and our Ansatz, Eq.(2.13), we arrive at a differential equation for $u(\rho, \omega)$

$$(\nabla^2 + s^2)u(\rho, \omega) = -\mu_0 q \delta_\rho(\rho) \; . \tag{2.14}$$

Here

$$s^2 \equiv \frac{\omega^2}{v^2}\left(\frac{n^2 v^2}{c^2} - 1\right) \equiv \frac{\omega^2 n^2}{c^2}\sin^2\theta_C \; , \tag{2.15}$$

according to the definition of θ_C, Eq.(2.8).

The source term of Eq.(2.14) is zero everywhere except on the z-axis. Thus we may solve this differential equation by considering a free field with a boundary condition at the z-axis. For $\rho > 0$, Eq.(2.14) reduces to a homogeneous equation

$$\frac{\partial^2}{\partial\rho^2}u(\rho, \omega) + \frac{1}{\rho}\frac{\partial}{\partial\rho}u(\rho, \omega) + s^2 u(\rho, \omega) = 0 \; , \quad \rho > 0 \; , \tag{2.16}$$

where we have written the Laplacian in cylindrical coordinates.

The boundary condition is

$$\lim_{\rho\to 0} \rho \frac{\partial}{\partial\rho}u(\rho, \omega) = -\frac{\mu_0 q}{2\pi} \; . \tag{2.17}$$

This condition can be found by integrating Eq.(2.14) over an infinitesimal disk about the origin of the $\rho\phi$-plane as follows. We begin by making the assumption that $u(\rho)$ is well behaved for our purposes in $\rho = 0$. That is to say, if the function

is not finite we allow for $\rho = 0$ to be a pole of order 1, i.e., we assume

$$\lim_{\rho\to 0}\int_0^{2\pi} \mathrm{d}\phi \int_0^{\rho} \mathrm{d}\rho'\rho' u(\rho',\omega) = 0 \; . \tag{2.18}$$

Integrating the left-hand side of Eq.(2.14), we are then left with only the ∇^2-term, which we find by Gauss's theorem

$$\begin{aligned}\lim_{\rho\to 0}\int_0^{2\pi} \mathrm{d}\phi \int_0^{\rho} \mathrm{d}\rho'\rho' \boldsymbol{\nabla}\cdot\boldsymbol{\nabla} u(\rho',\omega) &= \lim_{\rho\to 0}\int_0^{2\pi} \mathrm{d}\phi\rho\hat{\boldsymbol{\rho}}\cdot\hat{\boldsymbol{\rho}}\frac{\partial}{\partial\rho}u(\rho,\omega) \\ &= \lim_{\rho\to 0} 2\pi\rho\frac{\partial}{\partial\rho}u(\rho,\omega) \; . \end{aligned} \tag{2.19}$$

Here we have expressed the $\boldsymbol{\nabla}$-operator in cylindrical coordinates by Eq.(A.2). The right-hand side of Eq.(2.14) is integrated by applying Eq.(C.5)

$$-\mu_0 q \lim_{\rho\to 0}\int_0^{2\pi} \mathrm{d}\phi \int_0^{\rho} \mathrm{d}\rho'\rho'\delta_\rho(\rho') = -\mu_0 q \; . \tag{2.20}$$

Thus the boundary condition results from equating the left-hand side, Eq.(2.19), with the right-hand side, Eq.(2.20), to give

$$\lim_{\rho\to 0}\rho\frac{\partial}{\partial\rho}u(\rho,\omega) = -\frac{\mu_0 q}{2\pi} \; . \tag{2.21}$$

We can now look for solutions of Eq.(2.16) which satisfy the boundary condition, Eq.(2.17). We define a function

$$f(\chi) \equiv u(\rho,\omega) \; , \quad \chi \equiv s\rho \; , \tag{2.22}$$

and reformulate Eq.(2.16) as a Bessel differential equation in χ

$$\chi^2\frac{\partial^2}{\partial\chi^2}f(\chi) + \chi\frac{\partial}{\partial\chi}f(\chi) + \chi^2 f(\chi) = 0 \; , \quad \rho > 0 \; , \tag{2.23}$$

with the boundary condition

$$\lim_{\rho\to 0}\chi\frac{\partial}{\partial\chi}f(\chi) = -\frac{\mu_0 q}{2\pi} \; . \tag{2.24}$$

Note that in the definition of χ, we define s as the positive square root of Eq.(2.15), making it proportional to the absolute value of ω

$$s \equiv \frac{|\omega|}{v}\sqrt{\frac{n^2v^2}{c^2} - 1} = \frac{|\omega|n}{c}\sin\theta_C \; . \tag{2.25}$$

The Bessel differential equation has two linearly independent solutions which may be expressed in different forms. We choose to express the solutions by the Hankel functions, to facilitate their description of a travelling wave (see

Appendix D). We write the solutions as

$$f^{(1)}(\chi) = \xi^{(1)} H_0^{(1)}(\chi) \,, \tag{2.26}$$

and

$$f^{(2)}(\chi) = \xi^{(2)} H_0^{(2)}(\chi) \,, \tag{2.27}$$

where ξ is a constant to be determined by the boundary condition. To find the constant, we evaluate the left-hand side of Eq.(2.24) using the asymptotic forms of the Hankel functions for a small argument, Eq.(D.6) and Eq.(D.7)

$$\begin{aligned} \lim_{\rho\to 0} \chi \frac{\partial}{\partial \chi} \xi^{(1)(2)} H_0^{(1)(2)}(\chi) &= \lim_{\rho\to 0} \chi \xi^{(1)(2)} \frac{\partial}{\partial \chi} \left(1 \pm i \frac{2}{\pi} (\ln(\chi/2) + \gamma) \right) \\ &= \pm i \frac{2}{\pi} \xi^{(1)(2)} \,. \end{aligned} \tag{2.28}$$

Requiring this to be equivalent to the right-hand side of Eq.(2.24), ξ becomes

$$\xi^{(1)(2)} = \pm i \frac{\mu_0 q}{4} \,. \tag{2.29}$$

The solutions are then

$$f^{(1)}(\chi) = i \frac{\mu_0 q}{4} H_0^{(1)}(\chi) \,, \tag{2.30}$$

and

$$f^{(2)}(\chi) = -i \frac{\mu_0 q}{4} H_0^{(2)}(\chi) \,. \tag{2.31}$$

Note that $f^{(1)*} = f^{(2)}$.

For a charge moving slower than the speed of light in the medium, we have from our definition of s, Eq.(2.25), that the argument χ is purely imaginary. Thus it can be seen from the large argument asymptotic forms of the Hankel function, Eq.(D.4), that $f^{(1)}$ will vanish exponentially with ρ. Conversely, $f^{(2)}$ will grow exponentially with ρ, which is clearly an unphysical solution. This confirms the absence of a radiative solution for velocities below the speed of light in the medium.

Conversely for a charge moving faster than the speed of light in the medium, Eq.(2.25) gives us a real argument χ. Consulting the large argument asymptotic forms of the Hankel functions, Eq.(D.4) and Eq.(D.5), the different domains can be characterized. For positive ω, $e^{i\omega t} H_0^{(1)}(\chi)$ will represent an incoming wave and $e^{i\omega t} H_0^{(2)}(\chi)$ an outgoing wave, and vice versa for negative ω. Our interest is in radiation emanating from the charge, and so we consider only the outgoing wave solutions

$$u(\rho, \omega) = \begin{cases} f^{(2)}(\chi) \,, & \text{if} \quad \omega \geq 0 \,, \\ f^{(1)}(\chi) \,, & \text{if} \quad \omega < 0 \,. \end{cases} \tag{2.32}$$

The Fourier transform of the vector potential is defined by our Ansatz, Eq.(2.13). Inserting $u(\rho, \omega)$ by Eq.(2.32) in the Ansatz, the vector potential

becomes

$$A_z(\boldsymbol{r},t) = \int_{-\infty}^{\infty} \frac{\mathrm{d}\omega}{2\pi} e^{i\omega t} A_z(\boldsymbol{r},\omega)$$
$$= \int_{-\infty}^{0} \frac{\mathrm{d}\omega}{2\pi} e^{i\omega t} e^{-i\omega z/v} f^{(1)}(\chi) + \int_{0}^{\infty} \frac{\mathrm{d}\omega}{2\pi} e^{i\omega t} e^{-i\omega z/v} f^{(2)}(\chi) \ . \tag{2.33}$$

The first term of this expression is simply the complex conjugate of the second term, due to the properties $f^{(1)*} = f^{(2)}$ and $\chi \propto |\omega|$. We may therefore write the vector potential as

$$A_z(\boldsymbol{r},t) = 2\mathrm{Re}\left\{ \int_{0}^{\infty} \frac{\mathrm{d}\omega}{2\pi} e^{i\omega t} A_z(\boldsymbol{r},\omega) \right\} \ . \tag{2.34}$$

We may therefore ignore the behaviour of $\boldsymbol{A}(\boldsymbol{r},\omega)$ in the $\omega < 0$ domain, and simplify notation by letting $|\omega| \to \omega$ in the expression for s, Eq.(2.25).

We are now ready to write an explicit expression for the Fourier transform of the vector potential, in the large ρ limit. Before writing it out, however, we simplify the notation using the wave vector $\boldsymbol{k}$, which we defined in Eq.(2.9). In the large argument limit, $u(\rho,\omega)$ is proportional to a factor $\exp[-is\rho]$, according to Eq.(D.5). Our Ansatz, Eq.(2.13), adds to this a factor $\exp[-i\omega z/v]$, and so we consider the expression

$$\frac{\omega z}{v} + s\rho = \frac{\omega n}{c}(z\cos\theta_C + \rho\sin\theta_C) = \boldsymbol{k}\cdot\boldsymbol{r} \ . \tag{2.35}$$

Note that our intuitive definition of the Cherenkov angle from Eq.(2.8) enters through s to define the direction of propagation of the radiation. With this observation, we are able to write the Fourier transform of the vector potential, in the large ρ limit, as

$$\boldsymbol{A}(\boldsymbol{r},\omega) = -i\hat{\mathbf{z}}\frac{\mu_0 q}{2}\sqrt{\frac{1}{2\pi s\rho}} e^{-i(\boldsymbol{k}\cdot\boldsymbol{r}-\pi/4)} \ , \quad \rho \gg 1 \ . \tag{2.36}$$

Having found the vector potential resulting from the current density in question, we are now ready to evaluate the corresponding physical fields.

Physical Fields

In order to solve Eq.(2.2) and Eq.(2.3) for the physical fields $\boldsymbol{E}(\boldsymbol{r},t)$ and $\boldsymbol{B}(\boldsymbol{r},t)$ we will need to take some derivatives of the vector potential. Using the $\boldsymbol{\nabla}$-operator as expressed in cylindrical coordinates by Eq.(A.2), we make a few observations based on the fact that $\boldsymbol{A}(\boldsymbol{r},t)$ is independent of ϕ, and proportional to $\hat{\mathbf{z}}$:

$$\boldsymbol{\nabla}\cdot\boldsymbol{A}(\boldsymbol{r},t) = \frac{\partial}{\partial z} A_z(\boldsymbol{r},t) \ , \tag{2.37}$$

and

$$\boldsymbol{\nabla}\times\boldsymbol{A}(\boldsymbol{r},t) = -\hat{\boldsymbol{\phi}}\frac{\partial}{\partial\rho} A_z(\boldsymbol{r},t) \ , \tag{2.38}$$

as well as

$$\boldsymbol{\nabla} A_z(\boldsymbol{r},t) = \left[\hat{\boldsymbol{\rho}}\frac{\partial}{\partial\rho} + \hat{\mathbf{z}}\frac{\partial}{\partial z}\right] A_z(\boldsymbol{r},t)\ . \tag{2.39}$$

We find from our Ansatz, Eq.(2.13), an explicit expression for the z-derivative

$$\frac{\partial}{\partial z}A_z(\boldsymbol{r},\omega) = -i\frac{\omega}{v}A_z(\boldsymbol{r},\omega)\ . \tag{2.40}$$

In order to evaluate the ρ-derivative, we consider the large ρ limit and express Eq.(2.36) explicitly in terms of ρ, using Eq.(2.35). The derivative contains a term proportional to $\rho^{-3/2}$, which we neglect, leaving

$$\frac{\partial}{\partial\rho}A_z(\boldsymbol{r},\omega) = -isA_z(\boldsymbol{r},\omega)\ , \quad \rho \gg 1\ . \tag{2.41}$$

We can find the electric field by Eq.(2.3) if we have an expression for the scalar potential. Eq.(2.37) allows us to express the Lorenz gauge condition, Eq.(2.4), as

$$\frac{\partial}{\partial t}V(\boldsymbol{r},t) = -\frac{c^2}{n^2}\frac{\partial}{\partial z}A_z(\boldsymbol{r},t)\ . \tag{2.42}$$

Inserting the Fourier transforms with respect to time in this equation, and applying Eq.(2.40), we find an expression for the scalar potential

$$V(\boldsymbol{r},\omega) = \frac{c^2}{n^2 v}A_z(\boldsymbol{r},\omega)\ , \tag{2.43}$$

and consequently

$$V(\boldsymbol{r},t) = \frac{c^2}{n^2 v}A_z(\boldsymbol{r},t)\ . \tag{2.44}$$

To find the electric field, we insert this expression in our definition of the scalar potential, Eq.(2.3)

$$\begin{aligned}\boldsymbol{E}(\boldsymbol{r},t) &= -\frac{c^2}{n^2 v}\boldsymbol{\nabla}A_z(\boldsymbol{r},t) - \hat{\mathbf{z}}\frac{\partial}{\partial t}A_z(\boldsymbol{r},t)\\ &= -\left[\hat{\boldsymbol{\rho}}\frac{c^2}{n^2 v}\frac{\partial}{\partial\rho} + \hat{\mathbf{z}}\left(\frac{c^2}{n^2 v}\frac{\partial}{\partial z} + \frac{\partial}{\partial t}\right)\right]A_z(\boldsymbol{r},t)\ .\end{aligned} \tag{2.45}$$

Here we have expressed the gradient by Eq.(2.39). We evaluate the operator within brackets by writing $A_z(\boldsymbol{r},t)$ in terms of its Fourier transform, according to Eq.(2.34). Applying Eq.(2.40) and Eq.(2.41), the operator then produces a factor

$$\hat{\boldsymbol{\rho}}\frac{c^2}{n^2 v}is + \hat{\mathbf{z}}\left(i\omega\frac{c^2}{n^2 v^2} - i\omega\right) = i\omega\sin\theta_C[\hat{\boldsymbol{\rho}}\cos\theta_C - \hat{\mathbf{z}}\sin\theta_C]\ , \tag{2.46}$$

where the right-hand side follows from the definitions of θ_C, Eq.(2.8), and s, Eq.(2.25). Note that this result is only valid in the large ρ limit, as we evaluated the ρ-derivative by Eq.(2.41).

Writing Eq.(2.45) out in full, we have

$$\boldsymbol{E}(\boldsymbol{r},t) = [\hat{\boldsymbol{\rho}}\cos\theta_C - \hat{\mathbf{z}}\sin\theta_C]\sin\theta_C 2\mathrm{Re}\left\{\int_0^\infty \frac{\mathrm{d}\omega}{2\pi} i\omega e^{i\omega t} A_z(\boldsymbol{r},\omega)\right\} \ , \ \rho \gg 1 \ . \tag{2.47}$$

We find the magnetic field in an equivalent manner. The curl of $\boldsymbol{A}(\boldsymbol{r},t)$ is given by Eq.(2.38) and Eq.(2.41). Thus Eq.(2.2) becomes

$$\boldsymbol{B}(\boldsymbol{r},t) = \hat{\boldsymbol{\phi}}\sin\theta_C \frac{n}{c} 2\mathrm{Re}\left\{\int_0^\infty \frac{\mathrm{d}\omega}{2\pi} i\omega e^{i\omega t} A_z(\boldsymbol{r},\omega)\right\} \ , \quad \rho \gg 1 \ . \tag{2.48}$$

Here we have also inserted the definition of s, Eq.(2.25).

We then insert our expression for $A_z(\boldsymbol{r},\omega)$, Eq.(2.36), in the above equations, and take the real part, to arrive at our final expressions for the physical fields in the large ρ limit

$$\boldsymbol{E}(\boldsymbol{r},t) = \frac{\boldsymbol{E}_0(\boldsymbol{r})}{\sqrt{\rho}} \int_0^\infty \frac{\mathrm{d}\omega}{2\pi}\sqrt{\omega}\cos\left(\omega t - \boldsymbol{k}\cdot\boldsymbol{r} + \frac{\pi}{4}\right) \ , \quad \rho \gg 1 \ , \tag{2.49}$$

and

$$\boldsymbol{B}(\boldsymbol{r},t) = \frac{\boldsymbol{B}_0(\boldsymbol{r})}{\sqrt{\rho}} \int_0^\infty \frac{\mathrm{d}\omega}{2\pi}\sqrt{\omega}\cos\left(\omega t - \boldsymbol{k}\cdot\boldsymbol{r} + \frac{\pi}{4}\right) \ , \quad \rho \gg 1 \ . \tag{2.50}$$

Here we have defined

$$\boldsymbol{E}_0(\boldsymbol{r}) \equiv [\hat{\boldsymbol{\rho}}\cos\theta_C - \hat{\mathbf{z}}\sin\theta_C]\mu_0 q\sqrt{\frac{c\sin\theta_C}{2\pi n}} \ , \tag{2.51}$$

$$\boldsymbol{B}_0(\boldsymbol{r}) \equiv \hat{\boldsymbol{\phi}}\mu_0 q\sqrt{\frac{n\sin\theta_C}{2\pi c}} \ . \tag{2.52}$$

We may now examine the radiation these fields carry by calculating the associated power spectrum.

Classical Power Spectrum

We wish to express the power radiated by the charge, and to that end we calculate the Poynting vector [12, p. 362]

$$\begin{aligned}\boldsymbol{S}(\boldsymbol{r},t) &= \frac{1}{\mu_0}\boldsymbol{E}(\boldsymbol{r},t)\times\boldsymbol{B}(\boldsymbol{r},t) \\ &= \hat{\boldsymbol{k}}\frac{\mu_0 q^2\sin\theta_C}{2\pi\rho}\left(\int_0^\infty \frac{\mathrm{d}\omega}{2\pi}\sqrt{\omega}\cos\left(\omega t - \boldsymbol{k}\cdot\boldsymbol{r} + \frac{\pi}{4}\right)\right)^2 \ , \quad \rho \gg 1 \ .\end{aligned} \tag{2.53}$$

We can use this expression to calculate the rate at which the charge emits energy.

We construct a surface in the shape of a cylinder around the path of the charge, such that the charge travels through the cylinder lengthwise in a span of time T (see Figure 2.3). Let the radius of the cylinder be denoted by ρ. The

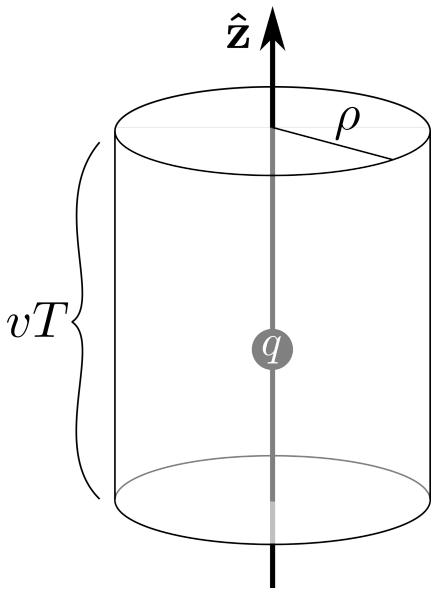

FIGURE 2.3: The charge q enclosed in a cylinder with radius ρ and length vT.

total energy, E_T, radiated through the surface of this cylinder in the time T is

$$E_T = \int_0^{2\pi} \mathrm{d}\phi\rho \int_{-vT/2}^{vT/2} \mathrm{d}z \int_{-T/2}^{T/2} \mathrm{d}t \hat{\boldsymbol{\rho}} \cdot \boldsymbol{S}(\boldsymbol{r}, t) \; . \tag{2.54}$$

Here we have neglected the contributions from the ends of the cylinder, as these become insignificant for sufficiently large T. The time dependence in Eq.(2.53) is contained in a product of cosines, which may be written as

$$\frac{1}{2}\cos\big((\omega+\omega')t - (\boldsymbol{k}+\boldsymbol{k}')\cdot\boldsymbol{r} + \pi/2\big) + \frac{1}{2}\cos\big((\omega-\omega')t - (\boldsymbol{k}-\boldsymbol{k}')\cdot\boldsymbol{r}\big) \; . \tag{2.55}$$

Here ω and ω' denote the variables of the two independent integrals in Eq.(2.53). Integrating this expression over time, the first term may be neglected as it oscillates with the frequency $(\omega+\omega')$. However, the second term makes a non-negligible contribution when $\omega \approx \omega'$. In the large T limit, the integral of the second term with respect to time approaches a delta function $\pi\delta(\omega-\omega')$.

Thus, integrating over time, then over ω', we may write

$$E_T = \frac{\mu_0 q^2 \sin\theta_C}{2\pi} \int_0^{2\pi} \mathrm{d}\phi \int_{-vT/2}^{vT/2} \mathrm{d}z \hat{\boldsymbol{\rho}} \cdot \hat{\mathbf{k}} \int_0^{\infty} \frac{\mathrm{d}\omega}{4\pi}\omega \; . \tag{2.56}$$

Noting that $\hat{\boldsymbol{\rho}} \cdot \hat{\mathbf{k}} = \sin\theta_C$, which is independent of ϕ and z, the energy emitted by the charge becomes simply

$$E_T = \frac{\mu_0 q^2}{4\pi} vT \sin^2\theta_C \int_0^{\omega_c} \mathrm{d}\omega\omega \; . \tag{2.57}$$

Here we have introduced a cut-off frequency ω_c to handle the divergent integral. The emitted power is quadratically divergent $\sim \omega_c^2$. This result is clearly

unphysical, as conservation of energy dictates the charge may not radiate an infinite amount of energy. In the classical theory, we deal with this by letting the index of refraction, and thereby the speed of light in the medium, depend on frequency, $n(\omega)$. This imposes a physical cut-off on the ω-integral. As previously discussed, the charge only radiates when moving at speeds greater than the speed of light in the medium, so the integral is only taken over those frequencies for which $n(\omega) \geq c/v$. Introducing a frequency dependence in the coefficient of refraction requires us to reconsider the previous calculations from the beginning (see for instance Ref. [10]). Such matters are outside the scope of this text, however, and we merely consider some finite cut-off frequency. A reasonable cut-off is the characteristic frequency of an electrically bound electron. At frequencies beyond this point, materials no longer exhibit dielectric properties [13]. The characteristic frequency varies between materials, but we may set as an approximate value $\omega_C = 10^{16}\,\mathrm{rad\,s^{-1}}$.

In spite of the above problem it is still worthwhile to consider the power spectrum of the radiation, $P(\omega)$. That is to say the energy emitted per unit time in the frequency interval from ω to $\omega + \mathrm{d}\omega$. Differentiating Eq.(2.57) with respect to T and ω, we find

$$P(\omega) = \frac{\mu_0 q^2}{4\pi}\omega v\left(1 - \frac{c^2}{n^2 v^2}\right) . \tag{2.58}$$

Here we have written $\sin^2\theta_C$ explicitly by Eq.(2.8). We may assume this power spectrum to be accurate in frequency ranges where the index of refraction can be considered constant.

2.2 Quantum Mechanics

We shall now consider the process of Cherenkov radiation to first order in perturbation theory. In spite of the large velocities involved, we shall first apply non-relativistic quantum mechanics to the problem. In addition to letting us compare the non-relativistic quantum mechanical results to those of the relativistic classical theory this section also serves to introduce concepts to be employed within relativistic quantum mechanics in subsequent sections.

We wish to calculate the rate of transition from a state of one free charged particle, to a state of one free charged particle plus one photon. In order to do this, we must quantize the electromagnetic field in the medium.

The Electromagnetic Field

Quantization of the macroscopic electromagnetic field in a linear, isotropic dielectric, with frequency independent permittivity ϵ, proceeds according to the standard second-quantization procedure for the electromagnetic field in vacuum (see, e.g., Ref. [14]). The method is only modified by substituting the permittivity of the medium for that of the vacuum: $\epsilon_0 \to \epsilon_0\epsilon = \epsilon_0 n^2$. We set the frame

to be the rest frame of the medium, and impose the Coulomb gauge

$$\boldsymbol{\nabla} \cdot \boldsymbol{A}(\boldsymbol{r}, t) = 0 \,, \tag{2.59}$$

and set the scalar potential in the absence of sources to zero

$$V(\boldsymbol{r}, t) = 0 \,. \tag{2.60}$$

The Coulomb gauge requires that plane waves in the field are transversely polarized $\boldsymbol{k} \cdot \boldsymbol{A}(\boldsymbol{r}, t) = 0$. With this in mind, we define a pair of linear polarization vectors $\boldsymbol{\epsilon}_{\boldsymbol{k}1}$, $\boldsymbol{\epsilon}_{\boldsymbol{k}2}$, for each wave vector $\boldsymbol{k}$ such that they form a right-handed basis with $\hat{\mathbf{k}}$

$$\begin{aligned} \boldsymbol{k} \cdot \boldsymbol{\epsilon}_{\boldsymbol{k}\lambda} &= 0 \,, \\ \boldsymbol{\epsilon}_{\boldsymbol{k}\lambda} \cdot \boldsymbol{\epsilon}_{\boldsymbol{k}\lambda'} &= \delta_{\lambda\lambda'} \,, \\ \boldsymbol{\epsilon}_{\boldsymbol{k}1} \times \boldsymbol{\epsilon}_{\boldsymbol{k}2} &= \hat{\mathbf{k}} \,. \end{aligned} \tag{2.61}$$

Moreover, we choose specific polarization vectors such that $\boldsymbol{\epsilon}_{\boldsymbol{k}1}$ lies in the scattering plane defined by $\boldsymbol{p}$ and $\boldsymbol{k}$, and $\boldsymbol{\epsilon}_{\boldsymbol{k}2}$ is perpendicular to this plane (see Figure 2.4). Defining θ to be the angle between the wave vector of the photon

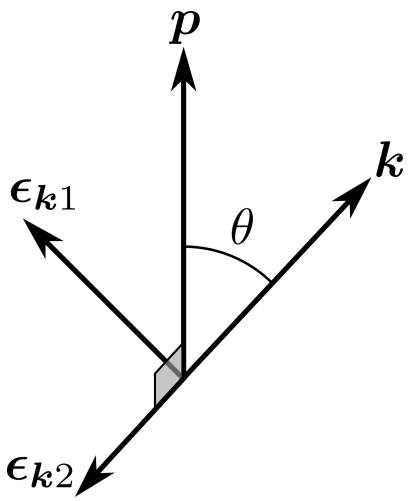

FIGURE 2.4: The linear polarization vectors, $\boldsymbol{\epsilon}_{\boldsymbol{k}1}$ and $\boldsymbol{\epsilon}_{\boldsymbol{k}2}$, form a right-handed basis with $\hat{\boldsymbol{k}}$. $\boldsymbol{\epsilon}_{\boldsymbol{k}1}$ lies in the plane spanned by $\boldsymbol{p}$ and $\boldsymbol{k}$, and $\boldsymbol{\epsilon}_{\boldsymbol{k}2}$ is perpendicular to this plane.

and the incoming particle's momentum, we may then write

$$\boldsymbol{p} \cdot \boldsymbol{\epsilon}_{\boldsymbol{k}\lambda} = \delta_{\lambda 1} p \sin\theta \,, \tag{2.62}$$

with $p = |\boldsymbol{p}|$.

The polarization of light may more generally be described in terms of elliptical polarization vectors. We define these as a linear combination of our previously defined linear polarization vectors

$$\boldsymbol{\epsilon}_{\boldsymbol{k}\alpha+} = \boldsymbol{\epsilon}_{\boldsymbol{k}1} \cos\alpha + i\boldsymbol{\epsilon}_{\boldsymbol{k}2} \sin\alpha \,, \tag{2.63}$$

and

$$\boldsymbol{\epsilon}_{\boldsymbol{k}\alpha-} = \boldsymbol{\epsilon}_{\boldsymbol{k}2}\cos\alpha + i\boldsymbol{\epsilon}_{\boldsymbol{k}1}\sin\alpha \ . \tag{2.64}$$

Here α is a parameter running from 0 to $\pi/2$. For the special case of $\alpha = \pi/4$ these elliptical polarization vectors describe circularly polarized light. The $\boldsymbol{\epsilon}_{\boldsymbol{k}+}$-vector then corresponds to right-handed light (helicity 1), and the $\boldsymbol{\epsilon}_{\boldsymbol{k}-}$-vector corresponds to left-handed light (helicity -1). In analogy to the case of circular polarization, we will refer to photons described by $\boldsymbol{\epsilon}_{\boldsymbol{k}\alpha+}$ as elliptically right-handed, and photons described by $\boldsymbol{\epsilon}_{\boldsymbol{k}\alpha-}$ as elliptically left-handed.

The free electromagnetic field, quantized in a cubical volume of side lengths L and volume $L^3 = V$ with periodic boundary conditions, can then be expressed as

$$\boldsymbol{A}(\boldsymbol{r},t) = \sum_{\boldsymbol{k}\lambda} A_{\boldsymbol{k}}\left[\boldsymbol{\epsilon}_{\boldsymbol{k}\lambda}a_{\boldsymbol{k}\lambda}e^{-i(\omega_{\boldsymbol{k}}t-\boldsymbol{k}\cdot\boldsymbol{r})} + \boldsymbol{\epsilon}^*_{\boldsymbol{k}\lambda}a^\dagger_{\boldsymbol{k}\lambda}e^{i(\omega_{\boldsymbol{k}}t-\boldsymbol{k}\cdot\boldsymbol{r})}\right] \ , \tag{2.65}$$

with

$$A_{\boldsymbol{k}} = \sqrt{\frac{\hbar}{2V\epsilon_0 n^2\omega_{\boldsymbol{k}}}} \ . \tag{2.66}$$

Here $a^\dagger_{\boldsymbol{k}\lambda}$ and $a_{\boldsymbol{k}\lambda}$ denote respectively creation and annihilation operators for each mode, and the time dependence is given in the Heisenberg picture. Note that the dispersion relation in the medium remains the same as in the classical theory, Eq.(2.7). The Hamiltonian is time-independent

$$H_\gamma = \sum_{\boldsymbol{k}\lambda}\hbar\omega_{\boldsymbol{k}}\left(a^\dagger_{\boldsymbol{k}\lambda}a_{\boldsymbol{k}\lambda} + \frac{1}{2}\right) \ . \tag{2.67}$$

Thus we may construct number eigenstates for the field as in the vacuum. We define a state containing n photons in the mode $\boldsymbol{k}\lambda$ by

$$a^\dagger_{\boldsymbol{k}'\lambda'}a_{\boldsymbol{k}'\lambda'}\left|n_{\boldsymbol{k}\lambda}\right\rangle = \delta_{\boldsymbol{k}'\boldsymbol{k}}\delta_{\lambda'\lambda}n_{\boldsymbol{k}\lambda}\left|n_{\boldsymbol{k}\lambda}\right\rangle \ . \tag{2.68}$$

Note that the states are orthogonal and normalized

$$\langle n_{\boldsymbol{k}'\lambda'}|n_{\boldsymbol{k}\lambda}\rangle = \delta_{\boldsymbol{k}'\boldsymbol{k}}\delta_{\lambda'\lambda} \ . \tag{2.69}$$

For simplicity, we denote one-photon states by $|\boldsymbol{k}\lambda\rangle$, and the vacuum state by $|0\rangle$.

The Charged Particle

We also need to introduce a charged particle to our system. The non-relativistic Hamiltonian of a free particle of mass m is

$$H_p = \frac{\boldsymbol{p}^2}{2m} \ . \tag{2.70}$$

Here $\boldsymbol{p}$ denotes the momentum operator. Eigenstates of momentum $|\psi_{\boldsymbol{p}}\rangle$ are thus also eigenstates of the Hamiltonian. In the position representation, where

$\boldsymbol{p} = -i\hbar\boldsymbol{\nabla}$, we may express these states as wave functions

$$\psi_{\boldsymbol{p}}(\boldsymbol{r}) = \frac{1}{\sqrt{V}} e^{i\boldsymbol{p}\cdot\boldsymbol{r}/\hbar} \,. \tag{2.71}$$

The constant $1/\sqrt{V}$ is chosen such that the wave functions are normalized to one in our quantization volume from before. The states are also orthogonal: $\langle\psi_{\boldsymbol{p}'}|\psi_{\boldsymbol{p}}\rangle = \delta_{\boldsymbol{p}'\boldsymbol{p}}$.

We now have an exactly solvable time-independent Hamiltonian for a system consisting of the free electric field and a free massive particle

$$H_0 = H_\gamma + H_p \,. \tag{2.72}$$

Eigenstates of this Hamiltonian may be written $|\psi_{\boldsymbol{p}}\rangle\,|n_{\boldsymbol{k}\lambda}\rangle$. In order to evaluate the transition rate of the process $|\psi_{\boldsymbol{p}}\rangle\,|0\rangle \to |\psi_{\boldsymbol{p}'}\rangle\,|\boldsymbol{k}\lambda\rangle$ we need to couple our particle to the electromagnetic field. Following the minimal coupling prescription [15, p. 78], we introduce a charge q to the particle by letting $\boldsymbol{p} \to \boldsymbol{p} - q\boldsymbol{A}$. The particle's Hamiltonian becomes

$$H_p \to \frac{\boldsymbol{p}^2}{2m} - \frac{q\boldsymbol{A}(\boldsymbol{r})\cdot\boldsymbol{p}}{m} + \mathcal{O}(\boldsymbol{A}^2(\boldsymbol{r})) \,. \tag{2.73}$$

Note that $\boldsymbol{p}\cdot\boldsymbol{A}\,|\psi\rangle = \boldsymbol{A}\cdot\boldsymbol{p}\,|\psi\rangle$, due to the Coulomb gauge condition $\boldsymbol{\nabla}\cdot\boldsymbol{A} = 0$. We have suppressed the time-dependence in $\boldsymbol{A}(\boldsymbol{r},t)$ by taking the initial time $t = 0$, and handling time evolution in the interaction picture. Neglecting the two-photon term $\mathcal{O}(\boldsymbol{A}^2(\boldsymbol{r}))$, we have the total Hamiltonian of our system, which may be viewed as a perturbation of the uncoupled Hamiltonian Eq.(2.72)

$$H = H_0 + H' \,, \tag{2.74}$$

where

$$\begin{aligned} H' &= -\frac{q\boldsymbol{A}(\boldsymbol{r})\cdot\boldsymbol{p}}{m} \\ &= -\frac{q}{m}\sum_{\boldsymbol{k}\lambda} A_{\boldsymbol{k}} \left[\boldsymbol{\epsilon}_{\boldsymbol{k}\lambda} a_{\boldsymbol{k}\lambda} e^{i\boldsymbol{k}\cdot\boldsymbol{r}} + \boldsymbol{\epsilon}^*_{\boldsymbol{k}\lambda} a^\dagger_{\boldsymbol{k}\lambda} e^{-i\boldsymbol{k}\cdot\boldsymbol{r}}\right]\cdot\boldsymbol{p} \,. \end{aligned} \tag{2.75}$$

We now have all the necessary elements to find the radiated power to first order in perturbation theory. With the Born approximation, we have the transition rate

$$\omega_R = \frac{2\pi}{\hbar}|\mathcal{M}_\lambda|^2\delta(E_f - E_i) \,. \tag{2.76}$$

Here E_f and E_i denote the energy of the final and initial states respectively, given by the unperturbed Hamiltonian, Eq.(2.72). $\mathcal{M}_\lambda$ represents the transition

amplitude $\langle \boldsymbol{k}\lambda| \langle \psi_{\boldsymbol{p}'}| H' |\psi_{\boldsymbol{p}}\rangle |0\rangle$. Evaluating the amplitude is a simple matter

$$\begin{aligned}\mathcal{M}_\lambda &= -\frac{q}{m} \langle \boldsymbol{k}\lambda| \langle \psi_{\boldsymbol{p}'}| \boldsymbol{A}(\boldsymbol{r}) \cdot \boldsymbol{p} |\psi_{\boldsymbol{p}}\rangle |0\rangle \\ &= -\frac{q}{m} \sum_{\boldsymbol{k}'\lambda'} A_{\boldsymbol{k}'} \langle \boldsymbol{k}\lambda| \langle \psi_{\boldsymbol{p}'}| e^{-i\boldsymbol{k}'\cdot\boldsymbol{r}} \boldsymbol{\epsilon}^*_{\boldsymbol{k}'\lambda'} \cdot \boldsymbol{p} |\psi_{\boldsymbol{p}}\rangle |\boldsymbol{k}'\lambda'\rangle \\ &= -\frac{q}{m} A_{\boldsymbol{k}} \boldsymbol{\epsilon}^*_{\boldsymbol{k}\lambda} \cdot \boldsymbol{p} \delta_{\boldsymbol{p}'+\hbar\boldsymbol{k},\boldsymbol{p}} \ . \end{aligned} \tag{2.77}$$

Here we have used the orthonormality relation of the number states, Eq.(2.69). The momentum-conserving Kronecker delta follows from evaluating the inner-product $\langle \psi_{\boldsymbol{p}'}| e^{-i\boldsymbol{k}\cdot\boldsymbol{r}} |\psi_{\boldsymbol{p}}\rangle$ explicitly in the position representation, Eq.(2.71).

Kinematics

Conservation of momentum allows us to write, with the non-relativistic definition of momentum $\boldsymbol{p} = m\boldsymbol{v}$,

$$\begin{aligned}E_f - E_i &= \frac{[\boldsymbol{p} - \hbar\boldsymbol{k}]^2}{2m} + \hbar\omega_{\boldsymbol{k}} - \frac{p^2}{2m} = \frac{\hbar^2 k^2}{2m} - \hbar k v \cos\theta + \hbar\omega_{\boldsymbol{k}} \\ &= \frac{\hbar\omega_{\boldsymbol{k}} n v}{c} \left(\frac{\hbar\omega_{\boldsymbol{k}} n}{2mvc} + \frac{c}{nv} - \cos\theta \right) \ . \end{aligned} \tag{2.78}$$

Here we have applied the dispersion relation Eq.(2.7) to eliminate k. With this we may write the delta function in Eq.(2.76) as

$$\delta(E_f - E_i) = \frac{c}{\hbar\omega_{\boldsymbol{k}} n v} \delta(\cos\theta - \cos\theta_C) \ . \tag{2.79}$$

Here we have defined

$$\cos\theta_C \equiv \frac{c}{nv} \left(1 + \frac{\hbar\omega_{\boldsymbol{k}} n^2}{2mc^2} \right) \simeq \frac{c}{nv} \ . \tag{2.80}$$

First-order perturbation theory is only valid in the limit $\hbar\omega_{\boldsymbol{k}} \ll mc^2$. Taking this limit, we find that the angle θ_C matches the Cherenkov angle as defined by Eq.(2.8) in the classical theory. Thus we see that the quantum mechanical theory affirms the classical expression of the Cherenkov angle, by demonstrating that the process $|\psi_{\boldsymbol{p}}\rangle |0\rangle \to |\psi_{\boldsymbol{p}'}\rangle |\boldsymbol{k}\lambda\rangle$ respects conservation of energy and momentum only if the photon is emitted at the angle θ_C defined by Eq.(2.80).

Inserting Eq.(2.79) in Eq.(2.76), we write the transition rate as

$$\omega_R = \frac{2\pi}{\hbar^2\omega_{\boldsymbol{k}}} \frac{c}{nv} |\mathcal{M}_\lambda|^2 \delta(\cos\theta - \cos\theta_C) \ . \tag{2.81}$$

Having found an expression for the transition rate, we are now equipped to calculate the power spectrum of the radiation.

Quantum Mechanical Power Spectrum

We may consider the total transition rate for the process by summing over the phase space of the final state. We only sum over the momentum and polarization states of the emitted photon, as the momentum of the charged particle is set to $\boldsymbol{p}' = \boldsymbol{p} - \hbar\boldsymbol{k}$ by momentum conservation

$$R \equiv \sum_{\boldsymbol{k}\lambda} \omega_R \, . \tag{2.82}$$

The total radiated power is found by multiplying the transition rate for each mode by its energy $\hbar\omega_{\boldsymbol{k}}$

$$P \equiv \sum_{\boldsymbol{k}\lambda} \omega_R \hbar\omega_{\boldsymbol{k}} \, . \tag{2.83}$$

We are interested in the limit of a continuous spectrum, i.e., the case where our quantization volume is infinitely large. Letting $V \to \infty$, the sum over wave modes approaches an integral in $\boldsymbol{k}$-space $\sum_{\boldsymbol{k}\lambda} \to V/(2\pi)^3 \int \mathrm{d}k k^2 \int \mathrm{d}\Omega$, where $\mathrm{d}\Omega$ denotes the solid angle $\mathrm{d}\Omega = \sin\theta \, \mathrm{d}\theta \, \mathrm{d}\phi$. In analogy to the classical theory we have here defined ϕ as the angle of rotation about $\boldsymbol{p}$. The prefactor is a consequence of moving from a discrete sum to a continuous integral, as the periodic boundary conditions permit $V/(2\pi)^3$ distinct wave modes within a unit volume in $\boldsymbol{k}$-space. Thus the power spectrum, $P(\omega_{\boldsymbol{k}})$, is given by the relation

$$P = \int \mathrm{d}\omega_{\boldsymbol{k}} P(\omega_{\boldsymbol{k}}) = \frac{V}{(2\pi)^3} \int \mathrm{d}k k^2 \int \mathrm{d}\Omega \sum_{\lambda} \omega_R \hbar\omega_{\boldsymbol{k}} \, . \tag{2.84}$$

Differentiating this equation with regard to $\omega_{\boldsymbol{k}}$, we have

$$\begin{aligned} P(\omega_{\boldsymbol{k}}) &= \hbar \frac{V}{(2\pi)^3} \frac{\mathrm{d}k}{\mathrm{d}\omega_{\boldsymbol{k}}} k^2 \omega_{\boldsymbol{k}} \int \mathrm{d}\Omega \sum_{\lambda} \omega_R \\ &= \hbar \frac{V}{(2\pi)^3} \left(\frac{\omega_{\boldsymbol{k}} n}{c}\right)^3 \int \mathrm{d}\Omega \sum_{\lambda} \omega_R \, , \end{aligned} \tag{2.85}$$

where we have used the dispersion relation, Eq.(2.7) to eliminate k. Note that these steps may be carried out identically with regard to the transition rate, Eq.(2.82), allowing us to similarly define a transition rate spectrum

$$R(\omega_{\boldsymbol{k}}) \equiv \frac{P(\omega_{\boldsymbol{k}})}{\hbar\omega_{\boldsymbol{k}}} \, . \tag{2.86}$$

To find the power spectrum, we need to evaluate the integral over the solid angle $\mathrm{d}\Omega$. The dependence of the transition rate ω_R on the solid angle is contained in the transition amplitude and the delta function. Due to the presence of the delta function, the $\mathrm{d}\theta$-integral serves to impose energy conservation on the amplitude by setting $\theta = \theta_C$, $E' = E - \hbar\omega_{\boldsymbol{k}}$. We define a new notation for

amplitudes with conservation of energy imposed, $\mathcal{M} \to \mathcal{S}$, and write

$$|\mathcal{S}_\lambda|^2 \equiv \int_0^\pi \mathrm{d}\theta \sin\theta |\mathcal{M}_\lambda|^2 \delta(\cos\theta - \cos\theta_C) = \left(\frac{qA_{\boldsymbol{k}}}{m}\right)^2 |\boldsymbol{\epsilon}_{\boldsymbol{k}\lambda} \cdot \boldsymbol{p}|^2 \tag{2.87}$$

We complete the solid angle integral by noting that the integral over ϕ trivially contributes a factor 2π.

Inserting Eq.(2.81) for the transition rate in Eq.(2.85), we write the power spectrum as

$$P(\omega_{\boldsymbol{k}}) = \frac{V}{2\pi\hbar}\left(\frac{\omega_{\boldsymbol{k}} n}{c}\right)^2 \frac{1}{v} \sum_\lambda |\mathcal{S}_\lambda|^2 \,. \tag{2.88}$$

The dependence of the transition amplitude on polarization is contained in the factor $|\boldsymbol{\epsilon}_{\boldsymbol{k}\lambda} \cdot \boldsymbol{p}|^2$, and we have

$$\sum_\lambda |\boldsymbol{\epsilon}_{\boldsymbol{k}\lambda} \cdot \boldsymbol{p}|^2 = p^2 \sin^2\theta_C \,, \tag{2.89}$$

as is easily seen due to the present choice of basis by Eq.(2.62). This choice of basis also makes the polarization of emitted light apparent. The power is emitted solely in the mode described by $\boldsymbol{\epsilon}_{\boldsymbol{k}1}$.

Inserting the classical momentum $\boldsymbol{p} = m\boldsymbol{v}$, and the Cherenkov angle by $\cos\theta_C = c/nv$, we find our final expression for the power spectrum

$$P(\omega_{\boldsymbol{k}}) = \frac{\mu_0 q^2}{4\pi} \omega_{\boldsymbol{k}} v \left(1 - \frac{c^2}{n^2 v^2}\right) \,. \tag{2.90}$$

Writing out $A_{\boldsymbol{k}}$ in the prefactor by Eq.(2.66), the dependence on our quantization volume, V, cancels as it should. Here we have also applied the relation $\epsilon_0 c^2 = 1/\mu_0$. This result is in exact agreement with the classical power spectrum, Eq.(2.58). It is quite remarkable that the non-relativistic theory of quantum mechanics reproduces the relativistic result derived in the classical theory. What is more, integrating the power spectrum over $\omega_{\boldsymbol{k}}$ to find the total emitted power, the quantum mechanical theory imposes a natural cut-off on the frequency due to the energy-conserving delta function present in the transition rate, Eq.(2.81). The energy of the photon, $\hbar\omega_{\boldsymbol{k}}$, can not be greater than the kinetic energy of the particle which emits it. In other words, the quantum mechanical theory allows us to evaluate the emitted power without introducing a frequency dependence in n. Using the non-relativistic kinetic energy, $E = mv^2/2$, we integrate the power spectrum to find the total emitted power

$$P = \frac{\mu_0 q^2}{4\pi} \frac{m^2 v^5}{8\hbar^2} \left(1 - \frac{c^2}{n^2 v^2}\right) \,. \tag{2.91}$$

Finally, we note that although the emitted power goes to zero as $\omega_{\boldsymbol{k}} \to 0$, the spectrum of the transition rate $R(\omega_{\boldsymbol{k}})$ is in fact independent of $\omega_{\boldsymbol{k}}$

$$R(\omega_{\boldsymbol{k}}) = \frac{\mu_0 q^2}{4\pi\hbar} v \left(1 - \frac{c^2}{n^2 v^2}\right) . \tag{2.92}$$

Equipment sensitive to a low-frequency radiation band should therefore detect the same number of photons as equipment sensitive to a high-frequency radiation band of equal width.

2.3 Relativistic Quantum Mechanics

By its nature, Cherenkov radiation involves massive and charged particles moving at a significant fraction of the speed of light. One should therefore expect the non-relativistic approximation to be inaccurate to a significant degree. With this motivation, we shall now calculate the Cherenkov effect to first order in perturbation theory, in relativistic quantum mechanics.

Dirac Hamiltonian and Spinors

The quantized electromagnetic field remains as in the non-relativistic theory, Eq.(2.65). For the massive particle, however, we must define a relativistic free Hamiltonian and corresponding eigenstates. We shall restrict the following calculations by assuming the charged particle to be a Dirac fermion. Doing so introduces spinors to the model (see Appendix F). We wish to examine how the transition rate depends on the orientation of these spinors, and to that end we solve the Dirac equation in an independent coordinate system defined by basis vectors $\hat{\mathbf{e}}_1$, $\hat{\mathbf{e}}_2$, and $\hat{\mathbf{e}}_3$. This allows us to alter the orientation of the spinors by simply rotating this coordinate system. Specifically, we parametrize the orientation of spinors by spherical coordinates ϕ and χ. As shown in Figure 2.5, we define ϕ in the manner of an azimuthal angle by projecting $\hat{\mathbf{e}}_3$ and $\boldsymbol{k}$ onto a plane perpendicular to $\boldsymbol{p}$ and setting ϕ to be the angle between these projections. We define χ as the polar angle between $\boldsymbol{p}$ and $\hat{\mathbf{e}}_3$.

Having defined the coordinate system, we now introduce the Dirac Hamiltonian

$$H_D = \left(c\boldsymbol{\alpha} \cdot \boldsymbol{p} + \beta m c^2\right) . \tag{2.93}$$

The corresponding eigenstates $|\psi_{\boldsymbol{p},s}\rangle$ may be expressed in the position representation as

$$\psi_{\boldsymbol{p},s}(\boldsymbol{r}) = \frac{1}{\sqrt{V}} u(\boldsymbol{p}, s) e^{i\boldsymbol{p}\cdot\boldsymbol{r}/\hbar} . \tag{2.94}$$

Here $u(\boldsymbol{p}, s)$ denotes a spinor, and the factor $1/\sqrt{V}$ ensures the wave function is normalized to one in our quantization volume.

Evaluating the process of Cherenkov radiation proceeds analogously to the non-relativistic theory. We introduce the free Hamiltonian

$$H_0 = H_\gamma + H_D , \tag{2.95}$$

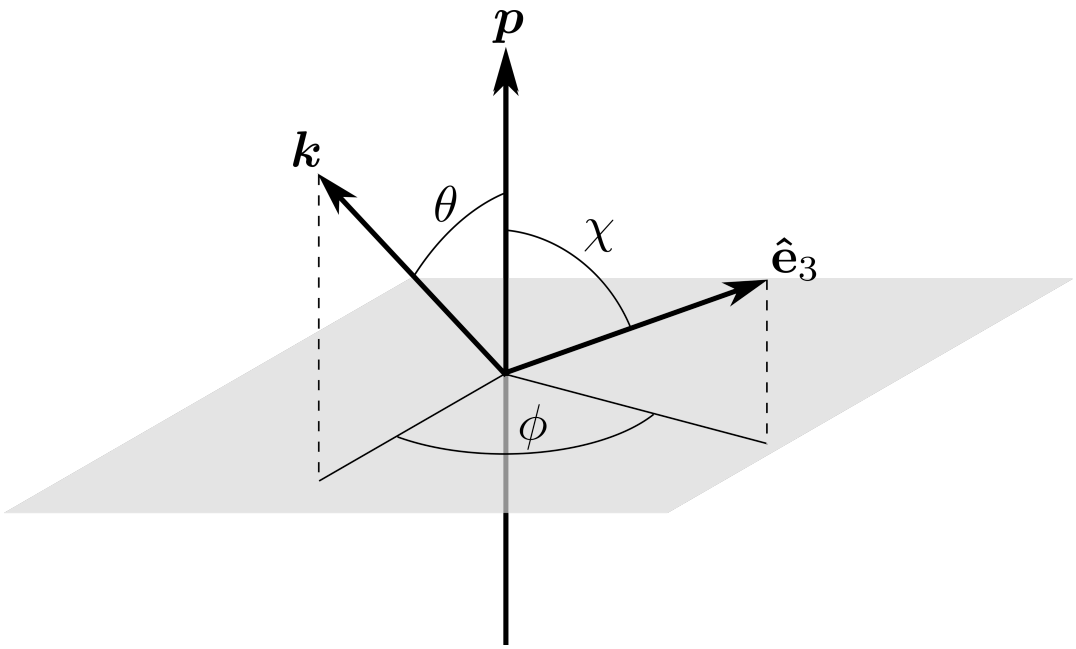

FIGURE 2.5: The orientation of the spin quantization axis, $\hat{\mathbf{e}}_3$, as it relates to particle and photon momenta. The orientation is parametrized by spherical coordinates ϕ and χ. The orientation of the remaining two axes, $\hat{\mathbf{e}}_1$ and $\hat{\mathbf{e}}_2$, is arbitrary.

where H_γ is defined as in Eq.(2.67). The time-independent eigenstates of H_0 are again denoted $|\psi_{\boldsymbol{p},s}\rangle\,|\boldsymbol{k}\lambda\rangle$, where $|\boldsymbol{k}\lambda\rangle$ is defined as in the non-relativistic theory, by Eq.(2.68). Having defined the uncoupled system, we couple the particle to the electromagnetic field by the minimal coupling prescription $\boldsymbol{p} \to \boldsymbol{p} - q\boldsymbol{A}$

$$H_D \to c\boldsymbol{\alpha}\cdot\boldsymbol{p} + \beta mc^2 - cq\boldsymbol{\alpha}\cdot\boldsymbol{A}(\boldsymbol{r})\ . \tag{2.96}$$

Note the absence of a two-photon term. We then express the Hamiltonian of the interacting system as a perturbation of the free Hamiltonian

$$H \equiv H_0 + H'\ , \tag{2.97}$$

where we have defined

$$H' \equiv -cq\boldsymbol{\alpha}\cdot\boldsymbol{A}(\boldsymbol{r})\ . \tag{2.98}$$

Calculating the transition amplitude is a more complicated affair than in the quantum mechanical theory. Before doing so, we will therefore address the kinematics of the process.

Kinematics

Momentum conservation will once again emerge when evaluating the relativistic transition amplitude. Anticipating this, we find a relativistic expression for the Cherenkov angle. Considering the delta function in Eq.(2.76), E_i and E_f are now given by the relativistic free Hamiltonian. Defining as before θ to be the angle between $\boldsymbol{p}$ and $\boldsymbol{k}$ (See Figure 2.5), and applying momentum

conservation, we have the relativistic Cherenkov angle as determined by V. L. Ginzburg (See Appendix G)

$$\cos\theta_C = \frac{c}{nv}\left(1 + \frac{\hbar\omega_{\boldsymbol{k}}}{2E}(n^2-1)\right) . \tag{2.99}$$

It is then straightforward to show that we may write the delta function $\delta(E_f - E_i)$ as

$$\delta(E_f - E_i) = \frac{c}{nv}\frac{E - \hbar\omega_{\boldsymbol{k}}}{\hbar\omega_{\boldsymbol{k}} E}\delta\left(\cos\theta - \cos\theta_C\right) . \tag{2.100}$$

Inserting this expression in Eq.(2.76), the transition rate becomes

$$\omega_R = \frac{2\pi}{\hbar^2\omega_{\boldsymbol{k}}}\frac{c}{nv}\frac{E - \hbar\omega_{\boldsymbol{k}}}{E}|\mathcal{M}_\lambda|^2\delta(\cos\theta - \cos\theta_C) . \tag{2.101}$$

Note the extra factor $(E - \hbar\omega_{\boldsymbol{k}})/E$ compared to the quantum mechanical expression in Eq.(2.82). The inverse of this factor will emerge to cancel it when we calculate the relativistic transition amplitude.

Transition Amplitude

The transition rate for the process $|\psi_{\boldsymbol{p},m}\rangle|0\rangle \to |\psi_{\boldsymbol{p}',l}\rangle|\boldsymbol{k}\lambda\rangle$ is evaluated in the interaction picture by the Born approximation, Eq.(2.76), as in the non-relativistic theory. The matrix element $\mathcal{M}_{m,l\lambda} = \langle\boldsymbol{k}\lambda|\langle\psi_{\boldsymbol{p}',l}|H'|\psi_{\boldsymbol{p},m}\rangle|0\rangle$ is found by the same process as before

$$\mathcal{M}_{m,l\lambda} = -cqA_{\boldsymbol{k}}u^\dagger(\boldsymbol{p}',l)\boldsymbol{\alpha}\cdot\boldsymbol{\epsilon}^*_{\boldsymbol{k}\lambda}u(\boldsymbol{p},m)\delta_{\boldsymbol{p}'+\hbar\boldsymbol{k},\boldsymbol{p}} . \tag{2.102}$$

Once again conservation of momentum emerges. Note the additional subscripts corresponding to the states of the spinors. The transition rate depends in general on the spin states of the charged particles. Thus, for a given initial state, we must sum over the spin states of the final particle in order to find the total transition amplitude. We do not yet sum over the polarization states of the photon, as we are interested in the dependence of the amplitude on photon polarization. Additionally, we assume the spin of the initial particle is unknown. In other words, the transition rate of interest is that which includes all spin states of the final particle, and where the spin of the initial particle is a statistical mixed state of up and down. Assuming either spin state is equally probable for the incoming particle, we write the "average" amplitude of the process by taking the squared modulus, summing over initial and final spin states, and dividing by 2

$$\langle|\mathcal{M}_\lambda|^2\rangle = \frac{(cqA_{\boldsymbol{k}})^2}{2}\sum_{l,m}|u^\dagger(\boldsymbol{p}',l)\boldsymbol{\alpha}\cdot\boldsymbol{\epsilon}^*_{\boldsymbol{k}\lambda}u(\boldsymbol{p},m)|^2 . \tag{2.103}$$

Conservation of charge dictates that the above sum is taken only over either particle states or antiparticle states. We simplify the calculation by introducing

the projection operator P_+ by Eq.(F.14), allowing us to sum over all spinors and thus apply the completeness relation, Eq.(F.17)

$$\begin{aligned}
&\sum_{l,m=1}^{2} \left[u^\dagger(\boldsymbol{p}',l)\alpha_i u(\boldsymbol{p},m)\right]^* \left[u^\dagger(\boldsymbol{p}',l)\alpha_j u(\boldsymbol{p},m)\right] \\
&= \sum_{l,m=1}^{4} \left[u^\dagger(\boldsymbol{p},m)P_+\alpha_i P'_+ u(\boldsymbol{p}',l)\right] \left[u^\dagger(\boldsymbol{p}',l)P'_+\alpha_j P_+ u(\boldsymbol{p},m)\right] \\
&= \sum_{m=1}^{4} u^\dagger(\boldsymbol{p},m)P_+\alpha_i P'_+\alpha_j P_+ u(\boldsymbol{p},m) \\
&= \mathrm{Tr}\left\{\alpha_i P'_+\alpha_j P_+\right\} \ .
\end{aligned} \tag{2.104}$$

Here we have used the cyclic property of the trace, as well as the properties of the projection operator, to simplify.

Summing repeated indices from 1 to 3, we can now write the amplitude Eq.(2.103) as

$$\langle|\mathcal{M}_\lambda|^2\rangle = \frac{(cqA_{\boldsymbol{k}})^2}{2}\mathrm{Tr}\left\{\alpha_i P'_+\alpha_j P_+\right\}(\boldsymbol{\epsilon}_{\boldsymbol{k}\lambda})_i(\boldsymbol{\epsilon}^*_{\boldsymbol{k}\lambda})_j \ . \tag{2.105}$$

Writing out the projection operators explicitly and applying the trace properties of the Dirac matrices, Eq.(F.5) and Eq.(E.6), the amplitude is thus proportional to the expression

$$\left[\left(1-\frac{m^2c^4}{EE'}\right)\delta_{ij} + \frac{c^2}{2EE'}\mathrm{Tr}\left\{\sigma_i\sigma_l\sigma_j\sigma_m\right\}p'_l p_m\right](\boldsymbol{\epsilon}_{\boldsymbol{k}\lambda})_i(\boldsymbol{\epsilon}^*_{\boldsymbol{k}\lambda})_j \ . \tag{2.106}$$

Evaluating the trace in the second term by Eq.(E.8), we write

$$\begin{aligned}
&\mathrm{Tr}\left\{\sigma_i\sigma_l\sigma_j\sigma_m\right\}p'_l p_m(\boldsymbol{\epsilon}_{\boldsymbol{k}\lambda})_i(\boldsymbol{\epsilon}^*_{\boldsymbol{k}\lambda})_j \\
&= 2(\boldsymbol{p}'\cdot\boldsymbol{\epsilon}_{\boldsymbol{k}\lambda})(\boldsymbol{p}\cdot\boldsymbol{\epsilon}^*_{\boldsymbol{k}\lambda}) + 2(\boldsymbol{p}'\cdot\boldsymbol{\epsilon}^*_{\boldsymbol{k}\lambda})(\boldsymbol{p}\cdot\boldsymbol{\epsilon}_{\boldsymbol{k}\lambda}) - 2(\boldsymbol{\epsilon}_{\boldsymbol{k}\lambda}\cdot\boldsymbol{\epsilon}^*_{\boldsymbol{k}\lambda})(\boldsymbol{p}'\cdot\boldsymbol{p}) \ .
\end{aligned} \tag{2.107}$$

Applying momentum conservation $\boldsymbol{p}' = \boldsymbol{p} - \hbar\boldsymbol{k}$, we have by the Coulomb gauge $\boldsymbol{p}'\cdot\boldsymbol{\epsilon}_{\boldsymbol{k}\lambda} = \boldsymbol{p}\cdot\boldsymbol{\epsilon}_{\boldsymbol{k}\lambda}$ and $\boldsymbol{p}'\cdot\boldsymbol{\epsilon}^*_{\boldsymbol{k}\lambda} = \boldsymbol{p}\cdot\boldsymbol{\epsilon}^*_{\boldsymbol{k}\lambda}$. Moreover, the polarization vectors are normalized, $\boldsymbol{\epsilon}_{\boldsymbol{k}\lambda}\cdot\boldsymbol{\epsilon}^*_{\boldsymbol{k}\lambda} = 1$. Thus, by Eq.(2.106) the average amplitude for the emission of a photon with polarization $\boldsymbol{\epsilon}_{\boldsymbol{k}\lambda}$ is

$$\langle|\mathcal{M}_\lambda|^2\rangle = \frac{(cqA_{\boldsymbol{k}})^2}{2}\left(1-\frac{m^2c^4}{EE'}+\frac{c^2}{EE'}\left(2|\boldsymbol{p}\cdot\boldsymbol{\epsilon}_{\boldsymbol{k}\lambda}|^2 - \boldsymbol{p}'\cdot\boldsymbol{p}\right)\right) \ . \tag{2.108}$$

Conservation of Energy

Due to the delta function present in the transition rate, Eq.(2.101), it will also become necessary to apply conservation of energy to this amplitude. We find an expression for the amplitude with energy conserved, $\langle|\mathcal{S}_\lambda|^2\rangle$, by setting

$\theta = \theta_C$, $E' = E - \hbar\omega_{\boldsymbol{k}}$ in Eq.(2.108)

$$\langle|\mathcal{S}_\lambda|^2\rangle = \frac{S_{\boldsymbol{k}}}{2}\left(\frac{E-\hbar\omega_{\boldsymbol{k}}}{E} - \frac{1}{\gamma^2} + \frac{c^2}{E^2}\left(2|\boldsymbol{p}\cdot\boldsymbol{\epsilon}_{\boldsymbol{k}\lambda}|^2 - \boldsymbol{p}'\cdot\boldsymbol{p}\right)\right)$$
$$= \frac{S_{\boldsymbol{k}}}{2}\left(\frac{v^2}{c^2} - \frac{\hbar\omega_{\boldsymbol{k}}}{E} + \frac{c^2}{E^2}\left(\delta_{\lambda 1} 2p^2\sin^2\theta_C - p^2 + p\hbar\frac{\omega_{\boldsymbol{k}} n}{c}\cos\theta_C\right)\right) . \quad (2.109)$$

Here we have applied momentum conservation and inserted the linear basis of polarization given by Eq.(2.62). We have also defined

$$S_{\boldsymbol{k}} \equiv (cqA_{\boldsymbol{k}})^2\frac{E}{E-\hbar\omega_{\boldsymbol{k}}} . \quad (2.110)$$

Simplifying, our final expression for the average relativistic transition amplitude becomes

$$\langle|\mathcal{S}_\lambda|^2\rangle = S_{\boldsymbol{k}}\left(\delta_{\lambda 1}\frac{v^2}{c^2}\sin^2\theta_C + \left(\frac{\hbar\omega_{\boldsymbol{k}}}{2E}\right)^2(n^2-1)\right) . \quad (2.111)$$

Here we have inserted the relativistic expression for $\cos\theta_C$ by Eq.(2.99).

Clearly, the average amplitude is independent of the orientation of the spinor axis $\hat{\mathbf{e}}_3$. Any effect this orientation may have on transition amplitudes will not emerge when we sum over the states of both spinors. In order to examine the effects of spinor orientation, we will therefore need to consider the individual transition amplitudes for each process. We note also that, in contrast to the non-relativistic theory, the relativistic theory introduces a non-zero transition amplitude for light polarized perpendicular to the scattering plane.

3 Relativistic Corrections

Relativistic quantum mechanics offers corrections to the quantities which were calculated in classical electrodynamics and quantum mechanics. In the following sections, we will detail the behaviour of the relativistic corrections to the Cherenkov angle and the power spectrum. The correction terms are found to be proportional to $\hbar/2E$. Therefore, whenever it is necessary to insert specific values of parameters for the purposes of an illustration or example, the following text will insert the mass of the electron in order to maximize any effects. The refraction coefficient used will typically be that of water ($n = 1.3$), and when a set velocity is needed the default will be $v = 0.9c$.

3.1 Cherenkov Angle

The Cherenkov angle, as derived in Appendix G, is given by the condition

$$\cos\theta_C = \frac{c}{nv}\left(1 + \frac{\hbar\omega_{\boldsymbol{k}}}{2E_{\boldsymbol{p}}}(n^2 - 1)\right) . \tag{3.1}$$

Here, the first term corresponds to the classical result, while the second term is a correction resulting from conservation of energy and momentum in relativistic kinematics. The correction to the Cherenkov angle indicates that the angle of emission for photons of high frequency is sharper than predicted by the classical theory. Curiously, this relativistic correction is larger the smaller the velocity of the incoming particle (see Figure 3.1). The correction is very small unless the particle velocity is close to threshold $v = c/n$, or photon energies are very large. Taking the example of an electron moving through water at $v = 0.9c$, the correction to the Cherenkov angle is less than 1 mrad for photons with frequencies below $10^{19}\,\mathrm{rad\,s^{-1}}$. For comparison, the Cherenkov angle resolution of the RICH 2 detector at LHCb is 0.68(2) mrad [5]. The refraction coefficient of water is less than one for frequencies above approximately $10^{16}\,\mathrm{rad\,s^{-1}}$, and so no photons with frequencies on the order of $10^{19}\,\mathrm{rad\,s^{-1}}$ may be emitted. In the absence of exotic materials possessing coefficients of refraction $n > 1$ at such high frequencies, detecting the relativistic correction to the Cherenkov angle would require a RICH detector with a prohibitively high angular resolution.

Another possibility for detecting the relativistic correction to the Cherenkov angle could be materials with large coefficients of refraction within the available frequency range. Due to the factor $(n^2 - 1)$ in Eq.(2.99) the correction is greater for larger n. As an example, Gallium Arsenide (GaAs) has a refraction coefficient of approximately 4 at a frequency $\omega \approx 7 \times 10^{15}\,\mathrm{rad\,s^{-1}}$. As shown in Figure 3.2, the relativistic correction to the Cherenkov angle would hypothetically be three times larger in GaAs than in water. Regrettably, GaAs is an

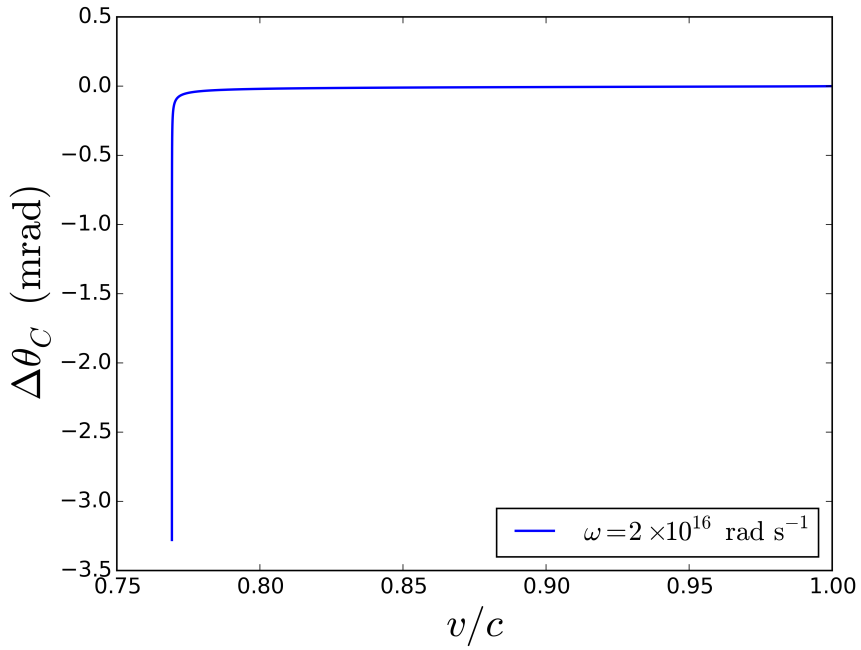

FIGURE 3.1: The relativistic correction $\Delta\theta_C$, to the Cherenkov angle for an electron in water as a function of particle velocity, for approximately the maximal experimentally accessible photon frequency.

ill-suited medium, as electrons may not travel freely through it. The penetration depth of an electron beam in GaAs is on the order of 1 µm [16]. However, it is possible to produce Cherenkov radiation by firing charged particles through a thin channel in an otherwise impenetrable medium [17, 18]. A more detailed treatment of whether it would be possible to test the relativistic correction to the Cherenkov angle in this manner is outside the scope of this thesis.

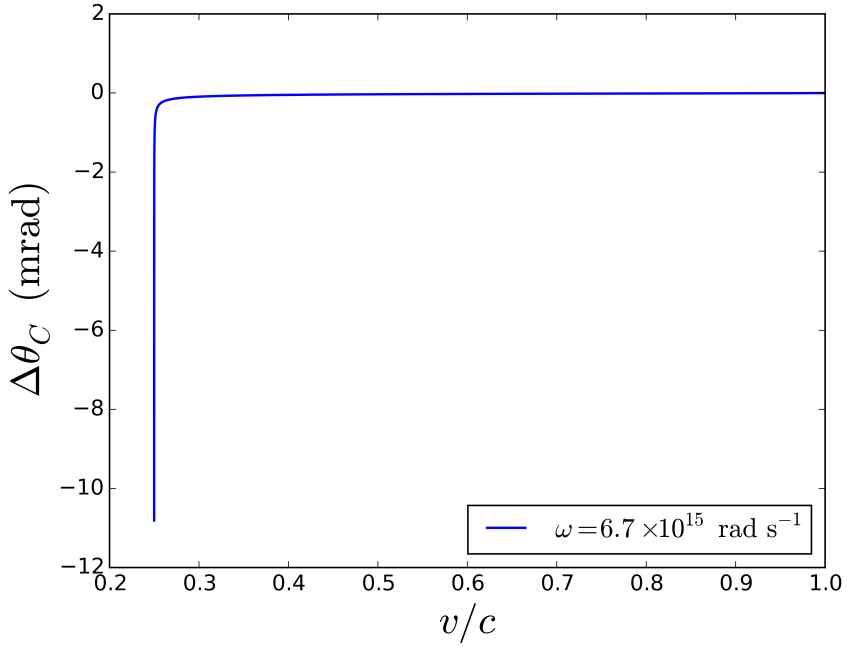

FIGURE 3.2: The relativistic correction $\Delta\theta_C$, to the Cherenkov angle for an electron in Gallium Arsenide as a function of particle velocity, for approximately the maximal experimentally accessible photon frequency.

3.2 Transition Rate and Power Spectrum

According to Ref. [19] A. Sokolov was the first to derive the power spectrum of Cherenkov radiation using relativistic quantum mechanics. We will here derive the same power spectrum, and the corresponding transition rate. Thereupon, we will comment on the feasibility of observing the resulting correction to the classical power spectrum.

Linear Polarization Modes

Having found an expression for the transition rates of each mode, Eq.(2.101), we may proceed to calculate the total transition rate

$$R = \sum_{\boldsymbol{k}\lambda} \omega_R \ . \tag{3.2}$$

We wish to examine the spectrum of this transition rate with regard to polarization and frequency in the limit of a continuous frequency spectrum. Thus we do not sum over the polarization states of the photon, and we take the limit of continuous frequencies by the same argument as in the non-relativistic theory.

Using Eq.(2.101), we write

$$R_\lambda(\omega_{\boldsymbol{k}}) = \frac{V}{(2\pi)^3}\left(\frac{n}{c}\right)^3 \omega_{\boldsymbol{k}}^2 \int \mathrm{d}\Omega \omega_R$$
$$= \frac{V}{(2\pi)^2}\left(\frac{n}{\hbar c}\right)^2 \frac{\omega_{\boldsymbol{k}}}{v}\frac{E-\hbar\omega_{\boldsymbol{k}}}{E}\int_0^{2\pi} \mathrm{d}\phi |\mathcal{S}_\lambda|^2 \ . \tag{3.3}$$

Here we have evaluated the $\mathrm{d}\theta$-part of the solid angle integral by imposing conservation of energy on the amplitude. In general we wish to consider ϕ-dependent effects, and so from Eq.(3.3) we define the angular distribution of the transition rate

$$R_\lambda(\omega_{\boldsymbol{k}}, \phi) \equiv \frac{\alpha}{2\pi}\frac{cq^2}{ve^2}\frac{|\mathcal{S}_\lambda|^2}{S_{\boldsymbol{k}}} \ , \tag{3.4}$$

where α denotes the fine-structure constant, and e denotes the elementary charge. Here we have also applied the definition of $S_{\boldsymbol{k}}$ by Eq.(2.110).

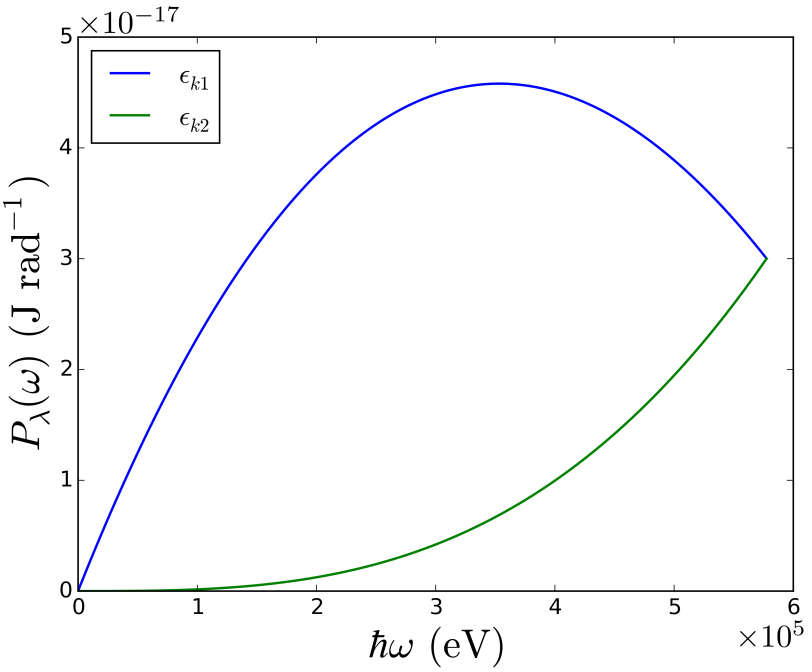

FIGURE 3.3: The power spectrum $P_\lambda(\omega)$, for each of the linear polarization modes for an electron moving through water at $0.9c$.

To find the power spectrum, we simply take $P_\lambda(\omega_{\boldsymbol{k}}) = \hbar\omega_{\boldsymbol{k}} R_\lambda(\omega_{\boldsymbol{k}})$. Considering a particle in an unknown initial state, we insert the average amplitude from Eq.(2.111) in Eq.(3.4). The amplitude is independent of ϕ, so integrating over ϕ trivially contributes a factor 2π. Thus we have the relativistic power spectrum

$$P_\lambda(\omega_{\boldsymbol{k}}) = \frac{\mu_0 q^2}{4\pi}\omega_{\boldsymbol{k}} v\left(\delta_{\lambda 1}\sin^2\theta_C + \frac{c^2}{v^2}\left(\frac{\hbar\omega_{\boldsymbol{k}}}{2E}\right)^2 (n^2-1)\right) \ . \tag{3.5}$$

Here we have also rewritten the prefactor to mirror that of the classical expression. Summing over photon polarizations and considering $\sin^2\theta_C = 1 - \cos^2\theta_C$, we recognize this as the classical power spectrum plus a correction term from relativistic quantum mechanics. Note that the relativistic correction to the Cherenkov angle also contributes.

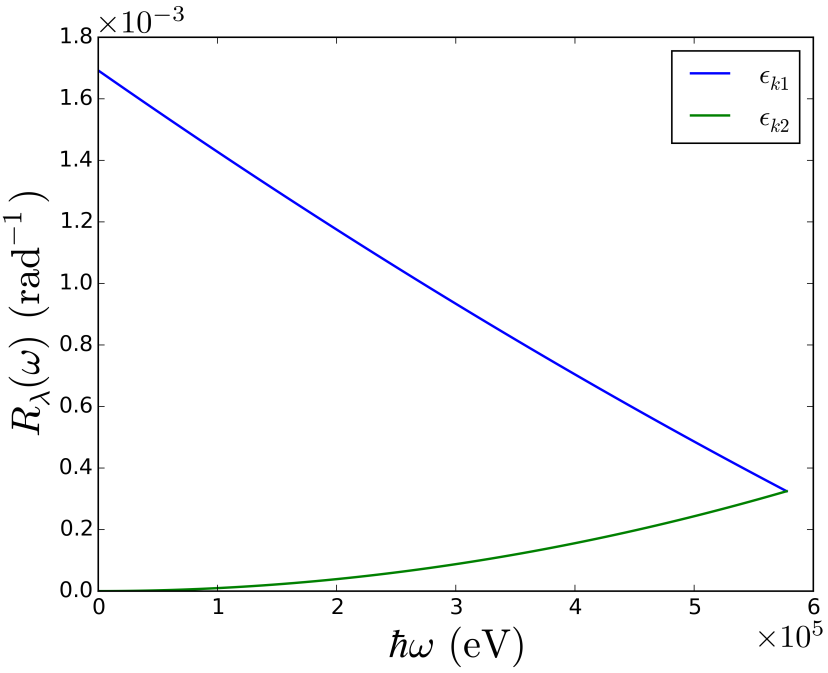

FIGURE 3.4: The transition rate spectrum $R_\lambda(\omega)$, for each of the linear polarization modes for an electron moving through water at $0.9c$.

Plotting the power spectrum and transition rate spectrum for each polarization mode (see Figure 3.3 and Figure 3.4), we note that although the emitted power goes to zero in the limit $\omega_{\boldsymbol{k}} \to 0$, the transition rate does not. We see also that for low photon energies the $\boldsymbol{\epsilon}_{\boldsymbol{k}1}$-mode dominates, in agreement with the classical and quantum mechanical theories.

Total Power Spectrum

It is also of interest to express explicitly the frequency dependence which relativistic quantum mechanics introduces to the total power spectrum. Inserting the Cherenkov angle by Eq.(2.99) in Eq.(3.5) and summing over photon polarization modes, we have

$$P(\omega_{\boldsymbol{k}}) = \frac{\mu_0 q^2}{4\pi}\omega_{\boldsymbol{k}} v\left(1 - \left(\frac{c}{nv}\right)^2 - \left(\frac{c}{nv}\right)^2\left(\frac{\hbar\omega_{\boldsymbol{k}}}{E}(n^2-1) - \left(\frac{\hbar\omega_{\boldsymbol{k}}}{2E}\right)^2(n^4-1)\right)\right). \quad (3.6)$$

This agrees with the expression of Sokolov as cited in Ref. [19]. In the low-frequency limit, the relativistic expression for the power spectrum matches the result from classical electrodynamics and quantum mechanics, Eq.(2.90). In the high-frequency domain, however, the power spectra diverge, as may be seen from Figure 3.5.

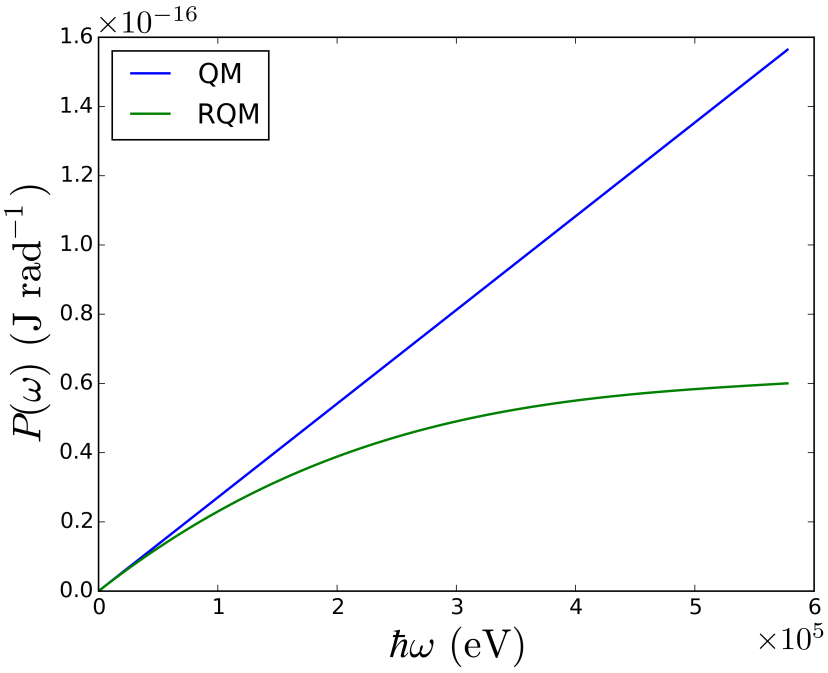

FIGURE 3.5: The power spectrum $P(\omega)$, for an electron moving through water at $0.9c$, as calculated in quantum mechanics and relativistic quantum mechanics respectively.

The power spectra diverge in general when the energy of the photon approaches the maximum allowed by conservation of energy. For an electron with velocity $v = 0.9c$, this maximum is greater than the rest-energy of the electron, and so the first-order perturbation theory we have applied becomes inaccurate in this region.

Estimate of Relativistic Correction

The factor $\hbar/E$ is on the order of $\sim 10^{-22}$ and so, calculating the relativistic correction, we neglect the term proportional to $(\hbar/E)^2$. We see that the classical power spectrum is proportional to $\omega_{\boldsymbol{k}}$, and the relativistic correction is proportional to $\omega_{\boldsymbol{k}}^2\hbar/E$. Thus, at $v = 0.9c$, $\omega_{\boldsymbol{k}} = 10^{16}\,\mathrm{rad\,s^{-1}}$, the relative correction to the power spectrum is on the order of $\sim 10^{-4}\,\%$. In order for the relative size of the correction to be on the order of $\sim 1\,\%$, one must consider frequencies of approximately $10^{20}\,\mathrm{rad\,s^{-1}}$.

The classical power spectrum approaches zero as $v \to c/n$, whereas the correction terms are approximately constant. Due to this it is possible to increase the relative size of the correction by decreasing the speed of the charged particle.

3.3 Remarks

The common feature of the relativistic corrections outlined above is that they are negligible unless the frequencies involved approach ω_{MAX} as given in Eq.(G.6). However, ω_{MAX} is prohibitively large for realistic particle velocities. As an example, for an electron moving at $0.9c$, we have a maximal photon energy of $\hbar\omega_{\mathrm{MAX}} \simeq 0.58\,\mathrm{MeV}$. This is greater than the rest-energy of the electron, making the first-order perturbation theory we have applied inaccurate. However, no known material possesses dielectric properties at such high frequencies ($\omega \sim 10^{20}\,\mathrm{rad\,s^{-1}}$), meaning Cherenkov radiation is experimentally inaccessible in this frequency range.

If the relativistic effects are to occur within an experimentally accessible frequency range, one must lower the speed of the charged particle to near threshold, so as to decrease ω_{MAX}. However, as the velocity approaches threshold, both the Cherenkov angle and the emitted power approach zero. Thus, any realistic attempt to detect the established relativistic corrections must probe radiation of very low intensity, emitted nearly parallel to the path of the charged particle. Due to these challenges, detecting the relativistic effects is not likely to be possible using current experimental techniques.

4 Polarization

In the following sections we will derive an expression for the transition amplitude of Cherenkov radiation emitted from an initial particle in a known spin-state. We will find that the polarization of the emitted light is dependent on the orientation of the spin of the initial particle. Thereupon we consider the feasibility of detecting these polarization effects. Finally, we consider the degree of entanglement between the spins of the final particles.

4.1 Initial Spin-Up State

In order to examine the effects of spinor orientation on the phenomenon, we need to consider an initial state with a specified spinor orientation. To this end, we calculate the transition amplitudes for the individual processes $|\psi_{\boldsymbol{p},1}\rangle\,|0\rangle \to |\psi_{\boldsymbol{p}',1}\rangle\,|\boldsymbol{k}\lambda\rangle$, and $|\psi_{\boldsymbol{p},2}\rangle\,|0\rangle \to |\psi_{\boldsymbol{p}',2}\rangle\,|\boldsymbol{k}\lambda\rangle$, and $|\psi_{\boldsymbol{p},1}\rangle\,|0\rangle \to |\psi_{\boldsymbol{p}',2}\rangle\,|\boldsymbol{k}\lambda\rangle$, and $|\psi_{\boldsymbol{p},2}\rangle\,|0\rangle \to |\psi_{\boldsymbol{p}',1}\rangle\,|\boldsymbol{k}\lambda\rangle$.

Individual Amplitudes

Since the expressions are quite simple, as seen in Eq.(2.102), we will simply evaluate them explicitly with the spinors from Appendix F. The calculations are contained in Appendix H. The notation used is

$$\mathcal{M}_{m,l\lambda} = \mathcal{M}\big(|\psi_{\boldsymbol{p},m}\rangle\,|0\rangle \to |\psi_{\boldsymbol{p}',l}\rangle\,|\boldsymbol{k}\lambda\rangle\big)\ . \tag{4.1}$$

The individual amplitudes are

$$\begin{aligned}
\mathcal{M}_{1,1\lambda} &= -M_{\boldsymbol{k}}\Big((\boldsymbol{p}\cdot\boldsymbol{\epsilon}^*_{\boldsymbol{k}\lambda})B + i[\boldsymbol{a}\times\boldsymbol{\epsilon}^*_{\boldsymbol{k}\lambda}]_3\Big)\ ,\\
\mathcal{M}_{2,2\lambda} &= -M_{\boldsymbol{k}}\Big((\boldsymbol{p}\cdot\boldsymbol{\epsilon}^*_{\boldsymbol{k}\lambda})B - i[\boldsymbol{a}\times\boldsymbol{\epsilon}^*_{\boldsymbol{k}\lambda}]_3\Big)\ ,\\
\mathcal{M}_{1,2\lambda} &= M_{\boldsymbol{k}}\Big([\boldsymbol{a}\times\boldsymbol{\epsilon}^*_{\boldsymbol{k}\lambda}]_2 - i[\boldsymbol{a}\times\boldsymbol{\epsilon}^*_{\boldsymbol{k}\lambda}]_1\Big)\ ,\\
\mathcal{M}_{2,1\lambda} &= -M_{\boldsymbol{k}}\Big([\boldsymbol{a}\times\boldsymbol{\epsilon}^*_{\boldsymbol{k}\lambda}]_2 + i[\boldsymbol{a}\times\boldsymbol{\epsilon}^*_{\boldsymbol{k}\lambda}]_1\Big)\ .
\end{aligned} \tag{4.2}$$

Here we have defined quantities $M_{\boldsymbol{k}}$, $\boldsymbol{a}$, and B, to allow compact expressions of the amplitudes and facilitate algebraic manipulations. The quantities are defined in Eq.(H.4), Eq.(H.5), and Eq.(H.6), respectively.

To begin, we verify the result from established theory. Considering the average amplitude

$$\langle|\mathcal{M}_\lambda|^2\rangle = \frac{1}{2}\left(|\mathcal{M}_{1,1\lambda}|^2 + |\mathcal{M}_{2,2\lambda}|^2 + |\mathcal{M}_{1,2\lambda}|^2 + |\mathcal{M}_{2,1\lambda}|^2\right) , \tag{4.3}$$

we note that the amplitudes come in pairs which are only distinguished by the relative sign of their terms. With complex numbers z and c, we have $|z+c|^2 + |z-c|^2 = |z|^2 + |c|^2$. Thus we may simply write

$$\langle|\mathcal{M}_\lambda|^2\rangle = M_{\boldsymbol{k}}^2\left(|\boldsymbol{p}\cdot\boldsymbol{\epsilon}_{\boldsymbol{k}\lambda}|^2 B^2 + |\boldsymbol{a}\times\boldsymbol{\epsilon}_{\boldsymbol{k}\lambda}|^2\right) . \tag{4.4}$$

This expression may be shown to correspond to that given in Eq.(2.108). It is also clear from Eq.(4.4) that the average amplitude is equal for left- and right-handed circularly polarized light. The polarization vector only appears within expressions of absolute value, and so the average amplitude does not distinguish between left- and right-handed circularly polarized light. In the interest of probing the phenomenon further, we shall sum over only the final spinor states.

Sum over Final Spinor States

Due to conservation of angular momentum, we expect light emitted from a particle in a known spin state to be in general elliptically polarized. With this in mind, we wish to calculate the amplitude

$$|\mathcal{M}_{1,\lambda}|^2 = |\mathcal{M}_{1,1\lambda}|^2 + |\mathcal{M}_{1,2\lambda}|^2 . \tag{4.5}$$

This expression may be evaluated in the same way as Eq.(4.3). Keeping in mind that now the cross-terms do not cancel, we write

$$|\mathcal{M}_{1,\lambda}|^2 = \langle|\mathcal{M}_\lambda|^2\rangle + M_{\boldsymbol{k}}^2 X_\lambda , \tag{4.6}$$

where the cross-terms are given by

$$\begin{aligned} X_\lambda \equiv iB(\boldsymbol{p}\cdot\boldsymbol{\epsilon}_{\boldsymbol{k}\lambda})[\boldsymbol{a}\times\boldsymbol{\epsilon}^*_{\boldsymbol{k}\lambda}]_3 - iB[\boldsymbol{a}\times\boldsymbol{\epsilon}_{\boldsymbol{k}\lambda}]_3(\boldsymbol{p}\cdot\boldsymbol{\epsilon}^*_{\boldsymbol{k}\lambda}) + \\ i[\boldsymbol{a}\times\boldsymbol{\epsilon}_{\boldsymbol{k}\lambda}]_1[\boldsymbol{a}\times\boldsymbol{\epsilon}^*_{\boldsymbol{k}\lambda}]_2 - i[\boldsymbol{a}\times\boldsymbol{\epsilon}_{\boldsymbol{k}\lambda}]_2[\boldsymbol{a}\times\boldsymbol{\epsilon}^*_{\boldsymbol{k}\lambda}]_1 . \end{aligned} \tag{4.7}$$

The first line of this expression is simplified by using the vector triple product

$$\boldsymbol{A}\times[\boldsymbol{B}\times\boldsymbol{C}] = (\boldsymbol{A}\cdot\boldsymbol{C})\boldsymbol{B} - (\boldsymbol{A}\cdot\boldsymbol{B})\boldsymbol{C} , \tag{4.8}$$

to write

$$(\boldsymbol{p}\cdot\boldsymbol{\epsilon}_{\boldsymbol{k}\lambda})[\boldsymbol{a}\times\boldsymbol{\epsilon}^*_{\boldsymbol{k}\lambda}] - (\boldsymbol{p}\cdot\boldsymbol{\epsilon}^*_{\boldsymbol{k}\lambda})[\boldsymbol{a}\times\boldsymbol{\epsilon}_{\boldsymbol{k}\lambda}] = \boldsymbol{a}\times\left[\boldsymbol{p}\times[\boldsymbol{\epsilon}^*_{\boldsymbol{k}\lambda}\times\boldsymbol{\epsilon}_{\boldsymbol{k}\lambda}]\right] , \tag{4.9}$$

for which the first line of Eq.(4.7) corresponds to the 3-component. The second line of Eq.(4.7) may be seen directly to correspond to the 3-component of the cross product $[\boldsymbol{a}\times\boldsymbol{\epsilon}_{\boldsymbol{k}\lambda}]\times[\boldsymbol{a}\times\boldsymbol{\epsilon}^*_{\boldsymbol{k}\lambda}]$, which may be simplified by using the vector

quadruple product

$$[\boldsymbol{A}\times\boldsymbol{B}]\times[\boldsymbol{C}\times\boldsymbol{D}]=\boldsymbol{A}\cdot[\boldsymbol{B}\times\boldsymbol{D}]\boldsymbol{C}-\boldsymbol{A}\cdot[\boldsymbol{B}\times\boldsymbol{C}]\boldsymbol{D}\,, \tag{4.10}$$

to write

$$[\boldsymbol{a}\times\boldsymbol{\epsilon}_{\boldsymbol{k}\lambda}]\times[\boldsymbol{a}\times\boldsymbol{\epsilon}^*_{\boldsymbol{k}\lambda}]=-\boldsymbol{a}\cdot[\boldsymbol{\epsilon}^*_{\boldsymbol{k}\lambda}\times\boldsymbol{\epsilon}_{\boldsymbol{k}\lambda}]\boldsymbol{a}\,. \tag{4.11}$$

Note that both terms in Eq.(4.7) are thus proportional to the cross product $\boldsymbol{\epsilon}^*_{\boldsymbol{k}\lambda}\times\boldsymbol{\epsilon}_{\boldsymbol{k}\lambda}$. Considering linear polarization, this product is zero by definition and so any dependence on linear polarization modes is contained in the $\langle|\mathcal{M}_\lambda|^2\rangle$ term. We are however interested in the general case of elliptical polarization. From the definitions of the elliptical basis vectors, Eq(2.63) and Eq.(2.64), we have

$$\boldsymbol{\epsilon}^*_{\boldsymbol{k}\alpha\pm}\times\boldsymbol{\epsilon}_{\boldsymbol{k}\alpha\pm}=\pm i\sin(2\alpha)\hat{\mathbf{k}}\,. \tag{4.12}$$

Applying this result to Eq.(4.9) and Eq.(4.11), we can write Eq.(4.7) more compactly

$$X_\pm=\mp\sin(2\alpha)\left[B\boldsymbol{a}\times[\boldsymbol{p}\times\hat{\mathbf{k}}]-(\boldsymbol{a}\cdot\hat{\mathbf{k}})\boldsymbol{a}\right]\cdot\hat{\mathbf{e}}_3\,. \tag{4.13}$$

Here, and in the following text, we use the subscript $\pm$ to indicate the state described by $\boldsymbol{\epsilon}_{\boldsymbol{k}\alpha\pm}$, i.e., we suppress the subscript α for notational brevity.

Eq.(4.13) may be made more transparent by re-expressing the vector within brackets. Applying Eq.(4.8) to the triple product term, the vector may be written

$$(\boldsymbol{a}\cdot\hat{\mathbf{k}})[B\boldsymbol{p}-\boldsymbol{a}]-B(\boldsymbol{a}\cdot\boldsymbol{p})\hat{\mathbf{k}}\,. \tag{4.14}$$

Applying momentum conservation to $\boldsymbol{a}$, we have by its definition, Eq.(H.5), $\boldsymbol{a}=(E-E')\boldsymbol{p}-(E+mc^2)\hbar\boldsymbol{k}$. With this, and recalling the definition of B, Eq.(H.6), we may arrange the vector into terms proportional to $\boldsymbol{p}$ and $\hat{\mathbf{k}}$ respectively

$$\begin{aligned}&(\boldsymbol{a}\cdot\hat{\mathbf{k}})[B\boldsymbol{p}-\boldsymbol{a}]-B(\boldsymbol{a}\cdot\boldsymbol{p})\hat{\mathbf{k}}\\&=(\boldsymbol{a}\cdot\hat{\mathbf{k}})\big[2(E'+mc^2)\boldsymbol{p}+(E+mc^2)\hbar\boldsymbol{k}\big]-B(\boldsymbol{a}\cdot\boldsymbol{p})\hat{\mathbf{k}}\\&=2(\boldsymbol{a}\cdot\hat{\mathbf{k}})(E'+mc^2)\boldsymbol{p}-\big(\boldsymbol{a}\cdot\big[\boldsymbol{p}B-\hbar\boldsymbol{k}(E+mc^2)\big]\big)\,\hat{\mathbf{k}}\,.\end{aligned} \tag{4.15}$$

Considering more closely the term proportional to $\hat{\mathbf{k}}$, we may apply momentum conservation $\boldsymbol{p}-\hbar\boldsymbol{k}=\boldsymbol{p}'$ to write

$$\boldsymbol{a}\cdot\big[\boldsymbol{p}B-\hbar\boldsymbol{k}(E+mc^2)\big]=\boldsymbol{a}\cdot\big[\boldsymbol{p}'(E+mc^2)+\boldsymbol{p}(E'+mc^2)\big]\,, \tag{4.16}$$

which by the definition of $\boldsymbol{a}$, Eq.(H.5), is equal to

$$p'^2(E+mc^2)^2-p^2(E'+mc^2)^2\,. \tag{4.17}$$

Writing the relativistic energy-momentum relation as

$$p^2c^2=(E+mc^2)(E-mc^2)\,, \tag{4.18}$$

Eq.(4.17) becomes

$$\frac{(E+mc^2)(E'+mc^2)}{c^2}\Big((E'-mc^2)(E+mc^2)-(E-mc^2)(E'+mc^2)\Big) \\ = 2(E+mc^2)(E'+mc^2)(E'-E)m\ . \tag{4.19}$$

Thus the vector with which we are concerned becomes simply

$$2(E+mc^2)(E'+mc^2)\left[\frac{(\boldsymbol{a}\cdot\hat{\mathbf{k}})}{E+mc^2}\boldsymbol{p}-m(E'-E)\hat{\mathbf{k}}\right]\ . \tag{4.20}$$

Inserting this expression in Eq.(4.13), we find an expression for $X_\pm$ which may in turn be inserted in Eq.(4.6) to give

$$|\mathcal{M}_{1,\pm}|^2=\langle|\mathcal{M}_\pm|^2\rangle\mp\sin(2\alpha)\frac{c^4q^2A_{\boldsymbol{k}}^2}{2E'E}\left[\frac{(\boldsymbol{a}\cdot\hat{\mathbf{k}})}{E+mc^2}\boldsymbol{p}+m(E-E')\hat{\mathbf{k}}\right]\cdot\hat{\mathbf{e}}_3\ . \tag{4.21}$$

Here we have also written out $M_{\boldsymbol{k}}$ explicitly by Eq.(H.4).

Conservation of Energy

We enforce conservation of energy on the amplitude by setting $\theta=\theta_C$ and $E'=E-\hbar\omega_{\boldsymbol{k}}$. We find the first term by an equivalent argument to that of Eq.(2.109) and Eq.(2.111), inserting the elliptical basis $\boldsymbol{\epsilon}_{\boldsymbol{k}\lambda}=\boldsymbol{\epsilon}_{\boldsymbol{k}\alpha\pm}$ instead of the linear basis

$$\langle|\mathcal{S}_\pm|^2\rangle=S_{\boldsymbol{k}}\left(\frac{1}{2}\frac{v^2}{c^2}\sin^2\theta_C\big(1\pm\cos(2\alpha)\big)+\left(\frac{\hbar\omega_{\boldsymbol{k}}}{2E}\right)^2(n^2-1)\right)\ . \tag{4.22}$$

Recall the definition of $S_{\boldsymbol{k}}$ from Eq.(2.110). Here we have also used the trigonometric relation $\cos(2x)=\cos^2x-\sin^2x$.

In order to impose conservation of energy on the second term of Eq.(4.21), we begin by noting that $\theta=\theta_C$ and $E'=E-\hbar\omega_{\boldsymbol{k}}$ gives

$$\boldsymbol{a}\cdot\hat{\mathbf{k}}=\boldsymbol{p}\cdot\hat{\mathbf{k}}\hbar\omega_{\boldsymbol{k}}-\hbar k(E+mc^2) \\ =\hbar\omega_{\boldsymbol{k}}\left(p\cos\theta_C-\frac{n}{c}(E+mc^2)\right)\ . \tag{4.23}$$

From this it follows that

$$|\mathcal{S}_{1,\pm}|^2-\langle|\mathcal{S}_\pm|^2\rangle=\mp S_{\boldsymbol{k}}\sin(2\alpha)\frac{\hbar\omega_{\boldsymbol{k}}c^2}{2E^2}\left[\frac{p\cos\theta_C}{E+mc^2}\boldsymbol{p}-\frac{n}{c}\boldsymbol{p}+m\hat{\mathbf{k}}\right]\cdot\hat{\mathbf{e}}_3\ . \tag{4.24}$$

In terms of the angles ϕ, χ, and θ, we have the dot products $\boldsymbol{p}\cdot\hat{\mathbf{e}}_3=p\cos\chi$ and $\hat{\mathbf{k}}\cdot\hat{\mathbf{e}}_3=\sin\chi\cos\phi\sin\theta+\cos\chi\cos\theta$. The dot product between $\hat{\mathbf{e}}_3$ and the expression within brackets then becomes

$$m\left(\gamma\cos\chi\left(\cos\theta_C-\frac{nv}{c}\right)+\sin\chi\cos\phi\sin\theta_C\right)\ . \tag{4.25}$$

Here we have applied the relativistic expressions $p = \gamma mv$ and $E = \gamma mc^2$. Thus after applying conservation of energy we may write the amplitude for elliptically polarized light as

$$|\mathcal{S}_{1,\pm}|^2 = S_{\boldsymbol{k}}\left(\frac{1}{2}\frac{v^2}{c^2}\sin^2\theta_C + \left(\frac{\hbar\omega_{\boldsymbol{k}}}{2E}\right)^2 (n^2-1)\pm \left(\frac{1}{2}\frac{v^2}{c^2}\sin^2\theta_C\cos(2\alpha) - \sin(2\alpha)\frac{\hbar\omega_{\boldsymbol{k}}}{2E}F(\chi,\phi)\right)\right), \quad (4.26)$$

where we have defined

$$F(\chi,\phi) \equiv \cos\chi\left(\cos\theta_C - \frac{nv}{c}\right) + \frac{1}{\gamma}\sin\chi\cos\phi\sin\theta_C\,. \quad (4.27)$$

It is clear from Eq.(4.26) that the polarization of emitted light depends on the orientation of the spinor.

4.2 Detecting Polarization

With a general expression for the amplitudes of different polarizations of light, we may consider the degree of polarization of light emitted in a realistic experimental setup. In order to study the polarization of Cherenkov radiation,

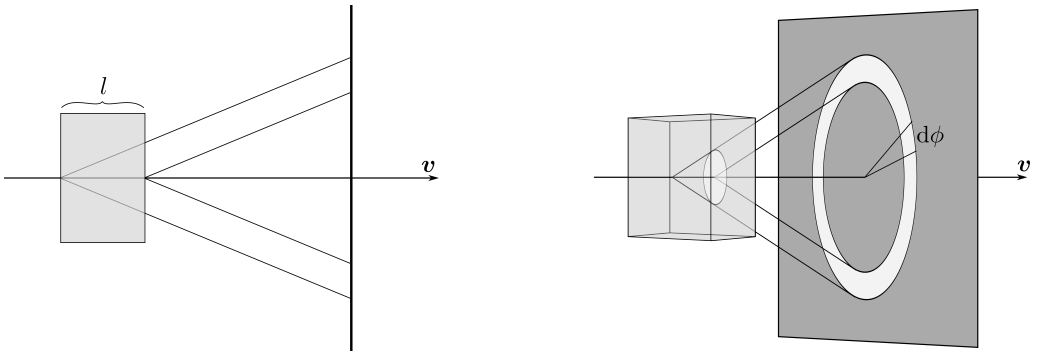

(a) (b)

FIGURE 4.1: Side view (a) and perspective view (b) of a RICH-detector. A particle moving at speed v through a medium of length l emits radiation in a conical shell which forms a circle on the detector plane.

one would require an experimental setup based on the principles of a RICH-detector (see Figure 4.1). The purpose of a conventional RICH-detector is to reconstruct the Cherenkov angle from the circle of light formed on the detector plane. In attempting to detect polarization effects, the Cherenkov angle is of no interest. As we shall see, the matter of interest would be the distribution of the number of detected photons, with regard to ϕ, on the circle of light. More precisely, we wish to measure said distribution for specific polarizations of light.

Consider an electron moving at constant speed v through some dielectric medium of length l. Downstream from the medium, a detector sensitive to

photons in the frequency band $\omega \in [\omega_m, \omega_M]$ is set up to register the emitted radiation. The number of photons emitted in a given polarization mode is

$$N_\lambda \equiv \frac{l}{v} R_\lambda \ . \tag{4.28}$$

Furthermore, the number of these photons which hit an angular element $\mathrm{d}\phi$ of the detector (see Figure 4.1b) is equal to $\mathrm{d}\phi N_\lambda(\phi) = \mathrm{d}\phi R_\lambda(\phi) l/v$, where we have set

$$R_\lambda(\phi) = \int_{\omega_m}^{\omega_M} \mathrm{d}\omega_{\boldsymbol{k}} R_\lambda(\omega_{\boldsymbol{k}}, \phi) \ . \tag{4.29}$$

With this we may consider how the number of photons emitted in each polarization mode depends on ϕ.

Linear Polarization

The presence of light polarized perpendicular to the scattering plane is evident from Eq.(2.111) in the established treatment of Cherenkov radiation. The corresponding amplitude is, however, proportional to $(\hbar\omega_{\boldsymbol{k}}/E)^2$. Thus for an electron moving at $v = 0.9c$ the amplitude of the perpendicularly polarized mode, $\boldsymbol{\epsilon}_{\boldsymbol{k}2}$, is smaller than that of the parallel mode, $\boldsymbol{\epsilon}_{\boldsymbol{k}1}$, by a factor

$$\frac{|\mathcal{S}_{1,2}|^2}{|\mathcal{S}_{1,1}|^2} \sim 10^{-44}\, \omega_{\boldsymbol{k}}^2 \ . \tag{4.30}$$

As a result, the degree of perpendicular polarization is approximately quadratic in $\omega_{\boldsymbol{k}}$, reaching $\sim 1\,\%$ at frequencies on the order of $\sim 10^{21}\,\mathrm{rad\,s^{-1}}$. Such frequencies, in addition to being several orders of magnitude larger than the upper frequency limit of known dielectrics, correspond to photon energies on the scale of the rest energy of the electron, making the perturbation theory we apply inaccurate. As a recourse to this, albeit a mild one, the degree of polarization may be increased by letting the velocity approach threshold, in order to decrease the total transition amplitude while slightly increasing the correction term. Furthermore, the correction term is proportional to $(n^2 - 1)$, making it sensitive to increases in the refraction coefficient.

We also note that the amplitudes of both linear modes of polarization are independent of the orientation of the initial spinor. In other words, even if it was possible to observe the perpendicularly polarized component, it could not be applied to study the spin degrees of freedom of the charged particle. Furthermore, the practical matter of fitting a RICH-detector with a polarizer to distinguish between linear polarization modes is non-trivial. Consider the circle of light incident on the detector plane in Figure 4.1b. At a given angle ϕ along the circle, the parallel direction of polarization is in fact perpendicular to the parallel direction of polarization at the angle $\phi + \pi/2$. In order to filter out the parallel mode of polarization, it would be necessary to fit the detector plane with a multitude of linear polarizers which, at every point along the circumference of the circle of light, are oriented perpendicular to its radius. Moreover, even if one were to construct such a circle of polarizers, its center

would need to exactly coincide with the central axis of the Cherenkov cone. Any misalignment would allow some proportion of the light polarized in the parallel mode to pass through the polarizer. At a frequency of $10^{16}\,\mathrm{rad\,s^{-1}}$, only one in every 10^{12} photons in the parallel mode would need to pass through the polarizer in order to drown out the perpendicularly polarized light.

Due to the factors outlined above, detecting the perpendicular polarization component which relativistic quantum mechanics introduces to the theory of Cherenkov radiation is not feasible with current experimental techniques. However, it may perhaps still be possible to observe some polarization effects, as the challenges related to detecting linear polarization do not apply to circular polarization.

Circular Polarization

Considering the circularly polarized basis ($\alpha = \pi/4$), we see from Eq.(4.26) that the amplitudes for left-handed and right-handed photons are nearly equal, as they should be for linearly polarized light. However, the amplitudes are separated by a term $\pm F(\chi,\phi)\hbar\omega_{\boldsymbol{k}}/2E$. Thus the amplitudes of left- and right-handed light depend on the orientation of the initial spinor. The basis of circular polarization poses therefore a more fertile paradigm for analysis than the basis of linear polarization. Additionally, the practical matter of separating circular modes of polarization is not hampered by the challenges involved with linear polarization. A right-handed photon is the same no matter which direction along the Cherenkov cone it is emitted, and so a single polarizer may be used to cover the entire detector plane. In the previous section we outlined how this is not the case for linear polarization.

The difference between the amplitudes of left-handed and right-handed photons emitted by an electron moving at $v = 0.9c$ is smaller than the total amplitude by a factor $\sim 10^{-22}\,\omega_{\boldsymbol{k}}$. In order for this difference to constitute 1 % of the total amplitude we need to consider frequencies on the order of $\sim 10^{20}\,\mathrm{rad\,s^{-1}}$. However, as we shall see, it might still be possible to detect this effect at frequencies as low as $10^{18}\,\mathrm{rad\,s^{-1}}$.

For a particle with charge $\pm|e|$, we note from Eq.(3.4) that the angular distribution of the transition rate may be written as

$$R_{1,\lambda}(\omega_{\boldsymbol{k}},\phi) = \frac{\alpha}{2\pi}\frac{c}{v}\frac{|\mathcal{S}_{1,\lambda}|^2}{S_{\boldsymbol{k}}}\ , \tag{4.31}$$

Applying the basis of circularly polarized light to Eq.(4.26), we define the angular distribution of the difference between the transition rates of the two modes as

$$\begin{aligned}\Delta R_{1,+}(\phi) &\equiv R_{1,+}(\phi) - R_{1,-}(\phi)\\ &= -\frac{\alpha}{2\pi}\frac{c}{v}\frac{\hbar}{E}\int_{\omega_m}^{\omega_M}\mathrm{d}\omega_{\boldsymbol{k}}\omega_{\boldsymbol{k}}F(\chi,\phi)\ .\end{aligned} \tag{4.32}$$

For comparison, we also find the angular distribution of the total transition rate

$$\begin{aligned} R_1(\phi) &= R_{1,+}(\phi) + R_{1,-}(\phi) \\ &= \frac{\alpha}{2\pi}\frac{c}{v}\int_{\omega_m}^{\omega_M} \mathrm{d}\omega_{\boldsymbol{k}} \frac{|\mathcal{S}_1|^2}{S_{\boldsymbol{k}}} \,, \end{aligned} \tag{4.33}$$

which, as we may see, is simply uniform.

As previously mentioned, the difference between transition rates is smaller than the total transition rate by a factor $\sim 10^{-22}\,\omega_M$. However, we now wish to consider whether the absolute magnitude of the difference is large enough for it to be observable regardless of its small relative size. We set the length of the dielectric medium to $l = 1\,\mathrm{m}$, and calculate the angular distribution of the expected difference between the number of right-handed and left-handed photons emitted as an electron traverses the medium

$$\Delta N_{1,+}(\phi) \equiv \frac{R_{1,+}(\phi)}{v} \,. \tag{4.34}$$

This quantity may be evaluated numerically for arbitrary input parameters n, v, ω_m, ω_M, and χ.

Helicity 1/2

Let us first consider an incoming particle of helicity 1/2, by setting $\chi = 0$. The difference in rates is then independent of ϕ, as may be seen from Eq.(4.27), and we consider the difference in number of emitted photons over the entire cone by taking the trivial integral over ϕ. The result is plotted as a function of velocity in Figure 4.2 and Figure 4.3. Here we have also assumed $\omega_m \ll \omega_M$, and therefore evaluated the integrals with $\omega_m = 0$.

In Figure 4.2 we have considered an electron moving through water with a realistic upper bound on the photon frequency. The expected difference between the number of photons in each polarization mode is then no more than 0.25. If, however, we consider some hypothetical material with a coefficient of refraction $n = 1.3$ at frequencies up to $10^{18}\,\mathrm{rad\,s^{-1}}$, the expected difference in number of photons increases by four orders of magnitude, as illustrated in Figure 4.3. As previously outlined, this difference is smaller than the total number of emitted photons by a factor of $\sim 10^{-4}$, however, the absolute magnitude of the effect is still on the order of 2000 photons. If the absolute uncertainty of the detector used in the experiment is small enough, one might be able to detect this effect in spite of its small relative size.

Note also that in contrast to the relativistic correction to the Cherenkov angle, the absolute magnitude of this effect is greatest at velocities significantly above threshold. As a result, attempting to detect the polarization effect does not require the experiment to probe radiation at small angles of emission or fine-tune the velocity of the electron beam to just above threshold.

This effect is also sensitive to increases in n. Therefore, as in our treatment of the relativistic correction to the Cherenkov angle, we have plotted $\Delta N_{1,+}$

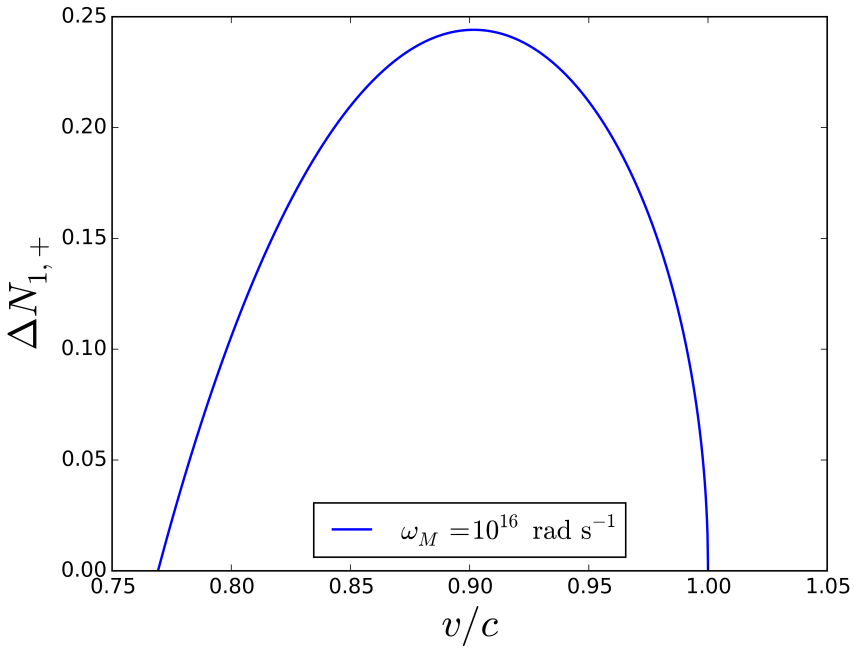

FIGURE 4.2: The difference between the number of right-handed photons and left-handed photons emitted per meter from an electron of helicity 1/2 moving through water, as a function of velocity.

for an electron moving through Gallium Arsenide in Figure 4.4. Here we see a significantly larger effect, which peaks at lower velocities.

We now consider some non-uniform photon emission distributions resulting from an initial electron polarized with $\chi \neq 0$.

Arbitrary Spinor Orientation

In this section we plot the angular density of the expected difference in number of photons, $\Delta N_{1,+}(\phi)$, for specific angles χ. In each case, we set the velocity to that for which the magnitude of the expected difference is maximal. The scenario under consideration is an electron moving through water. For aesthetic reasons we set the upper bound on photon frequency to $\omega_M = 10^{17}\,\mathrm{rad\,s^{-1}}$, such that $\Delta N_{1,+}(\phi)$ is on the order of ~ 10. Note that $\Delta N_{1,+}(\phi)$ is negative for certain ϕ. Polar plots are ill-suited for plotting negative valued functions, so we opt to plot the absolute value of the function and change the color of the graph to red wherever $\Delta N_{1,+}(\phi) < 0$. We see in Figures 4.5–4.7 various patterns of ϕ-dependence for the photon emission density. Due to this ϕ-dependence, a hypothetical experiment is not restricted to considering the difference in number of emitted photons at some angle ϕ in isolation. One may instead collect data at all ϕ simultaneously, and compare the observed distribution with the predictions shown in the figures. Such an experiment potentially allows for significantly enhanced precision compared to one where no ϕ-dependence is involved.

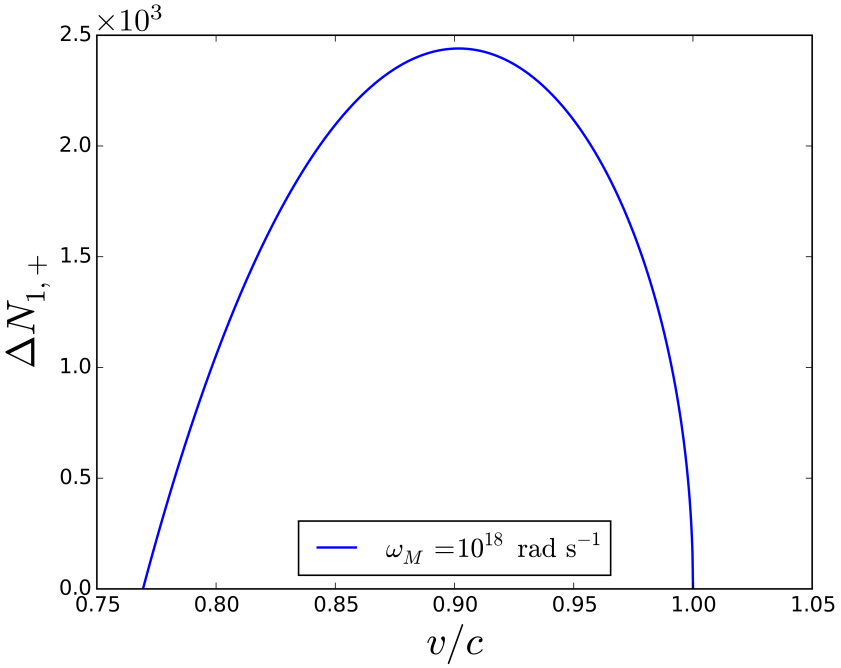

FIGURE 4.3: The difference between the number of right-handed photons and left-handed photons emitted from an electron of helicity 1/2 moving through water, as a function of velocity.

Velocity Dependence

Recalling the velocity dependence in Figure 4.2 and Figure 4.3, we now ask whether there is a similar velocity dependence in the difference in the number of emitted photons associated with other values of $\chi \neq 0$. As the previous section demonstrated, $\Delta N_{1,+}(\phi)$ is in general not uniform in ϕ. We must therefore be more specific. The point of interest is how $\Delta N_{1,+}(\phi)$ varies with velocity, not only for specific χ, but for specific ϕ as well. In Figures 4.8–4.10 we have evaluated the density of the difference in number of emitted photons, from an electron moving through one meter of water, numerically for various values of χ and ϕ, and plotted it as a function of velocity. As these figures illustrate, the velocity dependence of $\Delta N_{1,+}(\phi)$ varies with χ and ϕ, forming a characteristic curve for each orientation of the initial spinor. This serves as another potential source of information regarding the particle, such that it might be possible to determine the spin polarization of a beam more precisely by varying the velocity of the beam and comparing measurements to the predicted curves.

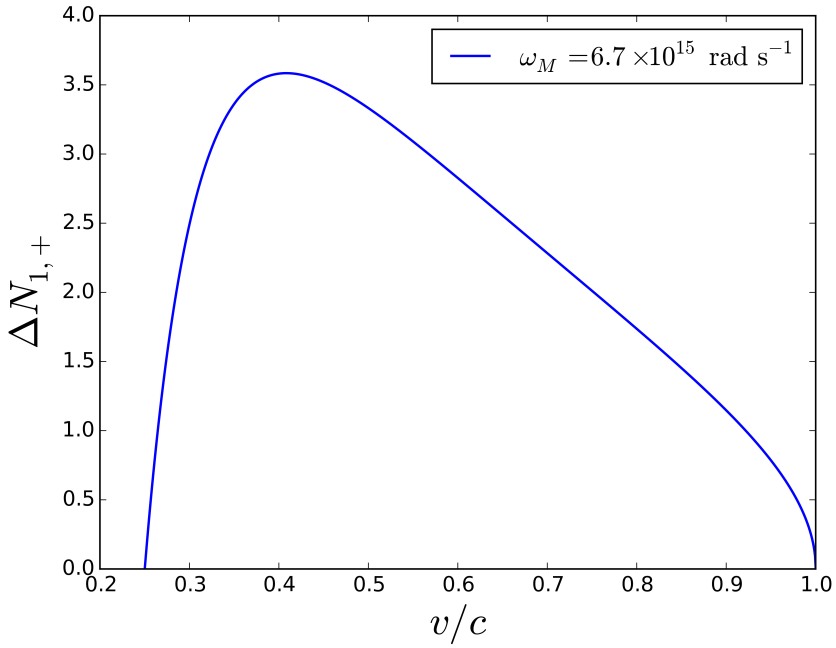

FIGURE 4.4: The difference between the number of right-handed photons and left-handed photons emitted from an electron of helicity 1/2 moving through one meter of Gallium Arsenide, as a function of velocity, for a realistic value of ω_M.

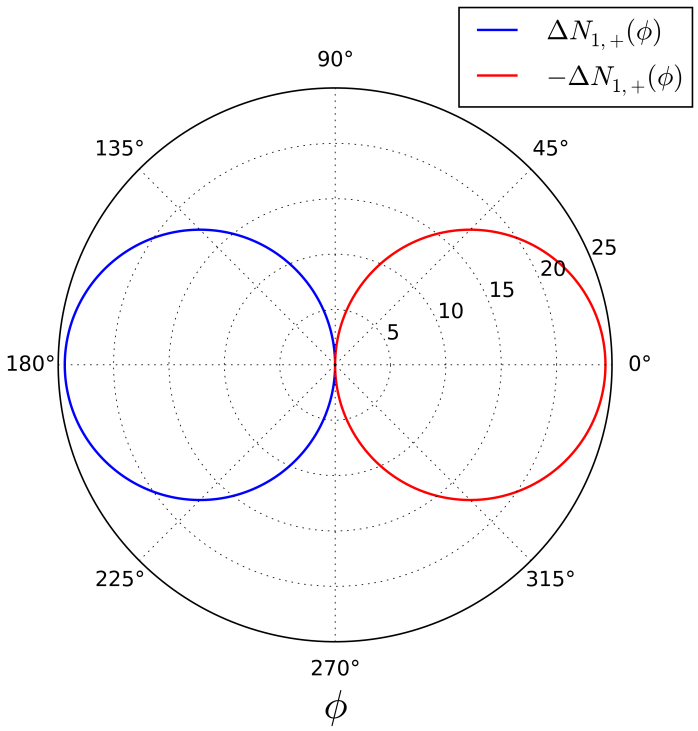

FIGURE 4.5: The angular distribution of the difference between the number of right-handed photons and left-handed photons emitted per meter, $\Delta N_{1,+}(\phi)$, from an electron moving through water. Plotted for $\chi = \frac{1}{2}\pi$, $v = 0.83c$, $\omega_M = 10^{17}\,\mathrm{rad\,s^{-1}}$.

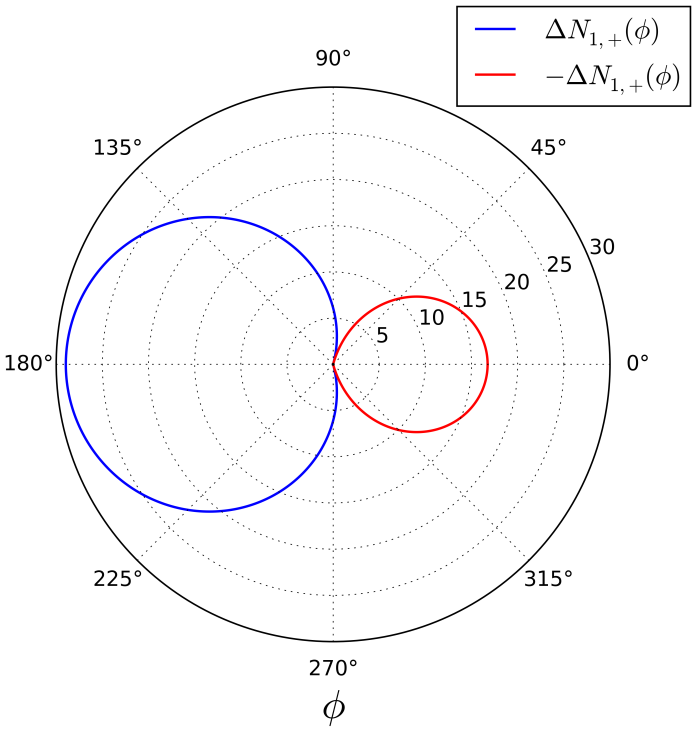

FIGURE 4.6: The angular distribution of the difference between the number of right-handed photons and left-handed photons emitted per meter, $\Delta N_{1,+}(\phi)$, from an electron moving through water. Plotted for $\chi = \frac{2}{5}\pi$, $v = 0.84c$, $\omega_M = 10^{17}\,\mathrm{rad\,s^{-1}}$.

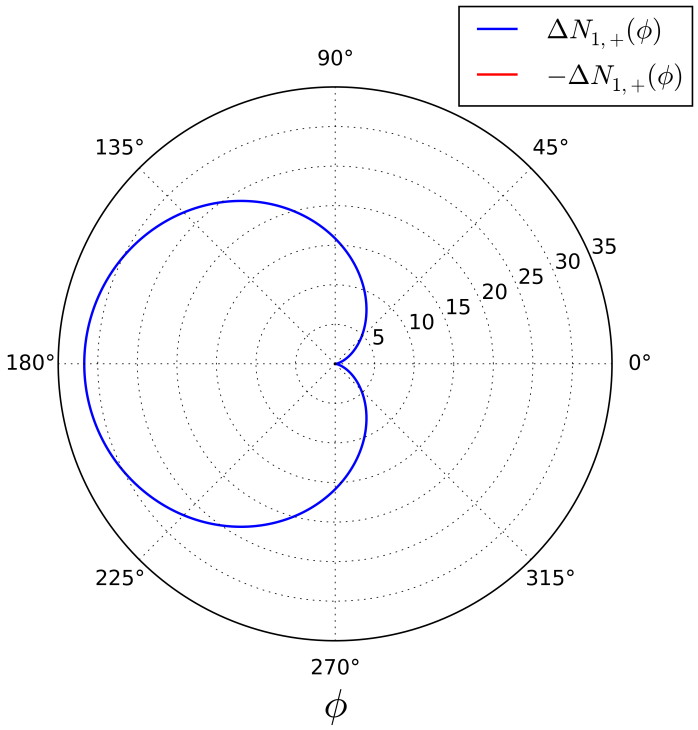

FIGURE 4.7: The angular distribution of the difference between the number of right-handed photons and left-handed photons emitted per meter, $\Delta N_{1,+}(\phi)$, from an electron moving through water. Plotted for $\chi = \frac{1}{4}\pi$, $v = 0.86c$, $\omega_M = 10^{17}\,\mathrm{rad\,s^{-1}}$.

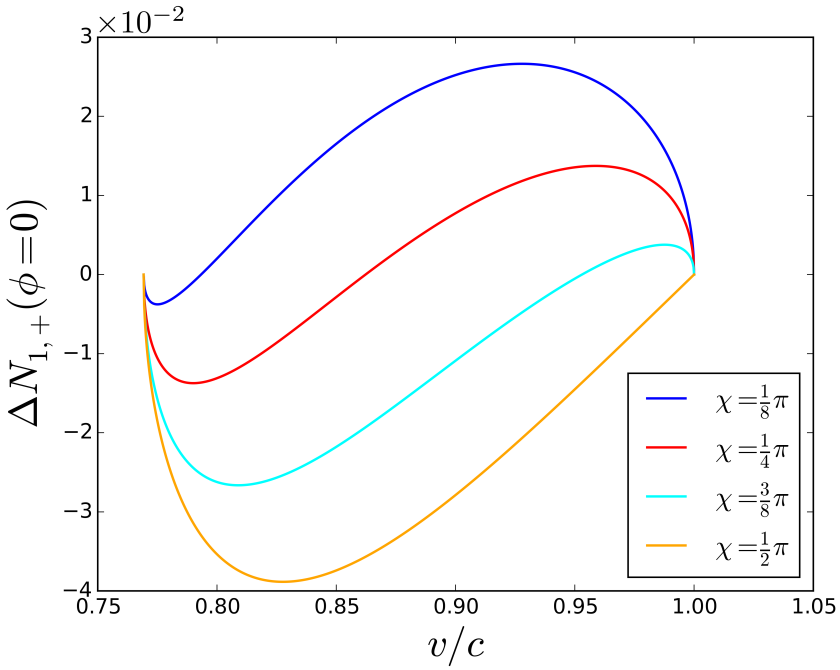

FIGURE 4.8: The angular density at $\phi = 0$ of the difference between the number of right-handed photons and left-handed photons emitted from an electron moving through one meter of water, as a function of velocity. Maximal frequency set to $\omega_M = 10^{16}\,\mathrm{rad\,s^{-1}}$.

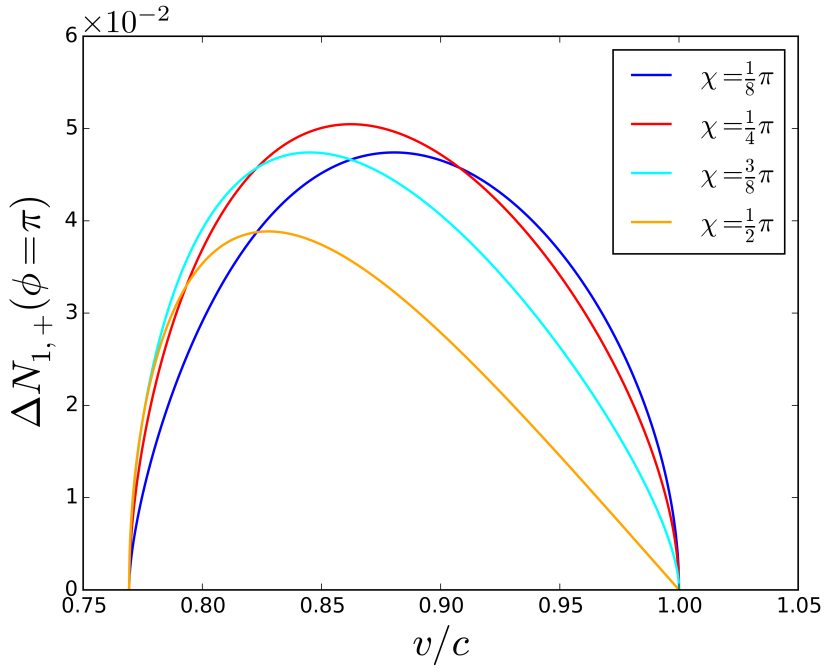

FIGURE 4.9: The angular density at $\phi = \pi$ of the difference between the number of right-handed photons and left-handed photons emitted from an electron moving through one meter of water, as a function of velocity. Maximal frequency set to $\omega_M = 10^{16}\,\mathrm{rad\,s^{-1}}$.

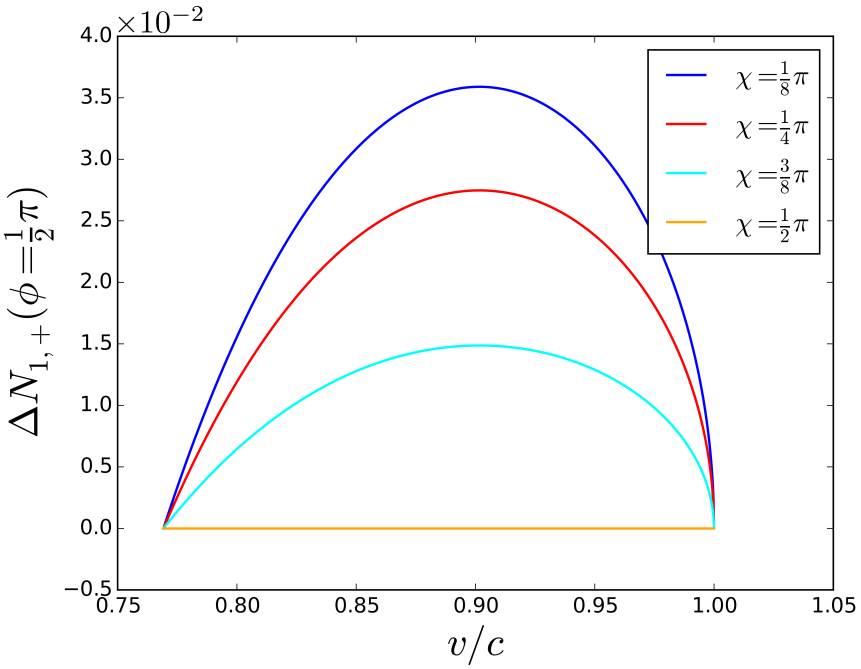

FIGURE 4.10: The angular density at $\phi = \frac{1}{2}\pi$ of the difference between the number of right-handed photons and left-handed photons emitted from an electron moving through one meter of water, as a function of velocity. Maximal frequency set to $\omega_M = 10^{16}\,\mathrm{rad\,s^{-1}}$.

5 Entanglement

Due to conservation of helicity, if an electron with helicity 1/2 emits a photon in the forward direction, the only physically possible process is that in which the spin of the electron flips and the emitted photon is right-handed (has helicity 1). This is the process corresponding to $\mathcal{S}_{1,2+}$. It is a simple matter to verify by Eqs.(4.2) that setting $\chi = 0$ and $\boldsymbol{k} \parallel \boldsymbol{p}$ results in $\mathcal{S}_{1,2-} = 0$ and $\mathcal{S}_{1,1\lambda} = 0$. In this event the final two-particle system is in a separable state denoted by $|\psi_{\boldsymbol{p}',2}\rangle\,|\boldsymbol{k}+\rangle$.

We consider the same scenario again, except now with the initial particle in a superposition of states with helicity 1/2 and $-1/2$. We set the state to

$$\frac{1}{\sqrt{2}}\Big(i\,|\psi_{\boldsymbol{p},1}\rangle + |\psi_{\boldsymbol{p},2}\rangle\Big)\,. \tag{5.1}$$

With this initial state, the amplitude $\mathcal{S}_{2,1-}$ also contributes to the emission of a photon. The state of the final two-particle system is now not separable. In fact the particles are maximally entangled. Normalizing the state of the final system, we arrive at one of the Bell basis states

$$\begin{aligned}&\frac{1}{|\mathcal{S}_{(1+2)}|}\Big(i\mathcal{S}_{1,2+}\,|\psi_{\boldsymbol{p}',2}\rangle\,|\boldsymbol{k}+\rangle + \mathcal{S}_{2,1-}\,|\psi_{\boldsymbol{p}',1}\rangle\,|\boldsymbol{k}-\rangle\Big)\\ &\qquad = \frac{1}{\sqrt{2}}\Big(|\psi_{\boldsymbol{p}',2}\rangle\,|\boldsymbol{k}+\rangle + |\psi_{\boldsymbol{p}',1}\rangle\,|\boldsymbol{k}-\rangle\Big)\,.\end{aligned} \tag{5.2}$$

Here we have noted from Eqs.(4.2) that $\mathcal{M}_{1,2+} = -i\mathcal{M}_{2,1-}$.

We wish to express the degree of entanglement in the final state, for a general state of the initial particle. To this end, we introduce the concurrence of a system as a measure of entanglement.

5.1 Concurrence

Adjusting the parameters χ and ϕ, the basis state $|\psi_{\boldsymbol{p},1}\rangle$ will correspond to some superposition of the helicity eigenstates. This allows us to consider entanglement in a general manner with regard to the state of the initial particle. Considering the event wherein an initial particle in the state $|\psi_{\boldsymbol{p},1}\rangle$ emits a photon with momentum $\boldsymbol{k}$, we write the normalized general state of the final

two-particle system as

$$\frac{1}{|\mathcal{S}_1|}\Big(\mathcal{S}_{1,1+}\left|\psi_{\boldsymbol{p}',1}\right\rangle\left|\boldsymbol{k}\alpha+\right\rangle+\mathcal{S}_{1,1-}\left|\psi_{\boldsymbol{p}',1}\right\rangle\left|\boldsymbol{k}\alpha-\right\rangle+ \\ \mathcal{S}_{1,2+}\left|\psi_{\boldsymbol{p}',2}\right\rangle\left|\boldsymbol{k}\alpha+\right\rangle+\mathcal{S}_{1,2-}\left|\psi_{\boldsymbol{p}',2}\right\rangle\left|\boldsymbol{k}\alpha-\right\rangle\Big)\,. \quad (5.3)$$

If this state is separable, it may be written on the form

$$\Big(a\left|\psi_{\boldsymbol{p}',1}\right\rangle+b\left|\psi_{\boldsymbol{p}',2}\right\rangle\Big)\otimes\Big(c\left|\boldsymbol{k}\alpha+\right\rangle+d\left|\boldsymbol{k}\alpha-\right\rangle\Big)\,. \quad (5.4)$$

Being able to decompose the state on this form is equivalent to stating that the quantity

$$C\equiv\frac{2}{|\mathcal{S}_1|}\left|\mathcal{S}_{1,1+}\mathcal{S}_{1,2-}-\mathcal{S}_{1,1-}\mathcal{S}_{1,2+}\right|\,, \quad (5.5)$$

equals zero. This quantity is referred to as the concurrence of the state [20]. For a maximally entangled state such as that given in Eq.(5.2), we have $C=1$, and for a separable state we have $C=0$. Due to this property, the concurrence serves as a useful measure of entanglement. The emitted photon is in general

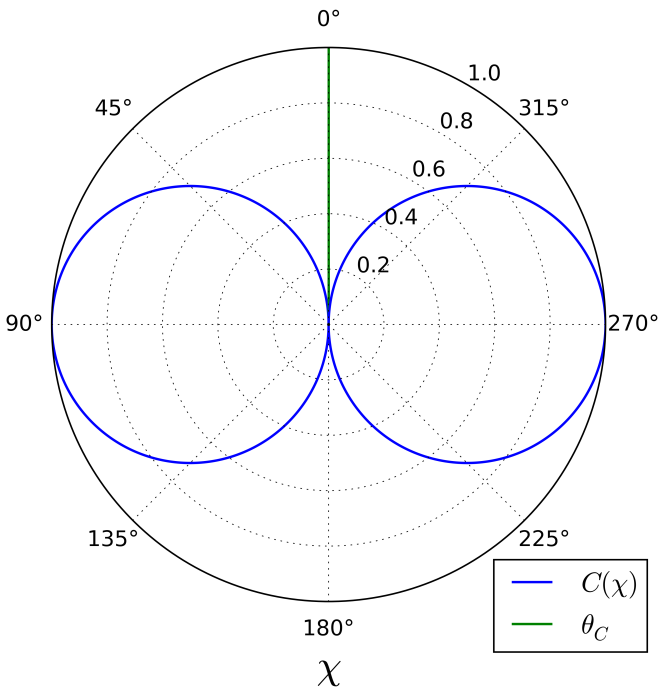

FIGURE 5.1: The concurrence, C, plotted as a function of χ for $\phi=0$ and $\phi=\pi$, represented by extending the range of χ on the polar axis. The direction of the emitted photon is illustrated by marking the angle θ_C. The system in question is an electron moving through water at $v=0.9c$, emitting a photon of frequency $\omega_{\boldsymbol{k}}=\omega_{\mathrm{MAX}}$ as given by Eq.(G.6).

entangled with the final particle. However, in the next section we will show that for any given momentum $\boldsymbol{k}$, of the emitted photon, there exists two orientations

of the initial spinor which result in a separable final state, and find analytical expressions for the corresponding parameters. Before doing so, however, we plot the concurrence as a function of χ in the plane given by $\phi = 0$ and $\phi = \pi$ as an initial qualitative approach.

Figure 5.1 confirms our initial two examples. If $\chi = 0$ the concurrence of the final state is zero, corresponding to a separable state. Conversely, if $\chi = \pi/2$, the concurrence of the final state is one, corresponding to a maximally entangled state. Additionally, although not shown in the figure, the concurrence is in this case independent of ϕ. If we were to plot the concurrence for all values of ϕ, the resulting shape would be a toroid.

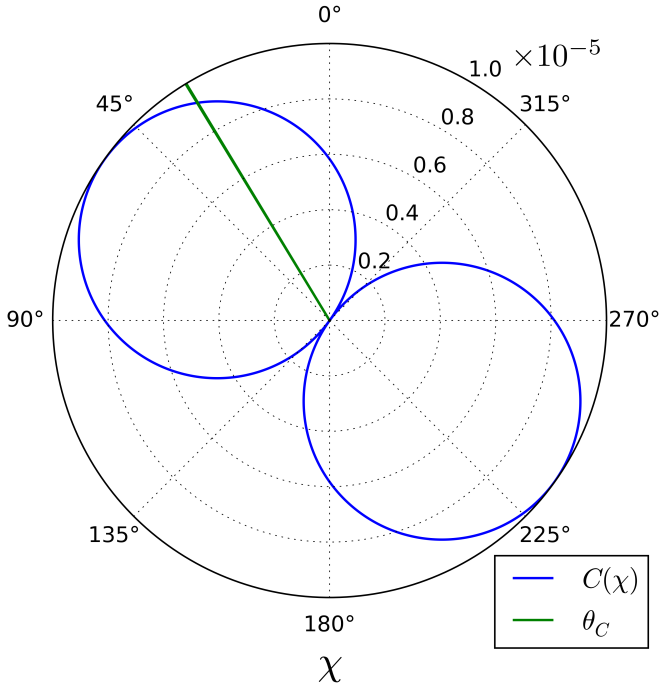

FIGURE 5.2: The concurrence, C, plotted as a function of χ for $\phi = 0$ and $\phi = \pi$, represented by extending the range of χ on the polar axis. The direction of the emitted photon is illustrated by marking the angle θ_C. The system in question is an electron moving through water at $v = 0.9c$, emitting a photon of frequency $\omega_{\boldsymbol{k}} = 10^{16}\,\mathrm{rad\,s^{-1}}$.

In Figure 5.2 we see a more general example, where the photon is not emitted in the forward direction. The toroidal shape remains, however, the axis of revolution is now tilted away from the path of the particle. We also see that the concurrence is in general quite small, here being on the order of $\sim 10^{-5}$.

Finally, Figure 5.3 shows an event occurring close to threshold velocity. Although the photon is emitted nearly parallel to the path of the particle, the toroid is here nearly perpendicular to the one shown in Figure 5.1. This demonstrates the distinction between an event where the Cherenkov angle approaches zero due to the classical dependence on velocity, and an event where the Cherenkov angle approaches zero due to the relativistic dependence on photon frequency.

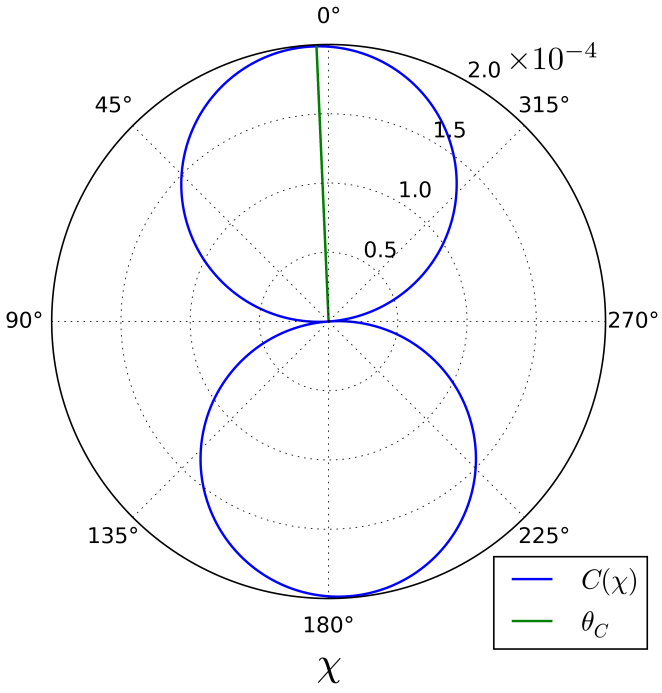

FIGURE 5.3: The concurrence, C, plotted as a function of χ for $\phi = 0$ and $\phi = \pi$, represented by extending the range of χ on the polar axis. The direction of the emitted photon is illustrated by marking the angle θ_C. The system in question is an electron moving through water at $v = 0.77c\,(= 1.001c/n)$, emitting a photon of frequency $\omega_{\boldsymbol{k}} = 10^{16}\,\mathrm{rad\,s^{-1}}$.

Hypothetically, if an experiment could set the velocity of a transversely polarized initial particle so close to threshold that the maximal frequency by Eq.(G.6) would lie within the frequency range where $n > 1$, it would be possible to observe the degree of entanglement in the final state to vary between 0 and 1 with the frequency of the emitted photon. However, such an experiment is probably not feasible, as it faces the same challenges outlined for relativistic corrections in Chapter 3.

5.2 Separable States

In this section we will show analytically that for any given $\boldsymbol{k}$ there exists parameters χ_0 and ϕ_0 such that the final state is separable. If the state of a two-particle system is separable, either component particle will be left in a pure quantum state after summing over the states of the other particle. To look for such states of our system, we therefore sum over the states of the final charged particle, then find a basis of polarization by the parameter α such that the state of the photon is $|\boldsymbol{k}\alpha_0+\rangle$. In other words, we find the parameters α_0, χ_0, and ϕ_0 by requiring that $|\mathcal{S}_{1,-}|^2$ becomes zero. As the squared modulus of the amplitude is a positive number, we note that any zero of the function must coincide with a global minimum. We therefore begin by finding the extrema of the amplitude with respect to α

Minimal Basis

To find the extrema of the amplitude, we set the partial derivative to zero

$$\frac{\partial}{\partial\alpha}|\mathcal{S}_{1,-}|^2 = S_{\boldsymbol{k}}\left(\frac{v^2}{c^2}\sin^2\theta_C\sin(2\alpha) + \cos(2\alpha)\frac{\hbar\omega_{\boldsymbol{k}}}{E}F(\chi,\phi)\right) = 0\ . \tag{5.6}$$

Thus, for a given spinor orientation, χ, ϕ, there are polarization bases given by $\alpha = \alpha_0$ for which $|\mathcal{S}_{1,-}|^2$ is extremal, where

$$\tan(2\alpha_0) = -\frac{\hbar\omega_{\boldsymbol{k}}}{2E}\frac{F(\chi,\phi)}{\frac{1}{2}\frac{v^2}{c^2}\sin^2\theta_C}\ . \tag{5.7}$$

Recalling α is restricted to the range $[0,\pi/2]$, we have two extrema of the amplitude: a minimum corresponding to the $\cos(2\alpha_0) \geq 0$ solution, and a maximum corresponding to the $\cos(2\alpha_0) < 0$ solution.

Inserting the $\cos(2\alpha_0) \geq 0$ solution in Eq.(4.26), we write the amplitude in the minimal basis as

$$|\mathcal{S}_{1,-}|^2\big|_{\alpha_0} = S_{\boldsymbol{k}}\Bigg(\frac{1}{2}\frac{v^2}{c^2}\sin\theta_C + \left(\frac{\hbar\omega_{\boldsymbol{k}}}{2E}\right)^2(n^2-1) - \sqrt{\left(\frac{1}{2}\frac{v^2}{c^2}\sin^2\theta_C\right)^2 + \left(\frac{\hbar\omega_{\boldsymbol{k}}}{2E}\right)^2 F^2(\chi,\phi)}\Bigg)\ . \tag{5.8}$$

Here we have applied the trigonometric identity $\cos(\arctan(x)) = 1/\sqrt{1+x^2}$. From Eq.(5.8) we see that the amplitude is zero when

$$F^2(\chi,\phi) = \left(\frac{nv}{c} - \cos\theta_C\right)^2 + \frac{1}{\gamma^2}\sin^2\theta_C\ . \tag{5.9}$$

Here we have applied the relativistic definition of the Cherenkov angle, Eq.(2.99), in order to simplify.

Extremal Angles

Considering the form of Eq.(4.26), we see that a zero of the amplitude for left-handed light must correspond to a minimum of $F(\chi,\phi)$. We will therefore locate the global minimum, χ_0, ϕ_0, and show that $F(\chi_0,\phi_0)$ fulfils the condition given in Eq.(5.9). Setting the partial derivative with regard to ϕ to zero

$$\frac{\partial}{\partial\phi}F(\chi,\phi) = -\frac{1}{\gamma}\sin\chi\sin\phi\sin\theta_C = 0\ , \tag{5.10}$$

we have extrema at $\phi = 0$ and $\phi = \pi$. Setting the partial derivative with regard to χ to zero

$$\frac{\partial}{\partial\chi}F(\chi,\phi) = \frac{1}{\gamma}\cos\chi\cos\phi\sin\theta_C - \sin\chi\left(\cos\theta_C - \frac{nv}{c}\right) = 0\ , \tag{5.11}$$

we have extrema when

$$\tan\chi = \frac{\sin\theta_C\cos\phi}{\gamma(\cos\theta_C - nv/c)} \ . \tag{5.12}$$

Keeping in mind that $0 \leq \chi \leq \pi$ we conclude that the minimum of $F(\chi,\phi)$ is located at

$$\phi_0 = \pi \ , \tag{5.13}$$

and

$$\chi_0 = \arctan\left(\frac{\sin\theta_C}{\gamma(nv/c - \cos\theta_C)}\right) \ . \tag{5.14}$$

Evaluating $F(\chi_0,\phi_0)$ by Eq.(4.27), we find

$$F(\chi_0,\phi_0) = -\sqrt{\left(\frac{nv}{c} - \cos\theta_C\right)^2 + \frac{1}{\gamma^2}\sin^2\theta_C} \ , \tag{5.15}$$

which clearly fulfils the condition given in Eq.(5.9). Thus, for a given $\boldsymbol{k}$-vector there will always exist some spinor orientation, χ_0, ϕ_0, for which the photon is emitted in a pure state. Said pure state may be described as the state $|\boldsymbol{k}\alpha_0+\rangle$.

Having proven that a zero of the amplitude exists, we can find an explicit expression for α_0 by setting $|\mathcal{S}_{1,-}|^2 = 0$, which by Eq.(4.26) gives

$$F(\chi,\phi) = -\frac{2E}{\hbar\omega_{\boldsymbol{k}}}\frac{v^2}{c^2}\frac{\sin^2\theta_C\sin^2\alpha_0}{\sin(2\alpha_0)} - \frac{\hbar\omega_{\boldsymbol{k}}}{2E}\frac{(n^2-1)}{\sin(2\alpha_0)} \ . \tag{5.16}$$

Combining this with Eq.(5.7), we find

$$\cos(2\alpha_0) = \frac{\frac{1}{2}\frac{v^2}{c^2}\sin^2\theta_C}{\frac{1}{2}\frac{v^2}{c^2}\sin^2\theta_C + \left(\frac{\hbar\omega_{\boldsymbol{k}}}{2E}\right)^2(n^2-1)} \ . \tag{5.17}$$

This expression may also be reformulated as

$$\sin^2\alpha_0 = \frac{|\mathcal{S}_{1,2}|^2}{|\mathcal{S}_1|^2} \ . \tag{5.18}$$

Without commenting on this more rigorously, we can see intuitively that this relates to the definition of our elliptical basis vectors as superpositions of the linear polarization vectors by Eq.(2.63) and Eq.(2.64).

As we may see from the figures of Section **??**, there is a second spinor orientation corresponding to a separable state. Determining this orientation proceeds by the same math as presented above, but setting instead $|\mathcal{S}_{1,+}|^2 = 0$. Without doing so explicitly, we simply state that the second separable state occurs at $\chi = \pi - \chi_0$ and $\phi = 0$.

6 Conclusion

Modelling the source of Cherenkov radiation as a general spin polarized relativistic plane-wave introduces effects beyond the established relativistic corrections to the phenomenon. Said effects pertain to the polarization of emitted light, as presented in Chapter 4 (notably in Eq.(4.26)), and to the degree of entanglement between photon and charged particle, as presented in Chapter 5. Inquiry into the question of whether it would be possible to detect such effects experimentally is inconclusive. However, in particular the polarization effects presented in this thesis are potentially far simpler to detect than the established relativistic corrections as outlined in Chapter 3. This is primarily due to the ϕ-dependence of the effects, and the fact that they are present at velocities significantly above threshold.

If spin polarization effects were to be detected in accordance with the analysis of Chapter 4, they would have potential applications in experiment. A RICH-detector modified to register the angular distribution of polarized photons could be used to study the spin degrees of freedom of an electron beam. Such a device could prove a valuable experimental tool.

The effects are also interesting from a theoretical perspective. Presently, there is no classical theory of analogous effects, and intuitively it seems it would be challenging to construct such a theory within the assumptions presented in Section 2.1. Furthermore, if the phenomenon was to best be described as a charged particle interacting with an ensemble of dipoles, thereby causing them to radiate, it seems peculiar it should be possible for said particle to emerge from the medium in a pure quantum state, i.e., without having become entangled with any of the dipoles of the ensemble. In the event that the results of this thesis were to be confirmed experimentally, they would potentially constitute a compelling argument that it is in fact the charged particle itself which emits radiation.

Main desirable qualities of the material for the observation of relativistic effects in quantum mechanical Cherenkov radiation are as follows:

- As large a refraction coefficient, n, as possible.
- Dielectric properties at as high a frequency as possible.
- Penetrability to electrons. Although one may consider performing experiments with vacuum or waveguide channels allowing electrons to pass through an impenetrable medium.
- Homogeneity, in order to avoid the influence of unrelated effects on the experiment. The present results also assume the medium is isotropic, however, we have not considered whether anisotropic media would attenuate or amplify spin polarization effects.

It appears that the properties of currently known dielectrics lie just at the edge of what is required to observe the polarization effects discussed in the present thesis. It may perhaps be possible to employ metamaterials or other materials with exotic properties in order to detect these effects, however, such speculations are outside the scope of the thesis. One may also speculate that corresponding effects of greater magnitude may be present for spin-1 particles, as opposed to the spin-1/2 particles considered in the present thesis. Spin-1 particles are common subjects in RICH-detectors [5], and so it may be a worthwhile future endeavour to evaluate spin polarization effects for particles of integer spin as well. As a final cautionary remark, we note that the present discussion does not take into account dispersion, absorption, or scattering in the medium, and it is uncertain how these factors will affect the prospect of detecting spin polarization effects in practice.

A Notation and Conventions

Mathematics

Vectors are denoted by boldface symbols, $\boldsymbol{r}$, and the scalar product by $\boldsymbol{r}\cdot\boldsymbol{k}$. The norm of a vector is denoted $|\boldsymbol{r}| = r$. Vectors of unit length are denoted by a hat

$$\boldsymbol{r} = r\hat{\mathbf{r}} = x\hat{\mathbf{x}} + y\hat{\mathbf{y}} + z\hat{\mathbf{z}} \ . \tag{A.1}$$

The nabla operator is defined, in Cartesian and cylindrical coordinates respectively, as

$$\boldsymbol{\nabla} = \hat{\mathbf{x}}\frac{\partial}{\partial x} + \hat{\mathbf{y}}\frac{\partial}{\partial y} + \hat{\mathbf{z}}\frac{\partial}{\partial z} \ , \qquad \boldsymbol{\nabla} = \hat{\boldsymbol{\rho}}\frac{\partial}{\partial \rho} + \hat{\boldsymbol{\phi}}\frac{1}{\rho}\frac{\partial}{\partial \phi} + \hat{\mathbf{z}}\frac{\partial}{\partial z} \ . \tag{A.2}$$

The Laplace operator is defined, in Cartesian and cylindrical coordinates respectively, as

$$\nabla^2 = \frac{\partial^2}{\partial x^2} + \frac{\partial^2}{\partial y^2} + \frac{\partial^2}{\partial z^2} \ , \qquad \nabla^2 = \frac{\partial^2}{\partial \rho^2} + \frac{1}{\rho}\frac{\partial}{\partial \rho} + \frac{1}{\rho^2}\frac{\partial^2}{\partial \phi^2} + \frac{\partial^2}{\partial z^2} \ . \tag{A.3}$$

Fourier transforms use the following convention:

$$f(t) = \int_{-\infty}^{\infty} \frac{\mathrm{d}\omega}{2\pi} e^{i\omega t} f(\omega) \ , \qquad f(\omega) = \int_{-\infty}^{\infty} \mathrm{d}t e^{-i\omega t} f(t) \ , \tag{A.4}$$

$$f(\boldsymbol{r}) = \int_{-\infty}^{\infty} \frac{\mathrm{d}^3\boldsymbol{k}}{(2\pi)^3} e^{-i\boldsymbol{k}\cdot\boldsymbol{r}} f(\boldsymbol{k}) \ , \qquad f(\boldsymbol{k}) = \int_{-\infty}^{\infty} \mathrm{d}^3\boldsymbol{r} e^{i\boldsymbol{k}\cdot\boldsymbol{r}} f(\boldsymbol{r}) \ . \tag{A.5}$$

Physical Quantities

Unless noted otherwise, this thesis makes use of SI-units.

The permittivity and permeability of a linear medium are denoted $\epsilon\epsilon_0$ and $\mu\mu_0$ respectively, where ϵ_0 and μ_0 denote the permittivity and permeability of the vacuum, given by $\epsilon_0 = 1/\mu_0 c^2$. Additionally, the index of refraction is given by $n = \sqrt{\epsilon\mu}$.

Transition amplitudes in perturbation theory are denoted by

$$\mathcal{M}_{i,f} \equiv \langle f | \, H' \, | i \rangle \ , \tag{A.6}$$

where H' denotes the perturbation to the Hamiltonian. Summation over the states of a system is indicated by suppressing the corresponding subscript, e.g.,

$$|\mathcal{M}_i|^2 \equiv \sum_f |\, \langle f | \, H' \, | i \rangle \, |^2 \ . \tag{A.7}$$

B Tables

TABLE B.1: Some noteworthy coefficients of refraction. These are approximate values, as the coefficient of refraction in general depends on wavelength.

Material	n	at wavelength
water [2, p. 457]	1.34	500 nm
Gallium Arsenide [3]	4	270 nm
silica aerogel [4]	1.03	400 nm
C_4F_{10} [4]	1.0014	400 nm

TABLE B.2: Some noteworthy frequencies of light.

	ω ($\times 10^{15}\,\mathrm{rad\,s^{-1}}$)	$\hbar\omega$ (eV)	λ (nm)
ultraviolet C	6.73–18.8	4.44–12.4	280–100
LHCb RICH range [5]	3.14–9.42	2.07–6.21	600–200
visible light	2.51–4.96	1.65–3.26	750–380
electron rest energy equivalent	7.76×10^5	5.11×10^5	2.43×10^{-3}

C Delta Functions

The Dirac delta function $\delta(x)$ is defined as a distribution with the property

$$\int_{-\infty}^{\infty} \mathrm{d}x f(x)\delta(x) = f(0) \; . \tag{C.1}$$

In particular, we have

$$\lim_{\mu\to 0^-} \lim_{\nu\to 0^+} \int_{\mu}^{\nu} \mathrm{d}x\delta(x) = 1 \; . \tag{C.2}$$

One possible representation of the delta function is the limit of a box function with unit area

$$\delta(x) = \lim_{\epsilon\to 0} \begin{cases} \dfrac{1}{\epsilon} \; , & \text{if} \quad |x| \leq \epsilon \; , \\ 0 \; , & \text{if} \quad |x| > \epsilon \; . \end{cases} \tag{C.3}$$

Owing to the property of Eq.(C.1), the fourier transform of the delta function is simply $\delta(k) = 1$. Thus an alternative representation of the delta function is

$$\delta(x) = \int_{-\infty}^{\infty} \frac{\mathrm{d}k}{2\pi} e^{-ikx} \; . \tag{C.4}$$

When a plane is mapped in polar coordinates ρ, ϕ, it may be desirable to define a "radial delta function" $\delta_\rho(\rho)$ in order to emphasize the symmetry of the distribution with respect to rotation about the origin. Similarly to the expression $\delta(x)\delta(y)$, such a function should integrate to one on an infinitesimal area about the origin. Expressing this requirement in polar coordinates, we find that the radial delta function has the property

$$\lim_{\rho'\to 0} \int_{0}^{\rho'} \mathrm{d}\rho\rho\delta_\rho(\rho) = \frac{1}{2\pi} \; . \tag{C.5}$$

One possible representation of a radial delta function exhibiting this property is the limit of a rotationally symmetric step function:

$$\delta_\rho(\rho) = \lim_{\epsilon\to 0} \begin{cases} \dfrac{1}{\pi\epsilon^2} \; , & \text{if} \quad \rho \leq \epsilon \; , \\ 0 \; , & \text{if} \quad \rho > \epsilon \; . \end{cases} \tag{C.6}$$

D Hankel Functions

From Ref. [21].
In cylindrical systems one encounters the Bessel differential equation:

$$x^2 \frac{\mathrm{d}^2}{\mathrm{d}x^2} f(x) + x \frac{\mathrm{d}}{\mathrm{d}x} f(x) + (x^2 + \alpha^2) f(x) = 0 \; . \tag{D.1}$$

This equation has two linearly independent solutions: One which is regular in the origin, called the Bessel function of the first kind $J_\alpha(x)$, and one which is divergent in the origin, called the Bessel function of the second kind $Y_\alpha(x)$. Additionally, any linear combination of these solutions also constitutes a solution of the equation. When we wish to model waves in the system described by Eq. (D.1), the most convenient solutions are what we call the Hankel functions, also known as Bessel functions of the third kind:

$$H_\alpha^{(1)}(x) = J_\alpha(x) + i Y_\alpha(x) \; , \tag{D.2}$$

$$H_\alpha^{(2)}(x) = J_\alpha(x) - i Y_\alpha(x) \; . \tag{D.3}$$

In the large argument limit, the asymptotic forms of these functions are proportional to $e^{\pm ix}$. Specifically, for the case of $\alpha = 0$, the asymptotic forms are:

For $x \gg 1$:

$$H_0^{(1)}(x) = \sqrt{\frac{2}{\pi x}} e^{i(x - \pi/4)} \; , \tag{D.4}$$

$$H_0^{(2)}(x) = \sqrt{\frac{2}{\pi x}} e^{-i(x - \pi/4)} \; . \tag{D.5}$$

For $0 < x \ll 1$:

$$H_0^{(1)}(x) = 1 + i \frac{2}{\pi} (\ln(x/2) + \gamma) \; , \tag{D.6}$$

$$H_0^{(2)}(x) = 1 - i \frac{2}{\pi} (\ln(x/2) + \gamma) \; . \tag{D.7}$$

Here $\gamma = 0.57721...$ denotes the Euler-Mascheroni constant.

E Pauli Matrices

From Ref. [22, p. 433].
The Pauli matrices are a set of three traceless 2×2 matrices defined as

$$\sigma_1 = \begin{pmatrix} 0 & 1 \\ 1 & 0 \end{pmatrix} , \tag{E.1}$$

$$\sigma_2 = \begin{pmatrix} 0 & -i \\ i & 0 \end{pmatrix} , \tag{E.2}$$

$$\sigma_3 = \begin{pmatrix} 1 & 0 \\ 0 & -1 \end{pmatrix} . \tag{E.3}$$

They are Hermitian and unitary, and obey the relations

$$\sigma_i \sigma_j = \delta_{ij} + i\epsilon_{ijk}\sigma_k . \tag{E.4}$$

and

$$\sigma_i \sigma_j = 2\delta_{ij} - \sigma_j \sigma_i , \tag{E.5}$$

Here ϵ_{ijk} is the Levi-Civita symbol, with the convention $\epsilon_{123} = 1$. The trace of products of Pauli matrices is of particular interest in the evaluation of transition amplitudes. As the Pauli matrices are traceless, Eq.(E.4) implies

$$\mathrm{Tr}\left\{\sigma_i \sigma_j\right\} = 2\delta_{ij} . \tag{E.6}$$

Using Eq.(E.5) to iteratively commute the Pauli matrices, and evaluating the remaining traces by Eq.(E.6) as we go, gives

$$\mathrm{Tr}\left\{\sigma_i \sigma_l \sigma_j \sigma_m\right\} = 4\delta_{il}\delta_{jm} - 4\delta_{ij}\delta_{lm} + 4\delta_{im}\delta_{jl} - \mathrm{Tr}\left\{\sigma_i \sigma_l \sigma_j \sigma_m\right\} , \tag{E.7}$$

i.e.,

$$\mathrm{Tr}\left\{\sigma_i \sigma_l \sigma_j \sigma_m\right\} = 2\delta_{il}\delta_{jm} + 2\delta_{im}\delta_{jl} - 2\delta_{ij}\delta_{lm} . \tag{E.8}$$

F The Dirac Equation

We consider a particle with momentum $\boldsymbol{p}$ and mass m, in a Cartesian coordinate system defined by the unit vectors $\hat{\mathbf{e}}_1$, $\hat{\mathbf{e}}_2$, and $\hat{\mathbf{e}}_3$, as illustrated in Figure F.1.

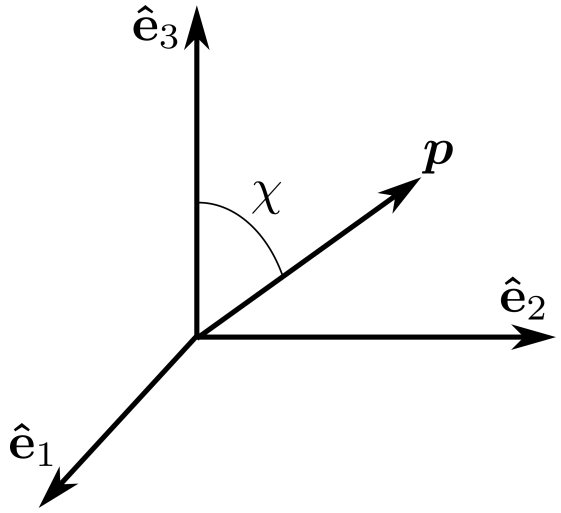

FIGURE F.1: The momentum vector $\boldsymbol{p}$, making an angle β with the 3-axis of the coordinate system.

The relativistic energy-momentum relation for a massive particle is

$$E = \sqrt{p^2c^2 + m^2c^4} \; . \tag{F.1}$$

Writing the Hamiltonian in terms of the momentum operator, we wish to avoid the square root in Eq.(F.1). As Dirac discovered in 1928 [23], this can be done by introducing non-commuting coefficients $\boldsymbol{\alpha} = (\alpha_1, \alpha_2, \alpha_3)$, and β

$$H_D = \left(c\boldsymbol{\alpha} \cdot \boldsymbol{p} + \beta mc^2\right) \; . \tag{F.2}$$

These coefficients are defined by the relations

$$\begin{aligned} \alpha_i^2 = \beta^2 = 1 \; , \\ \alpha_i\alpha_j + \alpha_j\alpha_i = 0 \; , \quad i \neq j \\ \alpha_i\beta + \beta\alpha_i = 0 \; , \end{aligned} \tag{F.3}$$

and may be represented by 4×4 matrices. Here, we shall use the representation

$$\boldsymbol{\alpha} = \begin{pmatrix} 0 & \boldsymbol{\sigma} \\ \boldsymbol{\sigma} & 0 \end{pmatrix} \; , \quad \beta = \begin{pmatrix} 1 & 0 \\ 0 & -1 \end{pmatrix} \; , \tag{F.4}$$

where $\boldsymbol{\sigma} = (\sigma_1, \sigma_2, \sigma_3)$ denotes a vector comprised of the Pauli matrices (See Appendix E). One may easily observe from Eq.(F.4) that a product of α- and β-matrices is traceless if either the number of α-matrices or the number of β-matrices is odd. Otherwise, the β-matrices may be eliminated by commutation, Eqs.(F.3), and we have

$$\mathrm{Tr}\left\{\alpha_i \dots \alpha_m\right\} = 2\mathrm{Tr}\left\{\sigma_i \dots \sigma_m\right\} \ . \tag{F.5}$$

Applying this notation, the Schrödinger equation of motion in the position representation reads

$$i\hbar\frac{\partial}{\partial t}\Psi(\boldsymbol{r},t) = \left(-i\hbar c\boldsymbol{\alpha}\cdot\boldsymbol{\nabla} + \beta mc^2\right)\Psi(\boldsymbol{r},t) \ . \tag{F.6}$$

This matrix equation is called the Dirac equation, and we suggest a plane wave solution

$$\Psi_{\boldsymbol{p},s}(\boldsymbol{r},t) = u(\boldsymbol{p},s)e^{-iE_{\boldsymbol{p}}t/\hbar}e^{i\boldsymbol{p}\cdot\boldsymbol{r}/\hbar} \ , \tag{F.7}$$

where u is a column matrix called a spinor. Inserting the plane wave solution in the Dirac equation, Eq.(F.6), we get an equation for the spinor

$$(E_{\boldsymbol{p}} - c\boldsymbol{\alpha}\cdot\boldsymbol{p} - \beta mc^2)u(\boldsymbol{p},s) = 0 \ . \tag{F.8}$$

This equation has four independent solutions which will not be derived here (see, e.g., Ref. [22, Chapter 7.1]). We write these solutions as two "particle states" with $E_{\boldsymbol{p}} = E$

$$u(\boldsymbol{p},1) = N\begin{pmatrix} 1 \\ 0 \\ \dfrac{cp_3}{E+mc^2} \\ \dfrac{cp_+}{E+mc^2} \end{pmatrix} \ , \tag{F.9}$$

$$u(\boldsymbol{p},2) = N\begin{pmatrix} 0 \\ 1 \\ \dfrac{cp_-}{E+mc^2} \\ \dfrac{-cp_3}{E+mc^2} \end{pmatrix} \ , \tag{F.10}$$

and two "antiparticle states" with $E_{\boldsymbol{p}} = -E$

$$u(\boldsymbol{p},3) = N \begin{pmatrix} \dfrac{-cp_3}{E+mc^2} \\ \dfrac{-cp_+}{E+mc^2} \\ 1 \\ 0 \end{pmatrix} , \tag{F.11}$$

$$u(\boldsymbol{p},4) = N \begin{pmatrix} \dfrac{-cp_-}{E+mc^2} \\ \dfrac{cp_3}{E+mc^2} \\ 0 \\ 1 \end{pmatrix} . \tag{F.12}$$

Note that E is still defined by Eq.(F.1). We have also defined $p_\pm = p_1 \pm ip_2$, and a normalization factor

$$N = \sqrt{\frac{E+mc^2}{2E}} , \tag{F.13}$$

chosen such that $u^\dagger u = 1$.

The particle states solve $(E - H_D)u = 0$, whereas the antiparticle states solve $(E + H_D)u = 0$. Using this, we construct projection operators,

$$P_+ = \frac{E + H_D}{2E} , \tag{F.14}$$

$$P_- = \frac{E - H_D}{2E} , \tag{F.15}$$

which project any spinor onto the particle states or the antiparticle states respectively. These operators are Hermitian, and obey the property

$$P_\pm^2 = P_\pm . \tag{F.16}$$

It may also be shown that the set of states is complete

$$\sum_s u_i(\boldsymbol{p},s) u_j^\dagger(\boldsymbol{p},s) = \delta_{ij} . \tag{F.17}$$

G Ginzburg's Energy Conservation

From Ref. [7].

Conservation of energy requires that the initial and final energies in a process are equal. In the case of Cherenkov radiation, this requirement reads

$$E_{\boldsymbol{p}} = E_{\boldsymbol{p}'} + \hbar\omega_{\boldsymbol{k}} \; . \tag{G.1}$$

Squaring this equation and applying the relativistic energy-momentum relation $E^2 = p^2c^2 + m^2c^4$, we have

$$p'^2c^2 = p^2c^2 + \hbar^2\omega_{\boldsymbol{k}}^2 - 2\hbar\omega_{\boldsymbol{k}}E_{\boldsymbol{p}} \; . \tag{G.2}$$

Conservation of momentum requires $\boldsymbol{p}' = \boldsymbol{p} - \hbar\boldsymbol{k}$. Thus, defining θ to be the angle between $\boldsymbol{p}$ and $\boldsymbol{k}$, we may write

$$c^2\hbar^2k^2 - 2c^2\hbar pk\cos\theta = \hbar^2\omega_{\boldsymbol{k}}^2 - 2\hbar\omega_{\boldsymbol{k}}E_{\boldsymbol{p}} \; . \tag{G.3}$$

Furthermore, the dispersion relation of light in a medium, $k = \omega n/c$, gives

$$cnp\cos\theta = \frac{\hbar\omega_{\boldsymbol{k}}}{2}(n^2 - 1) + E_{\boldsymbol{p}} \; . \tag{G.4}$$

Applying the relativistic expressions for momentum and energy, $p = \gamma mv$ and $E = \gamma mc^2$, where $\gamma = 1/\sqrt{1 - v^2/c^2}$ denotes the Lorentz factor, we may rewrite this expression as a constraint imposed on $\cos\theta$ by conservation of energy and momentum. We define the Cherenkov angle, θ_C, as the angle fulfilling this constraint

$$\cos\theta_C = \frac{c}{nv}\left(1 + \frac{\hbar\omega_{\boldsymbol{k}}}{2E_{\boldsymbol{p}}}(n^2 - 1)\right) \; . \tag{G.5}$$

Classically, light is emitted in the forward direction $\theta_C = 0$ when the particle reaches the threshold velocity. However, the emitted power goes to zero in this limit. In relativistic quantum mechanics, photons may in principle be emitted in the forward direction from a particle above threshold velocity due to the correction term in the Cherenkov angle. Setting $\cos\theta_C = 1$, we have by Eq.(G.5) an upper limit on the energy of the emitted photon

$$\hbar\omega_{\mathrm{MAX}} = \frac{nv/c - 1}{n^2 - 1}2E_{\boldsymbol{p}} \; . \tag{G.6}$$

H Amplitudes

This appendix contains the calculations of the transition amplitudes for the process $|\psi_{\boldsymbol{p}}\rangle\,|0\rangle \to |\psi_{\boldsymbol{p}'}\rangle\,|\boldsymbol{k}\lambda\rangle$ at tree level in relativistic quantum mechanics. The different amplitudes will be denoted by the notation

$$\mathcal{M}_{m,l\lambda} = \mathcal{M}\big(u(\boldsymbol{p},m) \to u(\boldsymbol{p}',l) + \boldsymbol{\epsilon}_{\boldsymbol{k}\lambda}\big)\ . \tag{H.1}$$

In the interest of keeping the calculations tidy, we begin by evaluating two matrix products which will appear repeatedly

$$\boldsymbol{\sigma}\begin{pmatrix} p_3 \\ p_+ \end{pmatrix} = \hat{\mathbf{e}}_1\begin{pmatrix} p_+ \\ p_3 \end{pmatrix} + i\hat{\mathbf{e}}_2\begin{pmatrix} -p_+ \\ p_3 \end{pmatrix} + \hat{\mathbf{e}}_3\begin{pmatrix} p_3 \\ -p_+ \end{pmatrix}\ , \tag{H.2}$$

and

$$\boldsymbol{\sigma}\begin{pmatrix} p_- \\ -p_3 \end{pmatrix} = \hat{\mathbf{e}}_1\begin{pmatrix} -p_3 \\ p_- \end{pmatrix} + i\hat{\mathbf{e}}_2\begin{pmatrix} p_3 \\ p_- \end{pmatrix} + \hat{\mathbf{e}}_3\begin{pmatrix} p_- \\ p_3 \end{pmatrix}\ . \tag{H.3}$$

We also define an expression which will emerge as a common prefactor for the amplitudes

$$M_{\boldsymbol{k}} \equiv \frac{c^2 q A_{\boldsymbol{k}} N' N}{(E+mc^2)(E'+mc^2)}\ , \tag{H.4}$$

as well as two quantities which allow us to write the amplitudes in a more compact manner

$$\boldsymbol{a} \equiv \boldsymbol{p}'(E+mc^2) - \boldsymbol{p}(E'+mc^2)\ , \tag{H.5}$$

and

$$B \equiv E + E' + 2mc^2\ . \tag{H.6}$$

With this, we are equipped to evaluate each amplitude.

Spin-up $\to$ Spin-up

The amplitude of the process is

$$\mathcal{M}_{1,1\lambda} = -cqA_{\boldsymbol{k}}u^\dagger(\boldsymbol{p}',1)\boldsymbol{\alpha}\cdot\boldsymbol{\epsilon}^*_{\boldsymbol{k}\lambda}u(\boldsymbol{p},1)\ . \tag{H.7}$$

We evaluate the matrix product

$$u^\dagger(\boldsymbol{p}',1)\boldsymbol{\alpha}\cdot\boldsymbol{\epsilon}^*_{\boldsymbol{k}\lambda}u(\boldsymbol{p},1)$$

$$= N'N\left[\begin{pmatrix}1 & 0 & \dfrac{cp'_3}{E'+mc^2} & \dfrac{cp'^*_+}{E'+mc^2}\end{pmatrix}\begin{pmatrix}0 & \boldsymbol{\sigma}\\ \boldsymbol{\sigma} & 0\end{pmatrix}\begin{pmatrix}1\\0\\\dfrac{cp_3}{E+mc^2}\\\dfrac{cp_+}{E+mc^2}\end{pmatrix}\right]\cdot\boldsymbol{\epsilon}^*_{\boldsymbol{k}\lambda}$$

$$= N'N\left[\frac{c}{E+mc^2}\begin{pmatrix}1 & 0\end{pmatrix}\boldsymbol{\sigma}\begin{pmatrix}p_3\\p_+\end{pmatrix}+\frac{c}{E'+mc^2}\begin{pmatrix}p'_3 & p'^*_+\end{pmatrix}\boldsymbol{\sigma}\begin{pmatrix}1\\0\end{pmatrix}\right]\cdot\boldsymbol{\epsilon}^*_{\boldsymbol{k}\lambda}\ . \quad \text{(H.8)}$$

Here, $N=\sqrt{(E+mc^2)/2E}$ and $p_\pm = p_1 \pm ip_2$, as defined in Appendix F. Apart from the prefactor, the second term in Eq.(H.8) is equal to the complex conjugate (excluding the polarization vector) of the first term, with the substitution $\boldsymbol{p}\to\boldsymbol{p}'$. Therefore we calculate only the first term explicitly, using Eq.(H.2)

$$\begin{pmatrix}1 & 0\end{pmatrix}\boldsymbol{\sigma}\begin{pmatrix}p_3\\p_+\end{pmatrix}\cdot\boldsymbol{\epsilon}^*_{\boldsymbol{k}\lambda} = [\hat{\mathbf{e}}_1 p_+ - i\hat{\mathbf{e}}_2 p_+ + \hat{\mathbf{e}}_3 p_3]\cdot\boldsymbol{\epsilon}^*_{\boldsymbol{k}\lambda} \quad \text{(H.9)}$$

$$= [\boldsymbol{p} - i(\hat{\mathbf{e}}_2 p_1 - \hat{\mathbf{e}}_1 p_2)]\cdot\boldsymbol{\epsilon}^*_{\boldsymbol{k}\lambda}$$

$$= \boldsymbol{p}\cdot\boldsymbol{\epsilon}^*_{\boldsymbol{k}\lambda} - i[\boldsymbol{p}\times\boldsymbol{\epsilon}^*_{\boldsymbol{k}\lambda}]_3\ . \quad \text{(H.10)}$$

The last step follows from the definition of the third component of the cross-product. Thus we have the expression

$$\mathcal{M}_{1,1\lambda} = -M_{\boldsymbol{k}}\Big[(\boldsymbol{p}\cdot\boldsymbol{\epsilon}^*_{\boldsymbol{k}\lambda} - i[\boldsymbol{p}\times\boldsymbol{\epsilon}^*_{\boldsymbol{k}\lambda}]_3)(E'+mc^2)+$$
$$(\boldsymbol{p}'\cdot\boldsymbol{\epsilon}^*_{\boldsymbol{k}\lambda} + i[\boldsymbol{p}'\times\boldsymbol{\epsilon}^*_{\boldsymbol{k}\lambda}]_3)(E+mc^2)\Big]\ . \quad \text{(H.11)}$$

Alternatively, in terms of the quantities $\boldsymbol{a}$ and B,

$$\mathcal{M}_{1,1\lambda} = -M_{\boldsymbol{k}}\Big[(\boldsymbol{p}\cdot\boldsymbol{\epsilon}^*_{\boldsymbol{k}\lambda})B + i[\boldsymbol{a}\times\boldsymbol{\epsilon}^*_{\boldsymbol{k}\lambda}]_3\Big]\ . \quad \text{(H.12)}$$

Spin-down → Spin-down

The amplitude of the process is

$$\mathcal{M}_{2,2\lambda} = -cqA_{\boldsymbol{k}}u^\dagger(\boldsymbol{p}',2)\boldsymbol{\alpha}\cdot\boldsymbol{\epsilon}^*_{\boldsymbol{k}\lambda}u(\boldsymbol{p},2)\ . \quad \text{(H.13)}$$

We evaluate the matrix product

$$
\begin{aligned}
& u^\dagger(\boldsymbol{p}',2)\boldsymbol{\alpha}\cdot\boldsymbol{\epsilon}^*_{\boldsymbol{k}\lambda}u(\boldsymbol{p},2) \\
&= N'N\left[\begin{pmatrix} 0 & 1 & \dfrac{cp'^*_-}{E'+mc^2} & \dfrac{-cp'_3}{E'+mc^2}\end{pmatrix}\begin{pmatrix} 0 & \boldsymbol{\sigma} \\ \boldsymbol{\sigma} & 0\end{pmatrix}\begin{pmatrix} 0 \\ 1 \\ \dfrac{cp_-}{E+mc^2} \\ \dfrac{-cp_3}{E+mc^2}\end{pmatrix}\right]\cdot\boldsymbol{\epsilon}^*_{\boldsymbol{k}\lambda} \\
&= N'N\left[\frac{c}{E+mc^2}\begin{pmatrix}0 & 1\end{pmatrix}\boldsymbol{\sigma}\begin{pmatrix}p_- \\ -p_3\end{pmatrix}+\frac{c}{E'+mc^2}\begin{pmatrix}p'^*_- & -p'_3\end{pmatrix}\boldsymbol{\sigma}\begin{pmatrix}0\\1\end{pmatrix}\right]\cdot\boldsymbol{\epsilon}^*_{\boldsymbol{k}\lambda}\,.
\end{aligned}
\tag{H.14}
$$

Again the second term is equal to the complex conjugate of the first term, with the substitution $\boldsymbol{p}\to\boldsymbol{p}'$. Therefore we calculate only the first term explicitly, using Eq.(H.3)

$$
\begin{aligned}
\begin{pmatrix}0 & 1\end{pmatrix}\boldsymbol{\sigma}\begin{pmatrix}p_- \\ -p_3\end{pmatrix}\cdot\boldsymbol{\epsilon}^*_{\boldsymbol{k}\lambda} &= [\hat{\mathbf{e}}_1 p_- + i\hat{\mathbf{e}}_2 p_- + \hat{\mathbf{e}}_3 p_3]\cdot\boldsymbol{\epsilon}^*_{\boldsymbol{k}\lambda} \\
&= [\boldsymbol{p}+i(\hat{\mathbf{e}}_2 p_1 - \hat{\mathbf{e}}_1 p_2)]\cdot\boldsymbol{\epsilon}^*_{\boldsymbol{k}\lambda} \\
&= \boldsymbol{p}\cdot\boldsymbol{\epsilon}^*_{\boldsymbol{k}\lambda} + i[\boldsymbol{p}\times\boldsymbol{\epsilon}^*_{\boldsymbol{k}\lambda}]_3\,.
\end{aligned}
\tag{H.15}
$$

Thus we have the expression

$$
\begin{aligned}
\mathcal{M}_{2,2\lambda} = -M_{\boldsymbol{k}}\Big[&\big(\boldsymbol{p}\cdot\boldsymbol{\epsilon}^*_{\boldsymbol{k}\lambda} + i[\boldsymbol{p}\times\boldsymbol{\epsilon}^*_{\boldsymbol{k}\lambda}]_3\big)\big(E'+mc^2\big)+ \\
&\big(\boldsymbol{p}'\cdot\boldsymbol{\epsilon}^*_{\boldsymbol{k}\lambda} - i[\boldsymbol{p}'\times\boldsymbol{\epsilon}^*_{\boldsymbol{k}\lambda}]_3\big)\big(E+mc^2\big)\Big]\,.
\end{aligned}
\tag{H.16}
$$

Alternatively, in terms of the quantities $\boldsymbol{a}$ and B,

$$
\mathcal{M}_{2,2\lambda} = -M_{\boldsymbol{k}}\Big[(\boldsymbol{p}\cdot\boldsymbol{\epsilon}^*_{\boldsymbol{k}\lambda})B - i[\boldsymbol{a}\times\boldsymbol{\epsilon}^*_{\boldsymbol{k}\lambda}]_3\Big]\,. \tag{H.17}
$$

Spin-up → Spin-down

The amplitude of the process is

$$
\mathcal{M}_{1,2\lambda} = -cqA_{\boldsymbol{k}}u^\dagger(\boldsymbol{p}',2)\boldsymbol{\alpha}\cdot\boldsymbol{\epsilon}^*_{\boldsymbol{k}\lambda}u(\boldsymbol{p},1)\,. \tag{H.18}
$$

We evaluate the matrix product

$$\begin{aligned}
\mathcal{M}_{1,2\lambda} &\propto u^{\dagger}(\boldsymbol{p}',2)\boldsymbol{\alpha}\cdot\boldsymbol{\epsilon}^{*}_{\boldsymbol{k}\lambda}u(\boldsymbol{p},1)\\
&= N'N\left[\begin{pmatrix}0 & 1 & \dfrac{cp'^{*}_{-}}{E'+mc^2} & \dfrac{-cp'_3}{E'+mc^2}\end{pmatrix}\begin{pmatrix}0 & \boldsymbol{\sigma}\\ \boldsymbol{\sigma} & 0\end{pmatrix}\begin{pmatrix}1\\ 0\\ \dfrac{cp_3}{E+mc^2}\\ \dfrac{cp_+}{E+mc^2}\end{pmatrix}\right]\cdot\boldsymbol{\epsilon}^{*}_{\boldsymbol{k}\lambda}\\
&= N'N\left[\frac{c}{E+mc^2}\begin{pmatrix}0 & 1\end{pmatrix}\boldsymbol{\sigma}\begin{pmatrix}p_3\\ p_+\end{pmatrix}+\frac{c}{E'+mc^2}\begin{pmatrix}p'^{*}_{-} & -p'_3\end{pmatrix}\boldsymbol{\sigma}\begin{pmatrix}1\\ 0\end{pmatrix}\right]\cdot\boldsymbol{\epsilon}^{*}_{\boldsymbol{k}\lambda}\,.
\end{aligned}\tag{H.19}$$

Here both terms must be calculated explicitly. Evaluating the first term by Eq.(H.2), we find

$$\begin{aligned}
\begin{pmatrix}0 & 1\end{pmatrix}\boldsymbol{\sigma}\begin{pmatrix}p_3\\ p_+\end{pmatrix}\cdot\boldsymbol{\epsilon}^{*}_{\boldsymbol{k}\lambda} &= [\hat{\mathbf{e}}_1p_3+i\hat{\mathbf{e}}_2p_3-\hat{\mathbf{e}}_3p_+]\cdot\boldsymbol{\epsilon}^{*}_{\boldsymbol{k}\lambda}\\
&= [(\hat{\mathbf{e}}_1p_3-\hat{\mathbf{e}}_3p_1)-i(\hat{\mathbf{e}}_3p_2-\hat{\mathbf{e}}_2p_3)]\cdot\boldsymbol{\epsilon}^{*}_{\boldsymbol{k}\lambda}\\
&= [\boldsymbol{p}\times\boldsymbol{\epsilon}^{*}_{\boldsymbol{k}\lambda}]_2-i[\boldsymbol{p}\times\boldsymbol{\epsilon}^{*}_{\boldsymbol{k}\lambda}]_1\,.
\end{aligned}\tag{H.20}$$

For simplicity, we calculate the second term of Eq.(H.19) by its complex conjugate, allowing us to apply Eq.(H.3).

$$\begin{aligned}
\begin{pmatrix}1 & 0\end{pmatrix}\boldsymbol{\sigma}\begin{pmatrix}p'_{-}\\ -p'_3\end{pmatrix}\cdot\boldsymbol{\epsilon}^{*}_{\boldsymbol{k}\lambda} &= [-\hat{\mathbf{e}}_1p'_3+i\hat{\mathbf{e}}_2p'_3+\hat{\mathbf{e}}_3p'_{-}]\cdot\boldsymbol{\epsilon}^{*}_{\boldsymbol{k}\lambda}\\
&= [-(\hat{\mathbf{e}}_1p'_3-\hat{\mathbf{e}}_3p'_1)-i(\hat{\mathbf{e}}_3p'_2-\hat{\mathbf{e}}_2p'_3)]\cdot\boldsymbol{\epsilon}^{*}_{\boldsymbol{k}\lambda}\\
&= -[\boldsymbol{p}'\times\boldsymbol{\epsilon}^{*}_{\boldsymbol{k}\lambda}]_2-i[\boldsymbol{p}'\times\boldsymbol{\epsilon}^{*}_{\boldsymbol{k}\lambda}]_1\,.
\end{aligned}\tag{H.21}$$

Thus we have the expression

$$\begin{aligned}
\mathcal{M}_{1,2\lambda} = -M_{\boldsymbol{k}}\Big[&\big([\boldsymbol{p}\times\boldsymbol{\epsilon}^{*}_{\boldsymbol{k}\lambda}]_2-i[\boldsymbol{p}\times\boldsymbol{\epsilon}^{*}_{\boldsymbol{k}\lambda}]_1\big)\big(E'+mc^2\big)-\\
&\big([\boldsymbol{p}'\times\boldsymbol{\epsilon}^{*}_{\boldsymbol{k}\lambda}]_2-i[\boldsymbol{p}'\times\boldsymbol{\epsilon}^{*}_{\boldsymbol{k}\lambda}]_1\big)\big(E+mc^2\big)\Big]\,.
\end{aligned}\tag{H.22}$$

Alternatively, in terms of the quantities $\boldsymbol{a}$ and B,

$$\mathcal{M}_{1,2\lambda} = M_{\boldsymbol{k}}\Big[[\boldsymbol{a}\times\boldsymbol{\epsilon}^{*}_{\boldsymbol{k}\lambda}]_2-i[\boldsymbol{a}\times\boldsymbol{\epsilon}^{*}_{\boldsymbol{k}\lambda}]_1\Big]\,.\tag{H.23}$$

Spin-down → Spin-up

The amplitude of the process is

$$\mathcal{M}_{2,1\lambda} = -cqA_{\boldsymbol{k}} u^{\dagger}(\boldsymbol{p}', 1)\boldsymbol{\alpha}\cdot\boldsymbol{\epsilon}^{*}_{\boldsymbol{k}\lambda} u(\boldsymbol{p}, 2)\ . \tag{H.24}$$

We evaluate the matrix product

$$\begin{aligned} &u^{\dagger}(\boldsymbol{p}', 1)\boldsymbol{\alpha}\cdot\boldsymbol{\epsilon}^{*}_{\boldsymbol{k}\lambda} u(\boldsymbol{p}, 2) \\ &= N'N\left[\begin{pmatrix} 1 & 0 & \dfrac{cp'_3}{E'+mc^2} & \dfrac{cp'^{*}_{+}}{E'+mc^2}\end{pmatrix}\begin{pmatrix} 0 & \boldsymbol{\sigma} \\ \boldsymbol{\sigma} & 0\end{pmatrix}\begin{pmatrix} 0 \\ 1 \\ \dfrac{cp_-}{E+mc^2} \\ \dfrac{-cp_3}{E+mc^2}\end{pmatrix}\right]\cdot\boldsymbol{\epsilon}^{*}_{\boldsymbol{k}\lambda} \\ &= N'N\left[\frac{c}{E+mc^2}\begin{pmatrix}1 & 0\end{pmatrix}\boldsymbol{\sigma}\begin{pmatrix}p_- \\ -p_3\end{pmatrix} + \frac{c}{E'+mc^2}\begin{pmatrix}p'_3 & p'^{*}_{+}\end{pmatrix}\boldsymbol{\sigma}\begin{pmatrix}0\\1\end{pmatrix}\right]\cdot\boldsymbol{\epsilon}^{*}_{\boldsymbol{k}\lambda}\ . \end{aligned} \tag{H.25}$$

Here, the first term may be taken directly from Eq.(H.21), substituting $\boldsymbol{p}' \to \boldsymbol{p}$

$$\begin{pmatrix}1 & 0\end{pmatrix}\boldsymbol{\sigma}\begin{pmatrix}p_- \\ -p_3\end{pmatrix}\cdot\boldsymbol{\epsilon}^{*}_{\boldsymbol{k}\lambda} = -[\boldsymbol{p}\times\boldsymbol{\epsilon}^{*}_{\boldsymbol{k}\lambda}]_2 - i[\boldsymbol{p}\times\boldsymbol{\epsilon}^{*}_{\boldsymbol{k}\lambda}]_1\ . \tag{H.26}$$

Similarly, we have the complex conjugate of the second term from Eq.(H.20), substituting $\boldsymbol{p} \to \boldsymbol{p}'$

$$\begin{pmatrix}0 & 1\end{pmatrix}\boldsymbol{\sigma}\begin{pmatrix}p'_3 \\ p'_+\end{pmatrix}\cdot\boldsymbol{\epsilon}^{*}_{\boldsymbol{k}\lambda} = [\boldsymbol{p}'\times\boldsymbol{\epsilon}^{*}_{\boldsymbol{k}\lambda}]_2 - i[\boldsymbol{p}'\times\boldsymbol{\epsilon}^{*}_{\boldsymbol{k}\lambda}]_1\ . \tag{H.27}$$

Thus we have the expression

$$\begin{aligned}\mathcal{M}_{2,1\lambda} = -M_{\boldsymbol{k}}\Big[&-\big([\boldsymbol{p}\times\boldsymbol{\epsilon}^{*}_{\boldsymbol{k}\lambda}]_2 + i[\boldsymbol{p}\times\boldsymbol{\epsilon}^{*}_{\boldsymbol{k}\lambda}]_1\big)\big(E'+mc^2\big) + \\ &\big([\boldsymbol{p}'\times\boldsymbol{\epsilon}^{*}_{\boldsymbol{k}\lambda}]_2 + i[\boldsymbol{p}'\times\boldsymbol{\epsilon}^{*}_{\boldsymbol{k}\lambda}]_1\big)\big(E+mc^2\big)\Big]\ .\end{aligned} \tag{H.28}$$

Alternatively, in terms of the quantities $\boldsymbol{a}$ and B,

$$\mathcal{M}_{2,1\lambda} = -M_{\boldsymbol{k}}\Big[[\boldsymbol{a}\times\boldsymbol{\epsilon}^{*}_{\boldsymbol{k}\lambda}]_2 + i[\boldsymbol{a}\times\boldsymbol{\epsilon}^{*}_{\boldsymbol{k}\lambda}]_1\Big]\ . \tag{H.29}$$

I Code

The following is an excerpt from the code used to produce the plots for this thesis. The full code can be found as an attachment to the digital version, or at https://github.com/JonasLW/Cherenkov-Radiation.git.

```
# Version: Python 2.7
from __future__ import division
import pylab as py
from scipy import integrate

# NOTE: These functions employ natural units. c = hbar = 1. Give
    masses and frequencies
#       in units of eV.

# Functions for basic quantities related to the physical system
def Gamma( v ):
    """Returns the Lorentz factor as a function of velocity."""
    return 1/py.sqrt(1-v**2)

def CosCh( n, m, v, w ):
    """Returns cosine of Cherenkov angle as function of refraction
        coefficient, mass, velocity, and frequency."""
    f = 2*Gamma(v)*m  # For readability
    result = ( 1 + (n**2-1)*w/f )/(n*v)
    if py.ndim(result) > 0:
        result[ result>1 ] = py.nan
        result[ result<0 ] = py.nan
    elif result > 1 or result < 0:
        result = py.nan
    return result

def ChAngle( n, m, v, w ):
    """Returns Cherenkov angle as function of refraction coefficient,
        mass, velocity, and frequency."""
    return py.arccos( CosCh(n,m,v,w) ) # Angle is always positive

def SinCh( n, m, v, w ):
    """Returns sine of Cherenkov angle as function of refraction
        coefficient, mass, velocity, and frequency."""
    return py.sin( ChAngle(n,m,v,w) )


# Amplitudes summed over final state spin
```

```
# Expressions do not include S_k, as this cancels in calculating
    physical quantities
def F( n, m, v, w, chi, phi ):
    """Function containing the spinor angle dependence of the squared
        amplitudes."""
    return py.sin(chi)*py.cos(phi)*SinCh(n,m,v,w)/Gamma(v) -
        py.cos(chi)*( n*v-CosCh(n,m,v,w) )

def TermOne( n, m, v, w ):
    """Recurring term in amplitudes."""
    return 0.5*( v*SinCh(n,m,v,w) )**2

def TermTwo( n, m, v, w ):
    """Recurring term in amplitudes."""
    return 0.5*w/( Gamma(v)*m )

def AmpMinSq( n, m, v, w, chi, phi, a ):
    """Returns squared transition amplitude of left-elliptical light,
        as function of spinor angles phi and chi, and basis a."""
    A = TermOne( n, m, v, w )
    B = TermTwo( n, m , v, w )
    return A + (n**2-1)*B**2 - py.cos(2*a)*A +
        py.sin(2*a)*B*F(n,m,v,w,chi,phi)

def AmpPlusSq( n, m, v, w, chi, phi, a ):
    """Returns squared transition amplitude of right-elliptical light,
        as function of spinor angles phi and chi, and basis a."""
    A = TermOne( n, m, v, w )
    B = TermTwo( n, m, v, w )
    return A + (n**2-1)*B**2 + py.cos(2*a)*A -
        py.sin(2*a)*B*F(n,m,v,w,chi,phi)

def AmpTotSq( n, m, v, w ):
    """Returns squared transition amplitude summed over polarization
        states."""
    A = TermOne( n, m, v, w )
    B = TermTwo( n, m, v, w )
    return 2*A + 2*(n**2-1)*B**2


def RateFac( v ):
    """Converts a squared transition amplitude into a transition rate
        density, in SI-units [1/rad].

    Integrate transition rate density over w and phi for total
        transition rate of process."""
    c = 299792458
    q = 1.6*10**(-19)
    h = 1.1*10**(-34)
    return 10**(-7)*q**2*c/(h*v*2*py.pi)
```

```
def RateTot( n, m, v, w, chi, phi, a ):
    return RateFac(v)*AmpTotSq(n,m,v,w)


# Utility functions for integration
def QuadArr( Func, a, b, args=()):
    """Integrates Func from a to b for args. One element of args may
       be array.

    Outputs array of integrated values.
    args is tuple of floats and/or ints and/or numpy arrays.
    Currently only one element of args may be array.
    The purpose of this function is to calculate an array of values
       where each element requires an integral."""
    l = 1
    for arg in args:
        if type(arg) is not float and type(arg) is not int:
            l = len(arg)
            break
    argarr = py.transpose( py.array([ py.ones(l)*arg for arg in args
       ]) )
    return py.array([ integrate.quad(Func,a,b,args=tuple(ars))[0] for
       ars in argarr ])

def IntegrateOmega( Func, n, m, v, wlims, chi, phi, a ):
    """Takes a function Func and integrates it over w.

    Func must take the appropriate arguments.
    wlims may be array used otherwise for plotting. Will then
       integrate over these values.
    Can not handle wlims input as meshgrid.
    Output in SI-units, however performs integral in natural units.
    Assumes Func output in SI-units."""
    h = 1.1*10**(-34)
    fac = 1.6*10**(-19)/h
    R = lambda W,N,M,V,CHI,PHI,A : py.nan_to_num(
       Func(N,M,V,W,CHI,PHI,A) )
    return fac*QuadArr( R, wlims[0], wlims[-1], args=(n,m,v,chi,phi,a)


# Sample script for numerical calculation and plotting of
# a quantity which contains an integral over omega.

res = 1000
n = 1.3                     # Refraction coefficient of medium
m = 5.11*10**5              # Particle mass (eV)
v = py.linspace( 1/n, 1, res ) # Particle velocity (c)
w = 6.59                    # Photon frequency (eV)
wlims = ( 0, w )            # Integration limits for photon frequency
```

```
chi = py.pi/2                # Spinor polar angle
phi = py.pi                  # Spinor azimuthal angle
a = py.pi/4                  # Polarization basis parameter (alpha)
c = 299792458

r = IntegrateOmega( RateTot, n, m, v, wlims, chi, phi, a )*2*py.pi
fig = py.figure()
ax = fig.add_subplot( 111 )
ax.plot( v, r, linewidth=1.5 )
ax.set_xlabel( '$v/c$' )
ax.set_ylabel( '$R$' )
fig.show()
```

Bibliography

[1] *Physical Review D, Review of Particle Physics*, 3rd ser. 86.1 (), edited by E. J. Weinberg, edited by D. L. Nordstrom.

[2] J. Miroslaw and G. R. Fournier, *Light Scattering by Particles in Water: Theoretical and Experimental Foundations* (Elsevier Science & Technology, 2011).

[3] G. E. Jellison, "Optical functions of GaAs, GaP, and Ge determined by two-channel polarization modulation ellipsometry", Optical Materials **1**, 151–160 (1992).

[4] D. L. Perego, "The RICH detectors of the LHCb experiment", Nuclear Physics B - Proceedings Supplements **197**, 358–361 (2009).

[5] The LHCb RICH Collaboration et al., "Performance of the LHCb RICH detector at the LHC", The European Physical Journal C, Particles and Fields **73** (2013).

[6] P. A. Cherenkov, "Visible emission of clean liquids by action of γ radiation", Doklady Akademii Nauk SSSR **2** (1934).

[7] V. L. Ginzburg, "Radiation by uniformly moving sources (Vavilov–Cherenkov effect, transition radiation, and other phenomena)", Physics-Uspekhi **39**, 973–982 (1996).

[8] A. F. Danilyuk, S. A. Kononov, E. A. Kravchenko, and A. P. Onuchin, "Aerogel Cherenkov detectors in colliding beam experiments", Physics-Uspekhi **58**, 503–511 (2015).

[9] V. L. Ginzburg, "Some remarks on the radiation of charges and multipoles uniformly moving in a medium", Physics-Uspekhi **45**, 341–344 (2002).

[10] L. D. Landau and E. M. Lifshitz, *Electrodynamics of Continuous Media*, 2nd ed. (Pergamon Press, 1963) Chap. 12.

[11] J. V. Jelley, *Cerenkov radiation and its applications* (Pergamon Press, 1958).

[12] D. Griffiths, *Introduction to Electrodynamics*, Pearson New International Edition, 4/E (Pearson, 2014).

[13] D. B. Sirdeshmukh, L. Sirdeshmukh, and K. G. Subhadra, *Atomistic Properties of Solids*, Vol. 147, Springer Series in Materials Science (Springer, 2011) Chap. 11.

[14] C. C. Gerry and P. L. Knight, *Introductory Quantum Optics*, 2nd ed. (Cambridge University Press, 2005) Chap. 2.

[15] M. E. Peskin and D. V. Schroeder, *An Introduction to Quantum Field Theory*, Student Economy Edition (Westview Press, 2016).

[16]R. U. Martinelli and C. C. Wang, "Electron-beam penetration in GaAs", Journal of Applied Physics **44**, 3350–3351 (1973).

[17]A. P. Potylitsyn, S. Y. Gogolev, and L. G. Sukhikh, "Angular distribution of coherent Cherenkov radiation from a bunch passing through a vacuum channel in the dielectric target", Nuclear Instruments and Methods in Physics Research Section B: Beam Interactions with Materials and Atoms **402**, 139–143 (2017).

[18]A. M. Cook, R. Tikhoplav, S. Y. Tochitsky, G. Travish, O. B. Williams, and J. B. Rosenzweig, "Observation of Narrow-Band Terahertz Coherent Cherenkov Radiation from a Cylindrical Dielectric-Lined Waveguide", Physical Review Letters **103**, 095003-1 –095003-4 (2009).

[19]G. N. Afanasiev, M. V. Lyubchenko, and Y. P. Stepanovsky, "Fine Structure of the Vavilov-Cherenkov radiation (and references cited therein)", Proceedings of the Royal Society of London A **462**, 689–699 (2006).

[20]L. Zhou and Y.-B. Sheng, "Concurrence Measurement for the Two-Qubit Optical and Atomic States", Entropy **17**, 4293–4322 (2015).

[21]M. Abramowitz and I. Stegun, *Handbook of Mathematical Functions with Formulas, Graphs, and Mathematical Tables*, Vol. 147 (United States Department of Commerce, National Bureau of Standards, 1964) Chap. 9.

[22]D. J. Griffiths, *Introduction to Elementary Particles*, 2nd ed. (Wiley-VCH, 2010).

[23]P. A. M. Dirac, "The quantum theory of the electron", Proceedings of the Royal Society of London A **117**, 610–624 (1928).